



Bucket wheel excavators operating under difficult mining conditions including unmineable inclusions and geological structures with excessive mining resistance

(BEWEXMIN)



EUR 30841 EN

Bucket wheel excavators operating under difficult mining conditions including unmineable inclusions and geological structures with excessive mining resistance (BEWEXMIN)

European Commission

Directorate-General for Research and Innovation

Directorate C – Clean Planet

Unit C.3 — Low Emission Future Industries

Contact Andrea Gentili

E-mail RTD-STEEL-COAL@ec.europa.eu

RTD-PUBLICATIONS@ec.europa.eu

European Commission

B-1049 Brussels

Manuscript completed in 2020.

This document has been prepared for the European Commission however it reflects the views only of the authors, and the Commission cannot be held responsible for any use which may be made of the information contained therein.

More information on the European Union is available on the internet (<http://europa.eu>).

Luxembourg: Publications Office of the European Union, 2020

PDF

ISBN 978-92-76-42005-7

ISSN 1831-9424

doi: 10.2777/875820

KI-NA-30-841-EN-N

© European Union, 2021.

Reuse is authorised provided the source is acknowledged. The reuse policy of European Commission documents is regulated by Decision 2011/833/EU (OJ L 330, 14.12.2011, p. 39).

For any use or reproduction of photos or other material that is not under the EU copyright, permission must be sought directly from the copyright holders.

All pictures, figures and graphs © Poltegor Instytut – Instytut Górnictwa Odkrywkowego, RFCR-CT-2015-00023 BEWEXMIN

Research Fund for Coal and Steel

Bucket wheel excavators operating under difficult mining conditions including unmineable inclusions and geological structures with excessive mining resistance

(BEWEXMIN)

Co-ordinator:
Adam Bajcar

Poltegor Instytut – Instytut Górnictwa Odkrywkowego
ul. Parkowa 25, 51-616 Wrocław, Poland

Authors:

Adam Bajcar, Barbara Rogosz, Marek Onichimuk, Marian Wygoda, Jacek Szczepiński
Poltegor Instytut – (POLT)

Petr Svoboda, Michal Rehor, Vlastimir Moni
Výzkumný ústav pro hnědé uhlí a.s. (VUHU)

Michalis Galetakis, Antonios Vafidis
The Research Committee of the Technical University of Crete (UCRE)
Theodore N. Michalakopoulos, George Apostolopoulos
National Technical University of Athens (NTUA)

Maria Lazar, Iosif Andras
Universitatea di Petrosani (UPETROS)

Christos Roumpos
Public Power Corporation AE (PPC)

Ionut Predoiu
Socitetatea Complexul Energetic OLTEANIA SA (CE OLTEANIA)

Jarosław Tokarczyk, Kamil Szewerda, Marek Dudek
Instytut Techniki Górniczej (KOMAG)

Marcin Olejnik, Tomasz Witalewski
PGE Górnictwo i Energetyka Konwencjonalna SA PGE PGIEK (PGEGIEK)

Grant Agreement RFR-CT-2015-00003

1 September 2015 to 31 August 2018

Final Report

Table of Contents

1	SUMMARY	5
2	SCIENTIFIC AND TECHNICAL DESCRIPTION OF THE RESULTS	7
2.1	Objectives of the project	7
2.2	Description of activities and discussion	11
2.2.1	WP-1. Optimal adaptation of currently exploited and new bucket-wheel excavators for mining of overburden including interlayers with excessive mining resistance and unmineable inclusions	11
2.2.1.1	WP-1.1. Construction solutions of mining equipment aiming at decrease of dynamic loads, especially impulse loads	11
2.2.1.2	WP 1-2 Method of definition of substitute calculation force of impact load for static calculations of strengths of bucket wheel excavator load carrying structure	16
2.2.1.3	WP 1-3 Research on real objects and analysis of dislocation of stress waves in excavator's bearing structure caused by impulse load of bucket wheel.....	25
2.2.1.4	WP 1-4 Experimental verification of correctness of selection of calculation values of load factors resulting from vibrations of load carrying structure during operation in selected conditions	28
2.2.1.5	WP 1-5 Assessment of selected excavator adjustment for operation under conditions including unmineable inclusions and geological structures with excessive mining resistance as well as definition of possible changes introduction increasing adjustment to operation in such conditions	36
2.2.2	WP-2. Monitoring system of bucket wheel excavator load carrying structure efforts and method of diagnostic signals analysis for current assessment of threats of load carrying structure damages as well as constant control of residual strength of the structure	39
2.2.2.1	WP-2.1. Method of monitoring of load carrying structure stresses along with selected parameters of excavators' operation as well as methods of load carrying structure efforts assessment on the basis of registered signals.....	39
2.2.2.2	WP 2.2 Definition of experimental methods of correlation of stresses in load carrying structure in measured points with the stresses in the areas of their concentration ..	42
2.2.2.3	WP-2.3 Definition of parameters of stresses distribution in bucket wheel excavator load carrying structure for different properties of mined materials on the basis of tests on real machines in exploitation conditions	47
2.2.2.4	WP-2.4 Experimental verification of obtained results through tests of the monitoring system in exploitation conditions	54
2.2.3	WP-3 Real-time mine-face inspection system, based on geophysical methods, capable to detect hard rock inclusions and geological formations which are difficult to be excavated by bucket-wheel excavators	59
2.2.3.1	WP-3.1 Collection and analysis of geological information for geophysical methods selection ..	59
2.2.3.2	WP-3.2 Report on field tests for the selection of the most appropriate geophysical method.	63
2.2.3.3	WP-3.3. Hardware development and installation on the BWE	68
2.2.3.4	WP-3.4 Development and testing of an automated algorithm for geophysical data processing and evaluation.....	71
2.2.3.5	WP-3.5 Development of the expert system.....	84
2.2.3.6	WP-3.6 Integration - final testing and evaluation.	87
2.2.4	WP-4 Management, coordination, and dissemination	91
2.3	Conclusions	93
2.4	Exploitation and impact of the research results	97
2.4.1	Actual applications	97
2.4.2	Technical and economic potential for the use of the results	97
2.4.3	Publications / conference presentations resulting from the project.....	99

2.4.4	Other aspects concerning the dissemination of results	101
3	LIST OF FIGURES	103
4	LIST OF TABLES	105
5	LIST OF ACRONYMS AND ABBREVIATIONS.....	107
6	REFERENCES.....	109

1 SUMMARY

The main aim of the BEWEXMIN project was to decrease failure frequency of bucket-wheel excavators operating in difficult mining conditions including unmineable inclusions and geological structures with excessive mining resistance, which are increasingly present at working faces of these machines. Within the project three substantial work packages were realized.

The work package 1 concerned construction solutions for mining equipment, aiming at a decrease of dynamic loads and especially impulse loads. Within this WP a simulation model of impulse load was proposed. The analysis was based on the theory of collision of hard bodies. Different models of collision impulse were analyzed and a scheme (timeframe) of the impulse load model was proposed for testing. Moreover, a method of definition of substitute calculation force of impact load for static calculations of strengths of bucket wheel excavator load carrying was completed. Within WP-1 a task focused on experimental values of parameters used in the method of determination of substitute strengths depending on impulse loads was also realized. This work package also included experimental verification of correctness of selecting calculation values of load factors resulting from vibrations of load carrying structure during operation in selected conditions as well as assessment of selected excavators' adjustment for operation under conditions characterized by unmineable inclusions and geological structures with excessive mining resistance.

Activities in the WP-2 were dedicated to definition of a method of monitoring of load carrying structure stresses along with selected parameters of excavators' operation as well as methods of load carrying structure efforts assessment on the basis of registered signals. This work package also included definition of efficiency value changes in the areas of stresses sensors installation in relation to fatigue strengths of neighbouring construction nod. During realization of this task a testing rig with a prototype measurement system was created. The testing rig was versatile because it was a reduced-scale model of a truss section and at the same time a quite real-scale model of a bolted or welded node (joint). Moreover, within the second work package parameters of stresses distribution in bucket wheel excavator load carrying structure for different properties of mined materials on the basis of tests on real machines in exploitation conditions were determined. Within this task long-term tests of load carrying structure conducted under real conditions of excavator operation in order to obtain data enabling constant monitoring and analysis were conducted. Also experimental verification of the obtained results through tests of the monitoring system in exploitation conditions was completed.

The third work package included collection and analysis of geological information for geophysical methods selection. Within this task, an extensive literature review on the geophysical methods used for the assessment of diggability of geological formations was conducted. The literature review on formations which occur frequently in the overburden or in the intermediate waste of brown coal deposits and especially in those exploited by continuous surface mining methods was performed.

Another objective of WP-3 was also to collect and analyse information required for the preliminary evaluation of geophysical methods to be used for the real-time assessment of the excavability of rock/soil types present at the mines operated by BEWEXMIN's industrial partners. The intention was to use these data for defining the requirements, specifications and limitations of the geophysical methods and equipment. Gathered data were analysed and evaluated in order to determine the most appropriate geophysical methods which were investigated during the field tests. Within WP-3, the most appropriate geophysical method to be used in a real-time mine-face inspection system, capable to detect hard rock inclusions and geological formations which are difficult to be excavated by bucket-wheel excavators, were also defined. Extensive field tests were conducted at the South Field mine Kozani Greece (PPC), at the Szczerbow Field, Belchatow mine, Poland (PGE) and at Husnicioara Field and Rociuta Mines, Romania (OLTENIA). The geophysical survey in PPC coal mine took place in April 2016. The geophysical survey at PGE mines, including test sites preparation and support during the field work, was performed in July 2016. The field tests in OLTENIA mines were also carried out in July 2016. The collected data were evaluated and the geophysical methods were ranked according to their suitability for real-time mine face inspection. Four different geophysical methods were used and evaluated in order to select the most appropriate. For their ranking not only their performance in hard rock detection but also the critical, technical and operational parameters related to mining operations and the working conditions were taken into account. A system capable to detect geological formations with excessive cutting resistance in real-time was completed and installed on the bucket wheel excavator.

An algorithm for automatic processing of data obtained from the geophysical sensor (Electro - Magnetic, EM) was developed as well as the expert system (ES), which can guide the operator of the BWE to avoid collisions of the excavating buckets with hard rock inclusions and avoid other

problems in material digging. A Fuzzy Inference System (FIS) was selected as the most appropriate type of expert system to carry out this task.

As a result the developed software was integrated with the geophysical hardware, tested and evaluated via field test in PPC's mines. These field tests included the operation of the BWE equipped with the detection system at faces where the hard rock inclusions had been mapped in detail, as well as in other sites where the locations of the hard formations were unknown. More specifically, the integration of the developed software-hardware into the overall system for real-time monitoring of the excavation process and its testing and evaluation was accomplished in 3 phases, the pre-integration, the integration and the final testing and evaluation.

2 SCIENTIFIC AND TECHNICAL DESCRIPTION OF THE RESULTS

2.1 Objectives of the project

Within the BEWEXMIN project activities were focused mainly on:

- construction solutions for mining equipment, aiming at a decrease of dynamic loads, especially impulse loads;
- method of definition of substitute calculation force of impact load for static calculations of strengths of bucket wheel excavator load carrying structure,
- monitoring of load carrying structure stresses along with selected parameters of excavators' operation as well as methods of load carrying structure efforts assessment on the basis of registered signals;
- research on real objects and analysis of dislocation of stress waves in excavator's bearing structure caused by impulse load of bucket wheel;
- experimental verification of correctness of selecting calculation values of load factors resulting from vibrations of load carrying structure during operation in selected conditions;
- definition of experimental methods of correlation of stresses in load carrying structure in measured points with the stresses in areas of their concentration;
- definition of parameters of stresses distribution in bucket wheel excavator load carrying structure for different properties of mined materials on the basis of test on real machines in exploitation conditions;
- development and installation of hardware on the BWE;
- development and testing of an automated algorithm for geophysical data processing and evaluation;
- development of expert system and its integration.

These overall objectives are given on a task per task basis below.

WP-1.1 Construction solutions of mining equipment aiming at decrease of dynamic loads, especially impulse loads

The objective of the task was to describe the requirements set for mining system of BWE for exploitation of structures with excessive mining resistance and with unmineable inclusions. Activities foreseen in this task were theoretical and included:

- analysis and theoretical definition of relationship between load occurring during exploitation of structures with excessive mining resistance and a number of buckets on a wheel;
- selection of system protecting from overload of a bucket wheel drive on the basis of simulation tests;
- elaboration of simulation model of impulse load;
- definition of bucket and wheel construction from the perspective of decrease of dynamics and improvement of operation effectiveness during exploitation of structures with excessive mining resistance based on theoretical analysis.

WP-1.2 Method of definition of substitute calculation force of impact load for static calculations of strengths of bucket wheel excavator load carrying structure

The main result of this task was a method of determination of value of force representing impulse loads during calculations of strengths of bucket wheel excavators load bearing structure. Within this task theoretical tests were conducted and they included:

- theoretical analysis of stresses in load carrying structure of bucket wheel excavator resulting from impulse load;
- definition of functional dependence of determination of computational substitute of impulse load and required experimental values.

WP-1.3 Research on real objects and analysis of dislocation of stress waves in excavator's bearing structure caused by impulse load of bucket wheel

The aim of this task was to obtain experimental material required for determination of substitute strength for impulse loads. The tests included:

- research program and method of research results analysis;
- verification of the program and arrangements with measurement contractors;
- tests of stresses in load carrying structure of real excavator during impulse loads;
- definition of unit force on bucket wheel in the area of extensometer localization during tests;
- analysis of obtained results and comparison of computational values with experimental values.

WP-1.4. Experimental verification of correctness of selection of calculation values of load factors resulting from vibrations of load carrying structure during operation in selected conditions.

Values of dynamic surpluses for calculations of load carrying structure resistance depending upon mass vibrations arising during exploitation of structures with excessive mining resistance were obtained as a main goal of this task. The activities foreseen in this task were experimental and were conducted on real machines during operation.

- Development of method of determination of dynamic surpluses depending on mass vibrations.
- Elaboration of research program for real bucket wheel excavators operating in structures with excessive mining resistance and arrangements with contractors.
- Definition of stresses of load carrying structure depending on mass loads in operation conditions.
- Definition, on the basis of research results, of dynamic surpluses depending on properties of structures with excessive mining resistance.

WP-1.5 Assessment of selected excavators adjustment for operation under conditions including unmineable inclusions and geological structures with excessive mining resistance as well as definition of possible changes introduction increasing adjustment to operation in such conditions

The result of the task is a concept and a range of necessary changes in SchRs 4000 excavator, in order to adjust it in as good as possible manner to real operating conditions.

WP-2.1 Method of monitoring of load carrying structure stresses along with selected parameters of excavators' operation as well as methods of load carrying structure efforts assessment on the basis of registered signals

Activities realized within this task had a theoretical character, and their main aim was to develop a method of assessment of load carrying structure on the basis of registered signals. It was also important to develop a vector of parameters of monitored measurement data as well as definition of rules of their analysis and interpretation in order to assess effort of construction elements depending on external loads connected with excavators operation. In order to obtain foreseen aim following objectives had to be set:

- definition of monitoring range and method of monitoring point distribution in order to monitor stresses in elements of the body structure;
- definition of areas of directional straining for localization of straining sensors, analysis of construction using MBS system to determine places where vibration sensors should be mounted;
- method of analysis of stresses in selected elements of the body in order to assess fatigue efforts of body structure;
- method of assessment of risks of load carrying structure damage based on registered signals.

WP-2.2 Definition of experimental methods of correlation of stresses in load carrying structure in measured points with the stresses in the areas of their concentration

Values of fatigue strength changes in the areas where measurement sensors were located in relation to fatigue strength of neighbouring nods were determined during conducted research. In order to obtain foreseen aim it was planned to:

- make an analysis of influence of geometry change on stresses distribution in areas foreseen for monitoring, including potential areas of stress accumulation using computer simulations;
- make stand tests on a model of construction nod using extensometer measurement systems in order to define instructions for construction of functional measurement systems enabling measurement of complicated stresses and monitoring of areas of construction nods;
- define experimental functions describing stress values in the area of stress accumulation, depending on stresses in the measurement points for selected construction nods of the body.

WP-2.3 Definition of parameters of stresses distribution in bucket wheel excavator load carrying structure for different properties of mined materials on the basis of tests on real machines in exploitation conditions

The main aim of this task was to construct monitoring measurement system for a bucket wheel excavator as well as realization of an experiment aiming at determination of parameters of stresses pattern.

WP-2.4 Experimental verification of obtained results through tests of the monitoring system in exploitation conditions

The main aim of experimental verification was to evaluate assumed solutions and obtained results by application of the measurement system for load carrying structure efforts monitoring. The basis for monitoring system was the measurement system installed on the bucket wheel excavator, recording stresses increase and parameters of drive system operation. Within this task, a dedicated software for the measurement system maintenance, data collection and storage as well as presentation was developed.

WP-3.1. Collection and analysis of geological information for geophysical methods selection

The objective of this task was to gather, compile and evaluate information about current geophysical methods used for the characterization of the geological formations with respect to their diggability by surface coal-mining equipment and particularly by bucket-wheel excavators.

WP-3.2. Field tests for the selection of the most appropriate geophysical methods

The objective of this task was to assess the capability of the most appropriate geophysical methods (derived from the previous review) in varying geological and mining conditions by performing field tests using conventional geophysical instrumentation in the coal-mines of the beneficiaries companies.

WP-3.3. Hardware development and installation on the BWE

The objective of this task was to develop a specialized hardware (based on existing geophysical instrumentation), installed on the bucket wheel slewing boom, and a dedicated software for acquisition, transmission and processing of the obtained measurements.

WP-3.4. Development and testing of an automated algorithm for geophysical data processing and evaluation

The objective of this task was to develop an algorithm for automated processing of the data obtained from the geophysical measurements (GPR and geoelectrics).

WP-3.5. Development of the expert system

The objective of this task was to build an expert system which can inform in advance the BWE operators about the occurrence of hard rock inclusions or difficult or even non-diggable geological formations. The reasoning of this expert system was based on data obtained from the geophysical instrumentation installed on BWE, on visual inspection of the mine's face and existing experiential knowledge regarding mining with use of BWE.

WP-3.6. Integration – final testing and evaluation

The objective of this task was integration of the developed software-hardware into the overall system for real-time monitoring of the excavation process and its testing and evaluation.

2.2 Description of activities and discussion

Results obtained within BEWEXMIN project are described for each task below.

2.2.1 WP-1. Optimal adaptation of currently exploited and new bucket-wheel excavators for mining of overburden including interlayers with excessive mining resistance and unmineable inclusions

The main aim of WP1 was to define requirements to be set during bucket wheel excavators (BWE) construction in order to obtain dynamic loads of a machine as low as possible and proper resistance of load carrying structure to these loads during exploitation of structures with excessive mining resistance and with unmineable inclusions. In order to obtain this aim it was necessary to:

- define requirements concerning mining system enabling decrease of amplitude for all kinds of dynamic loads;
- determine, on the basis of real excavators, values of maximal stresses in load carrying structure resulting from impulse loads during exploitation of structures with unmineable inclusions as well as coefficient of stresses resulting from mass vibrations in function of properties, included in exploited structure with excessive mining resistance;
- develop a method of definition of computational substitute strength enabling proper analysis of impulse loads arising when a bucket encounters unmineable inclusions.

Mass load coefficients and values of substitute strength defined on the basis of the conducted research enabled improvement of calculation methods of bucket wheel excavators load carrying structures.

2.2.1.1 WP-1.1. Construction solutions of mining equipment aiming at decrease of dynamic loads, especially impulse loads

A deep analysis of the construction parameters of the mining system of BWE in connection with its functional parameters related to the characteristics of the working face having as a result the main interactions between the mining systems of BWE and working face during the excavation process has been performed.

Also, a study regarding the possibilities/frequency of occurrence of structures with excessive resistance and unmineable inclusions in overburden rocks or lignite seam has been realised.

The main conclusions contained in D1-1 "Requirements set to mining system of bucket wheel excavator for exploitation of structures with excessive mining resistance and with unmineable inclusions" are listed below.

The economical design of BWEs in hard materials depends on numerous material characteristics, mechanical and operational parameters.

The material characteristics are decisive for the design of the BWE and the selection of the mining method.

A cutting force relative to the length of the cutting contours or cut cross section in relation to the bucket blades or the bucket itself is not sufficient for an optimum design of a BWE, especially for hard materials. This design does not consider the BWE geometry and the required mining method.

The method which should be given preference for the design of a BWE is the method using a fracture surface-related energy requirement, which considers the BWE geometry and mining method as well as the fracturing behaviour and the natural cleavage of the in-situ formation.

The wear of the cutting tools can be predicted by the wear intensity and wear dispersion on the surfaces of these bodies as a function of the material characteristics, mechanical and operational parameters.

A cost effective design of a BWE for a specific application is only possible on the basis of material characteristics determined by means of professional test methods and statistically proven databases of experienced manufacturers. A maximum efficiency of the BWE in operation is only guaranteed, if the selected BWE geometry and the mining method are in agreement with the material characteristics.

The continuous layers of hard formations cannot be generally excavated by BWEs. For their excavation, loosening operations by pre-excavation blasting works or the use of other types of machines, such as impact rippers, classic excavator and others, are required.

Seldom occurrences of boulders or short veins generally are managed by auxiliary measures. A common finding is that small (smaller than the bucket volume) are not excavated in proper sense,

but they are removed from soft embedding rock. Even in this case, they produce unwanted effects on mining system of BWE.

As a general remark, the threat to proper operation and structural safety of BWE resulting from well recognized, regular and continuous layers of hard formations is as important as the sudden encountering of small size and unrecognized hard boulders. The difference is as in risk theory: frequency of occurrence vs. extent of damages produced.

The boulders are of different shape and sizes (from irregular to round and from 0.1 to 15 m) as well as of different mineralogical compositions. They are embedded in a matrix material consisting of claystones, sands, gravel and loam (the overburden of the lignite deposit). These large variations, especially for the compressive strength, determine specific dynamic and stochastic impact loads acting on the BWEs which must be studied more thoroughly for each mine.

In most cases the BWEs can handle boulders ranging from 0.5 up to 1 m in size (depending on their mineralogical composition and strength). The larger ones usually require blasting works or mechanical disaggregation (using other machines).

Based on these findings, and events reported in literature, the identification and scoring of the negative impact of these inclusions on the mining system of BWE during the excavation process, and possible solutions by construction improvements aiming at limitation, mitigation and/or avoidance of negative impact of excavation in hard structures on the BWE mining system were stated.

The buckets intended for excavation the material with excessive cutting resistance and with non-mineable inclusions should:

- be obligatorily equipped with teeth;
- be shaped so as the teeth are the weakest structural link protecting the bucket framework against damage; a tooth pocket should be a successive protective element. The remaining elements (knife, knife support, bucket body, attachments) should be of elevated strength. The bucket should be dimensioned with the FEM method, the calculations should take into account real loads present on the bucket wheel. In calculations, the knife support and the bucket rim should be assumed as the main load bearing framework;
- be shaped so as the resulting effects of the bucket wheel ensure possibly low energy consumption per unit of mass (volume) of the excavated material;
- have bodies which allow their filling at possibly low resistances, and their fast emptying,
- be fully made out of steel plate (the bucket body) (as opposed to the body with chain mats) and, as needed, reinforced with additional ribs; sheet gouge thickness should be at least 10-15 mm;
- be made out of sheet gouge of considerable thickness (the knife support), min. 40-50 mm, and also additionally reinforced, as needed;
- be of the shape (the knife) which allows to select proper positioning angles for teeth (pockets);
- be made of abrasion resistant materials and then it should be subject to heat treatment (the knife). The knife should be min. 50 mm thick. To protect against intense abrasive wear, the knife surfaces should be additionally weld padded on their both sides,
- be fastened to the bucket wheel (the bucket) in four points: two front and two rear attachments;
- prevent excessive side clearance of the bucket fastening (the construction of the front attachments);
- be heat treated to eliminate internal (welding) stresses;
- be higher (the number of buckets on the bucket wheel) than that for excavators operating in easily- and medium-workable grounds. The number of buckets on the bucket wheel of a given excavator should be selected with modal analysis, so as excitation generated during working does not coincide with any resonance frequency.

The teeth intended for excavation of the materials with excessive cutting resistances and with unmineable inclusions should:

- be shaped and positioned on the bucket knife so as to get the self-sharpening process for the whole range of their wear;
- be as low as possible (the cutting edge angle β), however due to strength aspects and also abrasive wear, it should be within the range of $24^\circ \div 30^\circ$;
- the tooth clearance angle α should be within $15^\circ \div 18^\circ$, so together with the tool angle β amounts to the cutting angle $\delta = 39^\circ \div 48^\circ$, and the limit value of this angle should not exceed 55° ;
- feature high resistance (the tooth) to abrasive wear on its face and clearance surface, and it also should have high impact resistance in this zone to eliminate break and point chips when encountering hard inclusions, interlayers, etc.;

- feature appropriate high bending strength (the tooth) and resistance to cutting forces, selected to be the weakest element of the bucket and to protect it and other excavator assemblies against excessive impact loads;
- ensure (the way in which a tooth is fastened in the pocket) its fast and easy mounting/dismounting directly on excavator, and stable settlement;
- be relatively high (the number of teeth on the bucket) to protect the bucket knife against wear; this also reduces dynamic loads generated when the bucket goes in and out of the excavated ground;
- be as light as possible (the tooth) so as it can be mounted and dismounted by excavator crew;
- depend on the kind of excavated rocks (the technology used to manufacture the teeth): for rocks with high abrasive properties but without or with a small number of hard non-workable inclusions, more suitable is the technology using the materials without special resistance to abrasion and hardening the cutting edges by applying very hard metallic coatings. For rocks with high abrasive properties including also large number of hard inclusions and interlayers, more suitable is the technology of casting the whole tooth out of abrasion-resistant materials which is then subject of specialized heat treatment;
- enable production of large series using specialized automated production lines (the technology of teeth production -independently of its type) to ensure relatively low production costs and repeatable quality;
- be used bucket corners instead of teeth for hardly-workable rocks, which have both advantages and disadvantages. The advantages include much higher strength and durability than those of teeth, while disadvantages consist in high cutting resistances just after small wear, much higher than those for self-sharpening teeth; furthermore, strong corners do not provide such protection as teeth for mining system and supporting structure against effects of excessive impact loads;
- be used rippers or pre-cutters for rocks of especially high cutting resistances. They are located between buckets and are, like them, fastened on the bucket wheel, however their operating principles are different. The pre-cutters are substantially the buckets without bottoms so the excavated material is spilled out through open bottom to adjacent bucket. Rippers are the sliding out individual teeth provided with quick replaceable strikers which are crushing the excavated material thus facilitating its cutting off by teeth. Experiences gained so far confirm usefulness of both solutions for especially hardly-workable sediments.

The mechanism of bucket wheel drive in excavators operating in hardly-workable formations should:

- be of sufficient tangential cutting force enabling the nominal output at specific cutting resistance $k_L \geq 120\text{ kN/m}$;
- have effective and stable-during-operation protection against transmission of excessive dynamic loads to remaining components of mining system and load bearing structure;
- have secure, durable joint between bucket wheel and gearbox allowing fast assembly and disassembly;
- be able to control the rotary speed of the bucket wheel to adapt it to the properties of the excavated rock;
- feature as low torque as possible (high rotary speed components of the drive, like motor and clutch);
- take into account occurrence of rapid disconnections and braking actions resulting from impacts of the bucket wheel against hard non-workable inclusions (stones);
- be of electric type (the motor of bucket wheel drive); hydraulic drive is here of low usefulness.

The load bearing structure of BWEs operating in hardly-workable grounds should:

- be shaped on the basis of 3D modelling to get desired dynamic characteristic limiting the resonance phenomenon originating mainly during excavation process;
- contain mainly welding joints, the bolted joints should be reduced to minimum. Welded joints should be subject to detailed analysis using computer technique and laboratory examinations to reduce the phenomenon of stress concentration;
- ensure that rigidity of steel structures of chassis and superstructure are especially well coincided due to the durability of ball races. Larger inclination of the structure may exist for hard excavation and transport conditions. The ball races itself should have increased diameter and should be rather of double-row design. Application of trucks instead of ball race is excluded;
- be shaped (structural nodes) in order to avoid stress concentration within welded joints,
- be used (articulated joints) in connection points of main structural units to eliminate harmful effects of bending moments at points of rigidity step change;

- be of special care, as there exist excessive dynamic loads of impact nature, to ensure excavator stability by appropriate distribution of the masses of load bearing structure and mechanisms, and – as mentioned above – by enlarged diameter of the ball race;
- be shaped in order to ensure low height of dumping stations (chutes) (which should be made tight) and rectilinear run of belts; the number of chutes should be as low as possible;
- be located (the centre of superstructure gravity) as low as possible;
- be additionally protected against excessive effects of dynamic loads (strains) by continuous monitoring and evaluating the state of efforts of its elements, and as far as possible, by use of a system for current modification of force parameters of the main mechanisms of excavator.

The bucket wheel intended for excavation of rocks with excessive cutting resistances and including non-mineable inclusions, should:

- have relatively large rigidity of construction, and especially its hub;
- be designed so that the maximum stresses are located on buckets, while those on the construction of the wheel itself should be considerably lower;
- have secure, durable and quick mounting/dismounting joint with the shaft,
- be adapted (bucket wheel structure) for installation of increased number of buckets (see the description of requirements for the buckets);
- be selected (the angles of bucket wheel positioning in the boom head) in order to reduce the value of bending moment from digging force (turning the wheel in horizontal plane) and to facilitate excavated material dumping from buckets to conveyor (turning the wheel in vertical plane);
- be used (a fixed or rotary chute) as a unit receiving excavated material from the bucket wheel to the conveyor;
- be rotatable (the rear wall of dumping basket);
- be sealed out (all points of excavated material dumping);
- be protected (chute and other surfaces taking part in transporting the excavated material) against especially fast wear (mainly due to abrasion, and – to less degree – to impact wear).

As a part of the carried out tasks a theoretical analysis of dynamic load of a bucket wheel, which is the result of a bucket collision with an unmineable inclusion (boulders), was performed. The analysis was based on the theory of collision of hard bodies. Different models of collision impulse were analysed and a scheme (timeframe) of the impulse load model was proposed for testing.

At a work face of a bucket wheel excavator there are often rigid inclusions (boulders). When a bucket meets such obstacle there appears an additional dynamic load of the bucket wheel, and thus of the load-carrying structure of the machine. The size of the load to some extent depends on the size of the inclusion and a way it is seated in the excavated rocks. This may be a reason for a temporary change of the bucket wheel rotation speed, or even its complete halt. In this case, the speed change is gradual. However, if the inclusion is very large and firmly embedded in excavated material, what often occurs, the bucket wheel immediately stops and the load has an impulse character similar to constraint-based collision of a body. Then, the bucket wheel load is maximum and it should be taken into account in assessing the strength of the excavator's load-carrying structure. Thus, the studied simulation model of load should correspond to the constraint-based collision of the bucket wheel. In the impact theory it is often assumed that the halt and thereby the force of the collision do not occur in an infinitely short time but in a finite time increment which is very small in relation to the duration of studied the phenomenon. Thus, the collision force should be in this case a finite value. In simulation tests of the impact phenomenon a way of modelling of impulse load plays a key role. It should be possible to accurately reproduce the nature of the phenomenon, which is the interaction taking place between the colliding objects - a bucket of a bucket wheel excavator and a rigid inclusion. On the other hand, this model should be as simple as possible, engaging only the essential features of the modelled phenomenon, omitting the ones which play a secondary role in the analysed period of time.

The actual load during the stop of the bucket wheel to a large extent depends on the participation of elastic and plastic deformations of the mined material and the mining unit.

- In purely elastic deformation a loading force of the bucket increases up to a complete stop of the bucket wheel. Energy accumulated in the elastic deformation causes a return rotation of the bucket wheel and the bucket loading force decreases down to zero.
- In purely plastic deformation, the load after reaching a maximum value, which may take place at a decreasing rotation speed of the wheel, decreases until a complete stop of the movement.

Generally, a collision of a bucket with a rigid obstacle is never purely elastic or purely plastic phenomenon. Usually, when an obstacle is firmly embedded in excavated material it is close to

elastic collision with partial loss of kinetic energy which is used to produce surface waves. However, a collision similar to the plastic phenomenon can also occur when the inclusion is embedded in the plastic medium, and some components of the excavator are destroyed as an effect of the collision. Then, even a large part of the kinetic energy can be lost for the plastic deformation of the medium, caused by a move of embedded obstacle in the medium or the work done to break bucket wheel tooth, tear a bucket apart, damage bucket wheel shaft or other parts of the machine.

Theoretical considerations on the collision of elastic-plastic bodies and collision tests carried out for a number of metals and alloys indicate that the overall theoretical course of the contact force during collision, when it has only one extreme, can be schematically presented as in Figure 1. There are two phases in this model. The first one, when the contact force increases reaching a maximum (line-curve $P_1(t)$) and the second phase, when the contact force due to the stop of the drive is reduced to zero (line-curve - $P_{II}(t)$).

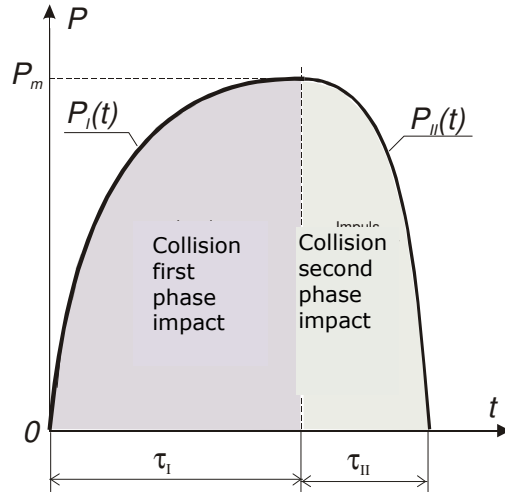


Figure 1 Theoretical scheme of the impact impulse

- P_m – Maximum value of contact force
- τ – Duration of impact (τ_I – the first phase of impact, τ_{II} – the second phase of impact).

The simplest way to illustrate the impulse load is a triangular model in Figure 2. In this model, the force of the impulse load increases in time according to the inclination of the side of the triangle, up to a value resulting from the kinetic energy of the rotating elements of the drive (P_g). The disadvantage of this model is that the contact force increase during the impact is constant, which is contrary to theoretical considerations.

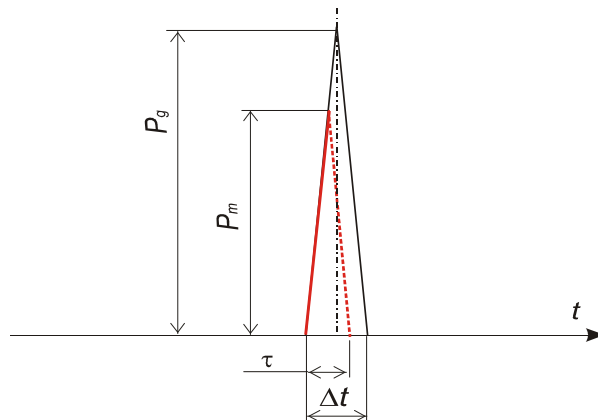


Figure 2. Triangular model of impulse load

where:

- P_m – Maximum value of contact force
- P_g – Limit value of contact force
- τ – Duration of impact
- Δt – Time

In the proposed model (Figure 3) the rate of load increase in time depends on the rotation speed of the bucket wheel, which during the first phase of the collision decreases from the nominal value to zero. The moment of immobilizing the wheel, resulting from the simulation, marks the end of the first phase of the collision, when the entire impulse energy is used for elastic and plastic deformations. In the second phase of the collision, when all the energy of the bucket wheel drive has already been given away, the value of contact force decreases. For this phase the model was simplified to linear reduction of force from the maximum value to zero.

In the proposed model the dependence of the impulse in the first phase of the collision is described by the function $P_I(t)$, and in the second phase of the collision – by the function $P_{II}(t)$.

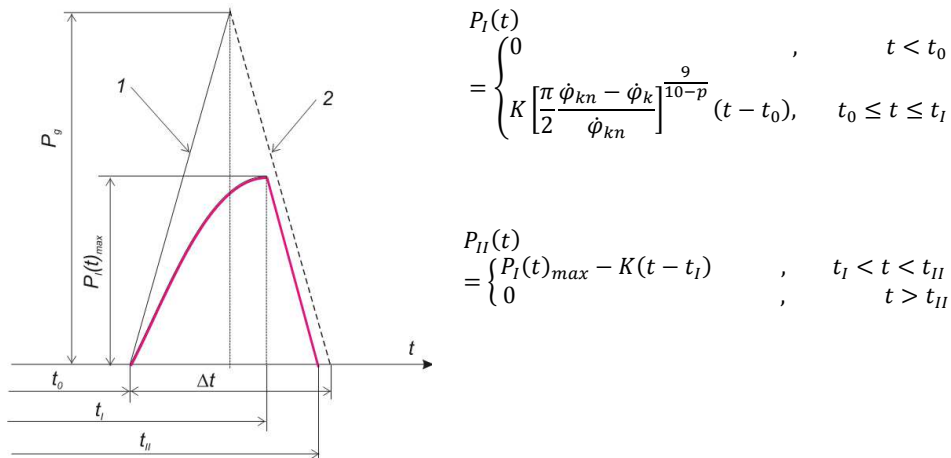


Figure 3. Proposed model of impulse force

WP 1.1 Major achievements:

- creating a database of existing, applicable solutions for subassemblies of BWE working in difficult mining conditions;
- development of simulation model of impulse load generated during the impact of the bucket with unmineable structure.

2.2.1.2 WP 1-2 Method of definition of substitute calculation force of impact load for static calculations of strengths of bucket wheel excavator load carrying structure

In order to obtain the aim of WP1 it was necessary to determine, on the basis of real excavators, values of maximal stresses in load carrying structure resulting from impulse loads during exploitation of structures with unmineable inclusions. Below the main values chosen to be monitored within the project are presented.

Load carrying structure of BWE is the boom, from structural point of view a truss (frame) pinned on the swivelling turret ensemble of the upper structure, and supported additionally by a set of ropes which are powered by a drum to realize the lowering/rising movement of the boom.

This is submitted to the resultant force at the shaft of the bucket wheel and a local reaction torque from the main gear which is fixed generally on a cantilever support in the lateral side of the front end of the boom.

Due to the randomly variable character of cutting, inertial and other dynamic character of the forces developed by the teeth, buckets and entire bucket wheel, it is subject of oscillations and vibrations, their cyclical character producing eventually overload on the members (beams) of the lattice structure and also in long term fatigue of the component material.

For this reason, the dynamic forces with a high degree of uncertainty in their crisp assessment are replaced by equivalent static forces in design stage.

For estimation of the remaining stress reserve at a certain amount of operating hours and under the action of different external – i.e. corrosion and weathering – causes, the values must be affected by additional safety factors.

Impulse of bucket impact in unmineable obstacle

The maximum value of the impact impulse occurs when the bucket that hits a not workable obstacle (stone) and the rotating components of the mining mechanism associated with its movement completely stop. The bucket wheel rotates at an angular speed ω_0 before the impact. The kinetic energy of this movement is related to the motion of the rotating masses of the bucket wheel drive and their (reduced to the axis of the bucket wheel) moment of inertia J . The motion of the bucket is stopped at the moment of impact and all kinetic energy of the drive system is replaced by the elastic strain of the bucket wheel boom.

In order to determine the kinetic energy, which the impact impulse gives to the end of the bucket wheel boom, the equation of momentum on the bucket before and during the collision has been used.

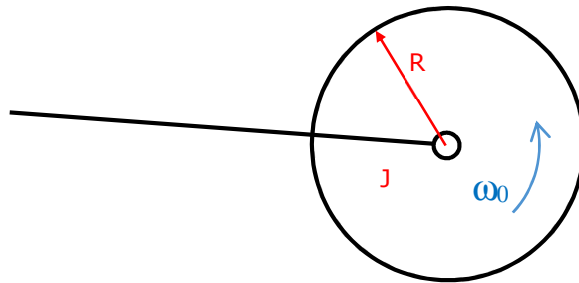


Figure 4 Bucket wheel and boom before hitting in the unmineable obstacle

Before impact (Figure 4) the moment of momentum is as follows:

$$L_0 = J \cdot \omega_0$$

Where J is the mass moment of rotating elements inertia reduced to the axis of bucket wheel.

L_0 can be also expressed as:

$$L_0 = R \cdot p_0$$

where: R is the bucket wheel radius, p_0 digging system momentum.

The digging system momentum on the bucket is equal to:

$$p_0 = \frac{J \cdot \omega_0}{R}$$

The momentum of the mining mechanism at the moment of collision (Figure 5) is the sum of the momentum p_1 of the bucket wheel boom movement with the drive, associated with the boom deflection and the momentum p_2 resulting from the rotary movement of the drive.

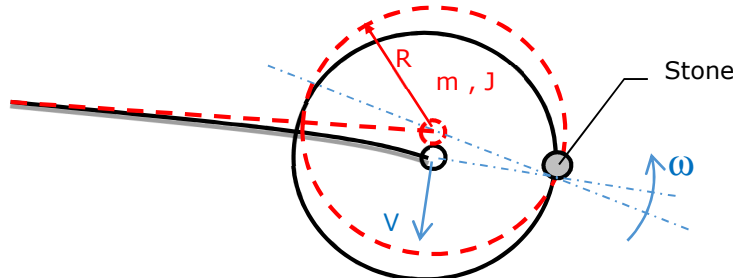


Figure 5 Bucket wheel and boom during impact in the unmineable obstacle

The motion momentum of bucket wheel head p_1 with the superstructure rotation mechanism is:

$$p_1 = m \cdot v$$

Moment of momentum L_2 of digging mechanism due to deflection of bucket wheel boom during the impact is:

$$L_2 = J \cdot \omega$$

Hence the momentum p_2 of bucket wheel on the bucket is equal to:

$$p_2 = \frac{J \cdot \omega}{R}$$

Since the total momentum of the system before and after the collision must be equal:

$$p_0 = p_1 + p_2$$

After substitution:

$$\begin{aligned}\frac{J \cdot \omega_0}{R} &= m \cdot v + \frac{J \cdot \omega}{R} \\ v &= \omega \cdot R \text{ and } v_0 = \omega_0 \cdot R \\ \frac{J \cdot \omega_0}{R^2} &= \frac{J \cdot v_0}{R^2} = m \cdot v + \frac{J \cdot v}{R^2} = m \cdot v \cdot \left(1 + \frac{J}{m \cdot R^2}\right) = m \cdot v \cdot \left(\frac{m \cdot R^2 + J}{m \cdot R^2}\right) \\ \frac{J \cdot v_0}{R^2} &= m \cdot v \cdot \left(\frac{m \cdot R^2 + J}{m \cdot R^2}\right) \\ \frac{m \cdot J \cdot v_0}{m \cdot R^2 + J} &= m \cdot v = p \quad (= p_1)\end{aligned}$$

Where p (equal to p_1) is the momentum of the head of bucket wheel boom which results from the impulse of hitting a bucket wheel into a non-mineable obstacle.

From the determined equation of the momentum of the bucket wheel, results that its speed at the moment of impact on a stone is:

$$v = \frac{J \cdot v_0}{m \cdot R^2 + J}$$

For this speed, the kinetic energy of the mining boom at the moment of impact is equal to:

$$E_k = \frac{m \cdot v^2}{2} = \frac{m}{2} \cdot \left(\frac{J \cdot v_0}{m \cdot R^2 + J}\right)^2$$

This kinetic energy is transformed to a large extent into the energy of the elastic deformation of the bucket wheel boom. It can be assumed that, at the moment of maximum deformation, the kinetic energy was transformed entirely into energy (potential energy of elasticity) of deformation.

$$E_k = E_p = \frac{1}{2} \cdot k \cdot f^2$$

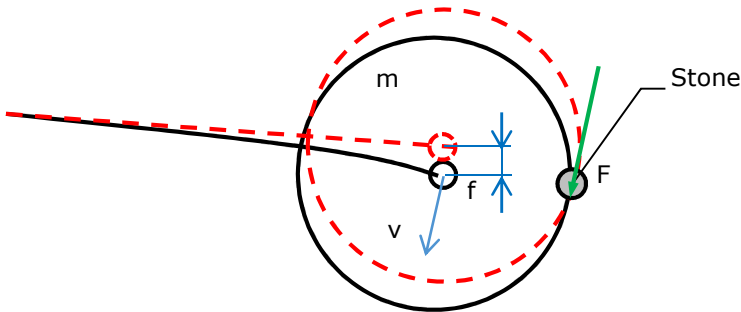


Figure 6 Deflection of the bucket wheel boom after impact

It can be assumed that the force F applied at the point of the impulse operation will cause the boom deflection f in proportion to the coefficient of elasticity k .

$$F = k \cdot f$$

Then

$$\frac{m}{2} \cdot \left(\frac{J \cdot v_0}{m \cdot R^2 + J}\right)^2 = E_k = E_p = \frac{1}{2} \cdot \frac{F^2}{k}$$

After transformation, the value of the impact impulse force is:

$$F = \frac{J \cdot v_0}{m \cdot R^2 + J} \cdot \sqrt{m \cdot k}$$

This is theoretically the maximum value of forces acting on the bucket wheel in contact with the ground. In practice, the value of the impact force with an unmineable obstacle is lower. This is because the model adopts a rigid embedding of an unmineable obstacle in the ground. In fact, when the bucket hits an unmineable obstacle, there are local deformations of the ground, which causes partial dissipation of energy in the ground. Secondly, in the drives of the bucket wheel, safeguards are used, which task is the reduction of the impact force. In spite of this, the maximum value of the impulse force may be the basis for calculating the strength of the load-bearing structure as an extreme load, because the used protection cuts only part of the drive energy and

with delay. Furthermore, the unmineable fractions may be so rigidly embedded that practically the energy dissipation in the ground will be negligibly small.

Derived dependence to calculate the impact force requires the determination of several parameters. These are the radius of the bucket wheel R , the peripheral speed of the bucket wheel v_0 and the mass of the drive (head) with the weight of the bucket wheel m . These parameters can be taken from the design of the bucket wheel drive and components used for this drive. For the SchRs4000 excavator (K45) the radius of the bucket wheel $R = 8.543\text{m}$, the weight of the mining drive head together with the moment lever is $m = 264738\text{kg}$ and the peripheral speed of the bucket wheel $v_0 = 2.577\text{m / s}$.

It is more difficult to obtain stiffness of the bucket wheel boom k and the value of the moment of inertia of rotating masses of the digging mechanism reduced to the axis of the bucket wheel J .

One of the methods of experimental determination of the value of the bucket wheel coefficient of elasticity is the measurement of the boom deflection under the influence of force of a known value, which loads the bucket wheel. It is possible experimentally for an already built machine. For designed machines, this value should be calculated, for example, by using MES.

The elasticity coefficient k can be determined by direct measurement of deflection (f) of the bucket wheel boom under the influence of vertical force (F) from the known weight (see Figure 7). The deflection (f) is in this case the difference (Δy) between the distance (y_0) between the unloaded bucket wheel boom and the ground and the distance (y) between the boom and the ground after loading the boom with force (F).

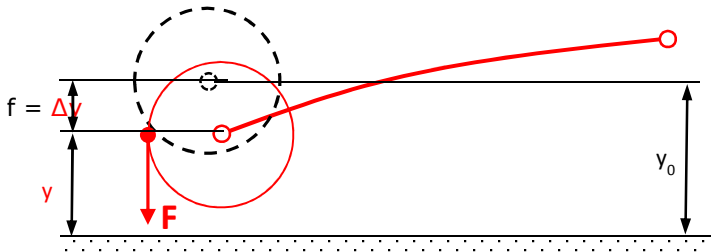


Figure 7 Diagram of boom deflection under the influence of vertical force

The elasticity coefficient can be also determined by indirect method. It consists in measuring the angles of inclination of tangents to the boom deflection line under the influence of the force (F) of the bucket wheel attachment (see Figure 8). The tangent values of the measured angles are the values of the derivative of the deflection line of the bucket wheel boom at the measuring points. After integrating the derivative thus obtained, a boom deflection line can be found. Knowing the deflection line of the bucket wheel boom, the value of the deflection (f) can be determined. In this case, the force (F) can be invoked as in the first method or by means of the rope system by force (S)

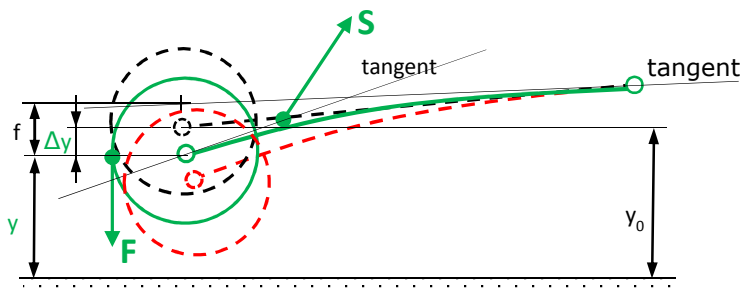


Figure 8 Diagram of deflection of the attached bucket wheel boom with winch force

Due to simpler technical implementation and greater safety, the second method has been selected to measure the deflection of the bucket wheel boom.

To measure the angle of inclination of the bucket wheel boom structure elements, acceleration sensors were selected.

All measuring sensors were located on the upper surface on the lower flange of the bucket wheel boom structure, at distances from the vertical movement axis of the boom, as shown in Figure 9 below.

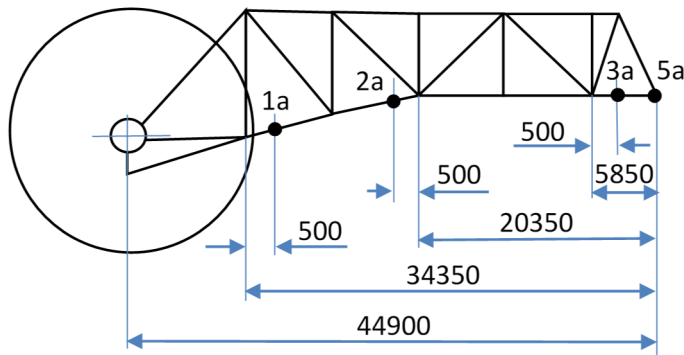


Figure 9 Diagram of distribution of measuring points

A load (bulldozer) was attached to the bucket via a U2A 20t force gauge, using sets of ropes (Figure 10).



Figure 10 Attachment of the auxiliary machine to the bucket

Using the winch of the excavator's bucket wheel boom rope system, the tension in the rope was induced. The force gauge readings for the measurement of the rope tension and the values of the acceleration sensor readings for the measurement of the boom deflection angles were read after stabilization of the load. Then, the loads were released by lowering the bucket wheel boom. After loosening the ropes connecting the bulldozer with the bucket, the readings of the measuring sensors were read again. This operation was repeated 3 times.

During these operations, the readings of the acceleration sensors and dynamometer were recorded. The acceleration values were converted into the value of the structure angle of inclination at the measuring points. On the basis of the difference between the values of the inclination angles with the load and without the load, increments of the inclination angles and their values in relation to the boom rotation axis were calculated. For the increments obtained, the corresponding tangent values were determined, which are values of the derivatives of the deflection line at a given measurement point. On the basis of the tangent values obtained in the measurement points, the derivative of the deflection line of the bucket wheel boom was approximated by a linear function.

Obtained results of deflection at selected points, for given loads ($j = 1, 2, 3$) are presented in Table 1 where the X coordinate indicates the distance between the point and the rotation axis of the

bucket wheel boom, the Y coordinate is the derivative value (tangent of the tangent) of the deflection line of the bucket wheel boom.

Table 1 Experimental values of boom deflections of the K45 bucket wheel excavator

j	i	1	2	3	F _j	K _j
	X _i [mm]	44900	33350	20850	kN	kN/mm
1	Y _{i,j} [mm]	58	33	12	203	3.500
2		68	39	15	210	3.088
3		83	47	18	243	2.928

The finite element method (FEM) is based on the creation of a discrete model based on the geometry of the boom structure, determination of boundary conditions by enforcing forces and determination of restraints, automatic generation of the discrete finite element model stiffness matrix, which allows determination of displacements of all finite element nodes and approximation of the bucket wheel axis displacement.

The numerical model used to determine the bucket wheel boom deflection mapped all the structural elements of the body assembly, i.e.: the bucket wheel boom, the counterweight boom, the fixed mast, the movable mast, the middle part and the platform of the body. All these elements were modelled with two-dimensional coating elements, which ensured a very accurate reproduction of stiffness of each of them. The shroud cables were modelled with beam elements with stiffness corresponding to the ropes mounted on the facility. The rope system rigging is designed to maintain the position of the mining boom required by the operator (hence, its flexibility is compensated by the winch) and therefore, it has been mapped with rigid elements, while maintaining full kinematics. The whole body was supported by flexible elements that represented the stiffness of the chassis assembly. The model was supplemented with mass elements representing the installed elements of the machine/electrical sections (e.g. gear, switchgear, etc.). The whole model was consistent with the location of the mass centres (individual elements and the entire body) in accordance with the proof of stability.

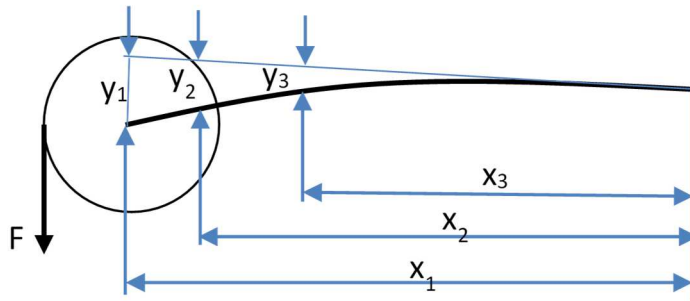


Figure 11 Diagram of boom deflection under the load (F)

For the theoretical values of the K45 excavator bucket wheel boom deflection for selected coordinates, counting from the bucket wheel boom vertical movement axis and for selected loads with vertical force (F) (see Figure 11), applied vertically to the edge of the bucket blade, obtained by the finite element method, see Table 2 below.

Table 2 Theoretical values of the SchRs4000 excavator bucket wheel boom deflections; (Bucket wheel boom vertical deflection under specific force)

j	i	1	2	3	F _j	K _j
	X _i [mm]	44900	33350	20850	kN	kN/mm
1	Y _j [mm]	61	45	27	200	3.279
2		76	56	34	250	3.289

On the basis of the experimental and theoretical values obtained for the deflection of the bucket wheel boom of the SchRS400 excavator (K45), the stiffness of the bucket wheel boom was assumed as **k = 3.28 kN / m**.

For calculating of the reduced moment of inertia of the bucket wheel drive it is necessary to build geometric model.

The mining mechanism of the SchRs4000 excavator (K45) is quite complicated and consists of many elements interacting with each other (Figure 12).

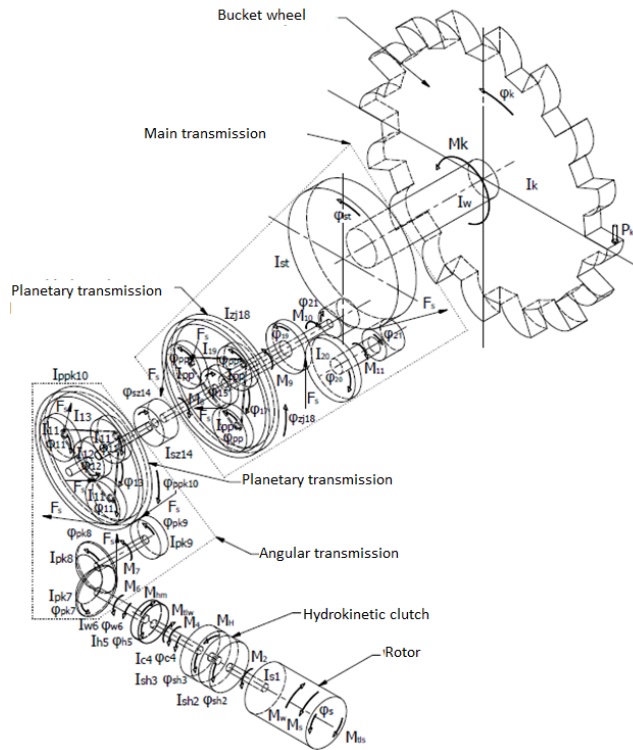


Figure 12 Model of the bucket wheel drive

It is a 3-drive unit. Each of the drives consists of an asynchronous motor with a power of 735kW and a rotational speed $n_0 = 987\text{rpm}$. The drive from the engine is transmitted through a hydrokinetic clutch, a fixed and articulated drive shaft, which ends with the brake drum of the drive and it is connected to the input shaft of the angle gear. This is a preliminary transmission.

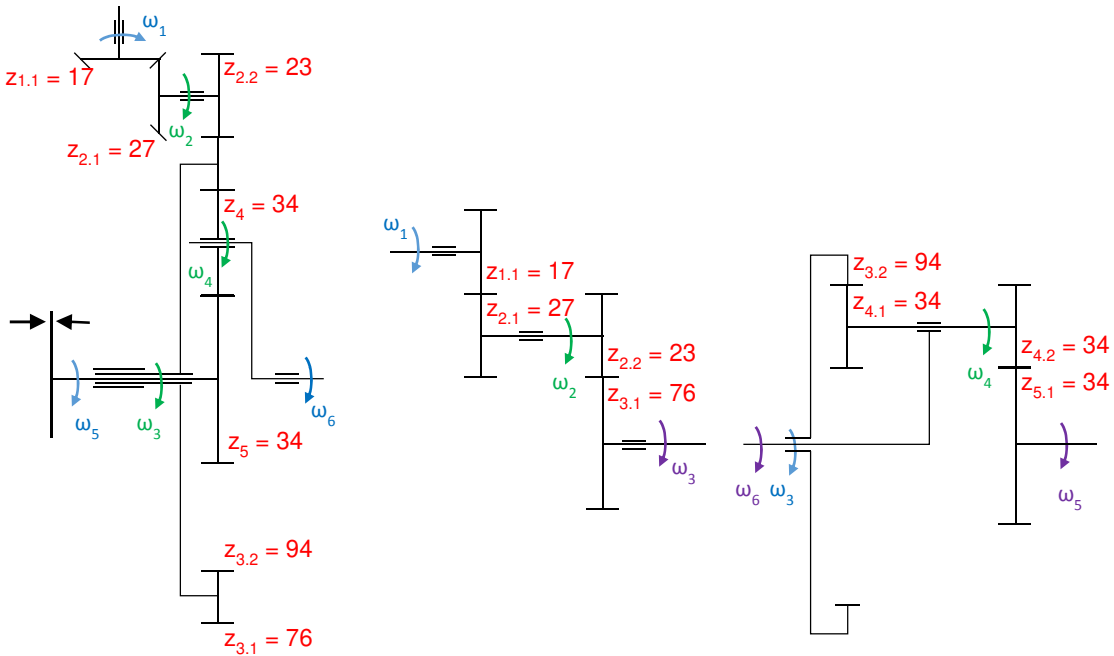


Figure 13 Kinematic scheme of the angular gearbox with equivalent scheme

The angular gearbox is equipped with a planetary stage (Figure 13). This stage acts as an overload clutch. A brake disc is installed on the central gear shaft. Opening of the brake results in switching

off the power transmission to the next stages of the bucket wheel drive. The output shaft of the angular gearbox transmits the drive through the toothed coupling to the main transmission.

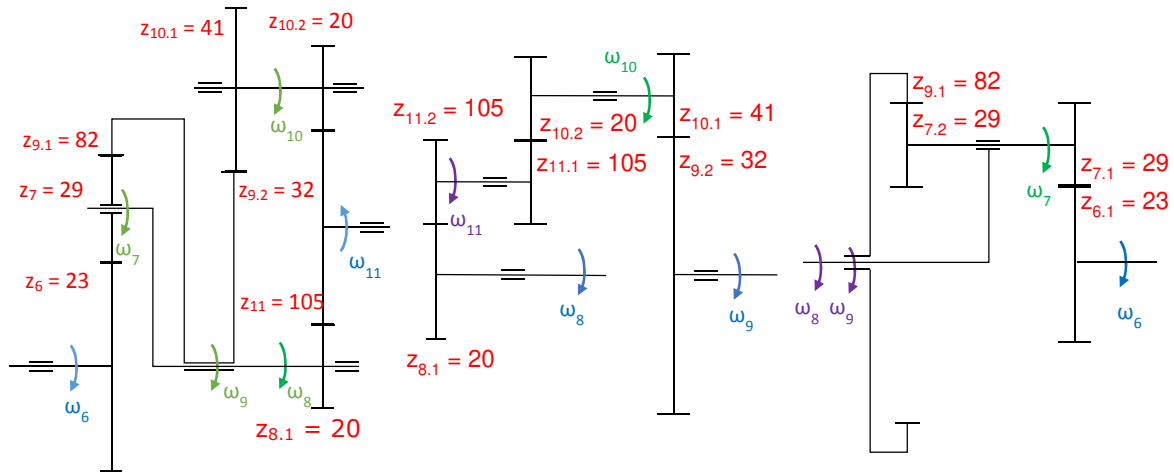


Figure 14 Kinematic scheme of main gearbox with equivalent diagram

The main transmission is a planetary gearbox (Figure 14). It has 3 drive inputs. Each of the inputs is connected with a separate planetary stage. Each of these stages in a 2-way manner, through the yoke shaft and the toothed ring shaft transmits the drive to the main wheel. This gear is mounted on the main shaft of the bucket wheel.

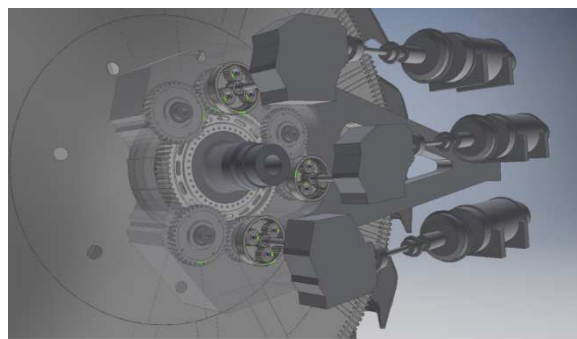


Figure 15 Geometrical model of the bucket wheel drive

Based on the assembly drawings, the drive geometric model was built. This model (Figure 15) allowed to determine mass values and axial moments of inertia of individual drive elements. Proceeding in sequence from the drive motor to the bucket wheel shaft, the reduced moments of inertia of the drive at the end of individual stages were calculated. This includes the efficiency of bearings and the meshing of individual gears. The results of calculations are presented in Tables 3 to 7, where:

- n_0 : input rotational speed,
- n_1 : output rotational speed,
- J_0 : moment of inertia of the previous stage,
- J moment of inertia of the stage,
- J_1 : moment of inertia reduced at the output,
- i : transmission ratio,
- η_1 : efficiency of bearings,
- η_2 : meshing efficiency,
- $\text{oš}_0/\text{oš}_1$: input shaft/output shaft ratio.

Table 3 Reduction of moments of inertia - Drive shaft

No	Element	n_0	J_0	$\frac{o\acute{s}_0}{o\acute{s}_1}$	i	J	η_f	η_z	n_1	J_1
		rpm	kg/m^2			kg/m^2			rpm	kg/m^2
1.1	Motor	987	0	1/1	47.00	0.99	1	987	46.53	47.00
1.2	Hydrokinetic clutch - input	987	46.53	1/1	29.02	0.99	1	987	47.80	29.02
1.3	Hydrokinetic clutch - output	987	74.80	1/1	10.20	0.99	1	987	84.15	10.20
1.4	Drive shaft	987	84.15	1/1	0.47	0.99	1	987	83.78	0.47
1.5	Articulated drive shaft	987	83.78	1/1	0.98	0.99	1	987	83.91	0.98
1.6	Brakes	987	83.91	1/1	2.20	1	1	987	86.11	2.20

Table 4 Reduction of moments of inertia - angular gearbox

No	Element	n_0	J_0	$\frac{o\acute{s}_0}{o\acute{s}_1}$	i	J	η_f	η_z	n_1	J_1
		rpm	kg/m^2			kg/m^2			rpm	kg/m^2
2.1	Shaft with cone wheel	987	86.11	1/1	1	1.22	0.99	0.9 ₉	987	86.46
2.2	Intermediate conical wheel	987	86.64	1/2	0.6296	5.91	0.99	0.9 ₉	621.44	230.68
2.3	Intermediate shaft with gear	621.44	230.68	2/2	1	1.76	0.99	0.9 ₉	621.44	230.12
2.4	Planetary gear rim	621.44	230.12	2/3	0.3026	37.37	0.99	0.9 ₉	188.07	2891.49
2.5	Planet wheels	188.07	2891.49	3/4	1.4688	0.76	0.985	0.9 ₄₁	276.23	1320.71
2.6	Planetary shaft (yoke)	276.23	1320.71	4/6	0.5	15.88	0.99	1	138.11	5293.06

Table 5 Reduction of moments of inertia - Main gearbox part 1

No	Element	n_0	J_0	$\frac{o\acute{s}_0}{o\acute{s}_1}$	i	J	η_f	η_z	n_1	J_1
		rpm	kg/m^2			kg/m^2			rpm	kg/m^2
3.1	Cogged clutch	138.11	5293.06	6/6	1	9.85	0.99	1	138.11	5250.01
3.2	Input shaft with a toothed wheel	138.11	5250.01	6/6	1	0.65	1	1	138.11	5250.66
3.3	Planetary wheels	138.11	5250.66	6/7	0.596 ₈	3.89	0.97	0.971	82.42	14317.05

Table 6 Reduction of moments of inertia - Main gearbox part 2a – the moment transfer

No	Element	n_0	J_0	$\frac{o\acute{s}_0}{o\acute{s}_1}$	i	J	η_f	η_z	n_1	J_1
		rpm	$10^3 kg/m^2$			kg/m^2			rpm	$10^3 kg/m^2$
3.4a	Toothed rim	82.42	14.32	7/9	0.2351	0	0.99	0.98	19.38	256.50
3.5a	Rim shaft with a toothed wheel	19.38	256.50	9/10	0.7805	0	0.99	0.98	15.12	416.88
3.6a	Intermediate stage of the rim	15.12	416.88	10/11	0.1905	0	1	1	2.88	11490.16
3.7a	Yoke shaft	82.42	14.32	7/8	0.1835	0	0.99	1	15.12	421.08
3.8a	Yoke's toothed wheel	15.12	421.08	8/11	0.1905	0	1	0.99	2.88	11605.93

Table 7 Reduction of moments of inertia - Main gearbox part 2b – inertia

No.	Element	n_0	J_0	$\frac{o_{\text{so}}}{o_s}$	i	J	η_f	η_z	n_1	J_1
		rpm	10^3kg/m^2			kg/m^2			rpm	10^3kg/m^2
3.4b	Toothed rim	82.42	0	7/9	0.2351	177.43	0.99	0.98	19.38	3.18
3.5b	Rim shaft with a toothed wheel	19.38	3.18	9/10	0.7805	285.52	0.99	0.98	15.12	5.63
3.6b	Intermediate stage of the rim	15.12	5.63	10/11	0.1905	0	1	1	2.88	155.18
3.7b	Yoke shaft	82.42	0	7/8	0.1835	92.37	0.99	1	15.12	2.72
3.8b	Yoke's toothed wheel	15.12	2.72	8/11	0.1905	92.37	1	0.99	2.88	77.43

The value of the reduced moment of inertia of the considered part of the drive due to the power flow in two ways (first way - through shaft 8, second way through shaft 9 – Figure 14) in the final stage of the main transmission was calculated according to the following dependence:

$$\frac{1}{3} I_{11a} = \frac{I_{3.6a} I_{3.8a}}{I_{3.3}} \left(\frac{n_{11}}{n_7} \right)^2 + (I_{3.6b} + I_{3.8b}) = 11603.2 \cdot 10^3 \text{kgm}^2$$

Taking into account 3 such drives $I_{11a} = 34809.6 \cdot 10^3 \text{kgm}^2$, the axis of the bucket wheel with the main gear rack and the bucket wheel with buckets $I_{11b} = 6386.96 \cdot 10^3 \text{kgm}^2$ reduced to the bucket wheel axis, the moment of inertia of the bucket wheel drive is $I_{11}=41196.56 \cdot 10^3 \text{kgm}^2$

Using the previously derived dependence on the value of the impact pulse of the bucket wheel into an unmineable obstacle:

$$F = \frac{J \cdot v_0}{m \cdot R^2 + J} \cdot \sqrt{m \cdot k}$$

and the mining drive parameters:

- bucket wheel radius $R=8.543 \text{m}$,
- weight of the mining drive $m=264738 \text{kg}$,
- peripheral speed of the bucket wheel $v_0=2.577 \text{m/s}$,
- stiffness of the bucket wheel boom $k=3.28 \text{kN/m}$,
- reduced moment of inertia of the drive $J = 41196560 \text{kgm}^2$,

the value of the maximum impact of the bucket wheel in unmineable obstacle, for the SchRs4000 excavator (K45), is $F_u = 1635 \text{kN}$. For this machine, the nominal value of the mining force is **$F_n = 700 \text{kN}$. The calculated value is 2.3 times higher than the nominal value.**

More results of works connected with WP 1-2 are shown in Deliverable D.1.2

WP 1.2 Major achievements:

- estimation of normal stresses value in selected places originating from natural load;
- determination of the values for variable digging forces: deformations, normal forces (axial), normal stresses;
- determination of natural frequency of K45 BWE superstructure.

2.2.1.3 WP 1-3 Research on real objects and analysis of dislocation of stress waves in excavator's bearing structure caused by impulse load of bucket wheel

The adopted research concept was based on the association of analytical method of kinematic descriptions and dynamic relations in the excavator-bucket-rock medium system and experimental methods of identification of resistance to mining and loads in the supporting structure. Hence, the research in this WP was divided into a theoretical part, the aim of which was to develop a mathematical model of extreme loads in the process of cutting tough workable soils with heavy-duty machines, and an experimental part, the aim of which was to verify the mathematical model using the measurements of real structures.

As a result of theoretical research, a mathematical model of the process of mining tough workable soils with heavy-duty working machines, in this case – bucket-wheel excavators for strip mining, has been developed

This model, unlike the current deterministic model, has been developed on the basis of the analysis of the process of cutting tough workable soils with tools of complex and continuous motion and the actual values and curves of extreme loads occurring during the operation of wheel excavators. It was created as a result of combination of statistical model of mining forces affecting the excavator's supporting structure with the hypothesis of unitary mining resistance. Therefore, the value of the mining force tangential component (F_{si}) on the bucket wheel was defined as follows:

$$F_{si}(\varphi, t) = p[k_A(\Omega)] \cdot A(\varphi, t) = \begin{cases} \frac{4\pi \cdot Q_t \sin \varphi}{(1 - \cos \varphi_u) \cdot z \cdot \omega_k \cdot D} \cdot p[k_A(\Omega)] & \text{for } 0 < \varphi \leq \varphi_u \\ 0 & \text{for } \varphi > \varphi_u \end{cases}$$

Such a combination allows the use of existing long-term experimental data from mining homogeneous soils with measurement data that prove the stochasticity of the process of mining heterogeneous soils. The basic novelty in relation to the current deterministic model, is the replacement of the constant unitary resistance k_A with experimentally determined statistical distribution $k_A(\Omega)$, where Ω is dimensional space of the process of mechanical mining of cohesive media with wheel excavators, defined in the project. In order to use the existing knowledge base, it was assumed that the expected value of the above distribution for homogeneous soils was exactly k_A . If the distribution is symmetrical, then the quantile order $p\{E[p\{E[k_A(\Omega)]\}]$ is equal to 0.5.

For the verification of the mathematical model developed, long-term tests of the mining resistance and loads (stresses) in the supporting structure of wheel excavators were carried out. Due to the specificity of mining plant operations, these tests were carried out during the normal operation of these machines. Since it was impossible to select the soil during the tests, it was decided to perform a so called passive experiment, by conducting tests on many excavators, working on different working levels of open pits, containing various types of soil. The tests were carried out on bucket-wheel excavators used in domestic brown coal mines. These excavators usually worked on the overburden in tough and very tough workable formations, with workability classes III – IV containing a large number of hard stony inclusions and quartz fractions with high friction properties. The tests were carried out for 1 year, which approximately gave approx. 4 months of continuous measurements.

Soil samples were taken for analysis before and during the tests, in order to determine the soil properties. The soil consisted mainly of various types of boulder clays, namely: sandy loams, grey and dark grey, light grey firm loams, light grey/rust-brown, yellow/rust-brown loams and clays: silty, grey and sandy. Boulder clays were characterised by the following average parameters: bulk density $\gamma = 19 - 22.7$ [kN/m³], natural humidity $W = 8.5-13.6$ %, while clays: bulk density $\gamma = 15.3 - 21.6$ [kN/m³], natural humidity $W = 14.2-39.8$ %.

As stated above, the tests were carried out in various soils also easily workable and medium workable (workability classes I and II), although excavators were selected to do this in such a way that most of the tests were performed in tough workable soils. In the case of easily workable and medium workable soils, these were mainly different types of sands: fine, medium and loamy sands, gravel with sand and all-ups. They were characterised by a bulk density $\gamma = 15.1-19$ [kN/m³], and natural humidity $W = 3-24$ %

Direct measurement of unitary mining resistances is not possible. Therefore, the indirect method was used to determine them, consisting in the measurement of the power N consumed by the bucket wheel drive and the cross-sectional area of the cut lump A and then, calculation of the value of $k_A(\Omega)$ basing on these values. In practice, it is difficult to measure the cross-section area of the lump being mined, hence it is performed indirectly by measuring the excavator manoeuvring movements.

As a result of experimental tests:

- the developed mathematical model was verified. The verification consisted in comparing the curves for the mining force tangential component, obtained as a result of stress measurements of the bucket wheel boom frame with the curves for this component, obtained as a result of measurements of the bucket wheel drive motor power output, carried out during mining resistance tests. As a result of the comparisons made, it was found that these distributions showed a consistent course of variation, which indicated that the proposed mathematical model was formulated correctly;
- a large set of research and test results was collected and archived in the form of unitary mining resistance k_A (W) histograms, characteristic for the domestic brown coal strip

mines. These histograms can be used, among others, for the design of new excavators intended to operate under specific geological and mining conditions of individual mines or strip mines;

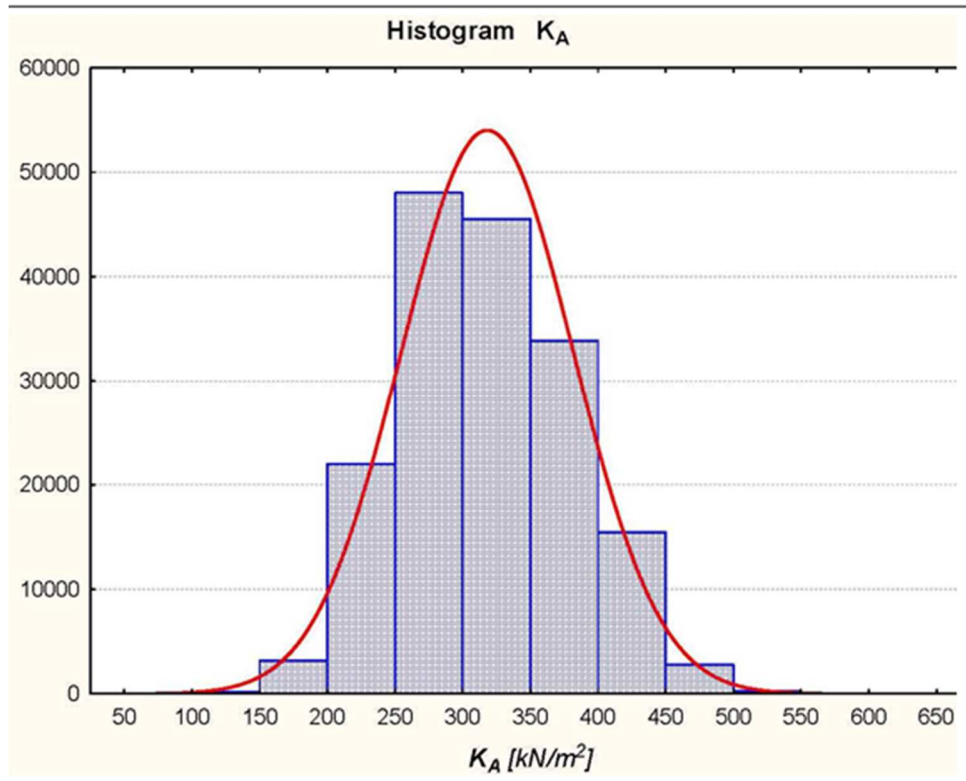


Figure 16 Histogram of the distribution of mining resistance values $kA(\Omega)$

In the excavator design process, the most important data are the data on the value of the mining force on the bucket wheel, since the supporting structure is dimensioned and the bucket wheel drive power is selected basing on this value. So far, the value of the mining force was selected basing on the deterministic model, which, as demonstrated in the project for inhomogeneous and tough workable soils, did not work. Currently, using the collected histograms, it is possible to determine the actual values of the mining force on the bucket wheel. This will enable dimensioning of the excavator's supporting structure allowing to minimise the probability of its damage, even while working in the most difficult geological and mining conditions occurring in a given mine or strip mine.

This is additionally helpful, because in the case of newly designed excavators, it is impossible to measure the actual values of mining forces on the bucket wheel before they are built. Hence, using the newly developed model it is enough to measure unitary resistance to mining on another excavator working in the same or similar geological and mining conditions, for which the newly designed excavator is intended (or use histograms accumulated as a result of the project, if they concern the same or similar operating conditions of the new excavator) and determine the values of the cross-sectional area of the lump A which result from the assumed capacity of the new excavator and thus, the volumes and dimensions of buckets, and calculate the value of the mining force component, F_{si} .

Detailed description of performed works is included in Deliverable D1-3

WP 1.3 Major achievements:

- Theoretical research:
 - determination of the dimensional space of the mechanical process of cutting cohesive media with machines of continuous operation,
 - modelling the resistance to mining cohesive media with wheel excavator working tools,
 - construction of a mathematical model of extreme loads for the process of cutting tough workable soils.
- Experimental tests:
 - development of a test programme for experimental verification of the obtained mathematical model,

- conducting a series of long-term tests of mining resistance and loads in the excavator supporting structure in the mining conditions of tough workable soils of domestic brown coal mines,
- statistical analysis of the test results and the final verification of the obtained mathematical model basing on them.

2.2.1.4 WP 1-4 Experimental verification of correctness of selection of calculation values of load factors resulting from vibrations of load carrying structure during operation in selected conditions.

In order to build a bucket wheel excavator's computational model, it is necessary to have a 3D model. If the 3D model of the machine is not available, its manufacturing takes place on the basis of available technical documentation in the form of 2D drawings, pictures of the machine and measurements made on the existing object. Geometric model intended for numerical simulations is usually a very simplified model, in which the selected components of the structure and the additional equipment found on it (does not affect the way the excavator operates), have been omitted. Components of the excavator's additional equipment, affecting the physical phenomena occurring during the movement are often replaced by concentrated mass or substituting elements that reflect the physical properties of simplified components.

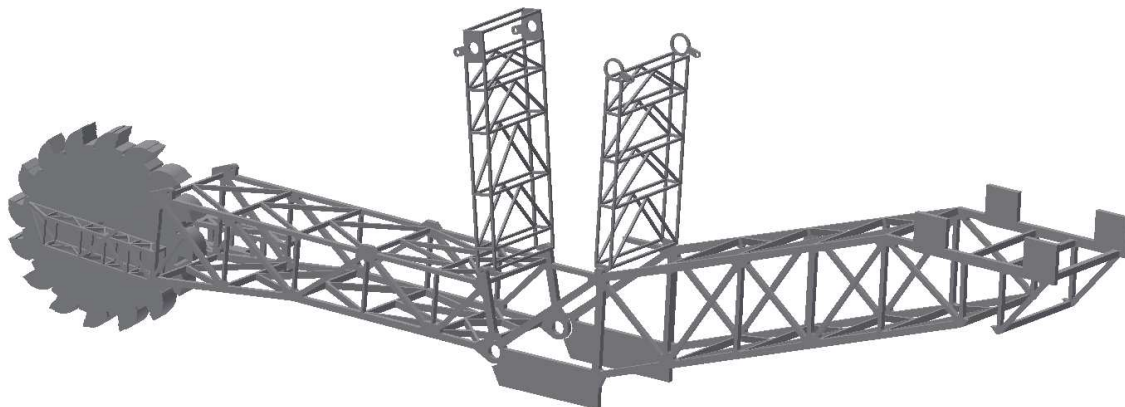


Figure 17 Geometric model of the bucket wheel excavator's body

Based on the presented geometric model, the physical model of the excavator was built by linking individual blocks with geometric constraints, elastic-damping components and elements such as ropes. In this model, individual blocks were assigned the mass and moment of inertia. The physical model of the excavator's body is devoid of equipment located on the real object. The equipment includes: electric motors, belt conveyors, operator's cabins, etc. The mass of the elements omitted in the model was taken into consideration by adding it to the mass of one of the structure solids. So, the correct mass of the complete body of the excavator was maintained. The physical model of the excavator's body is shown in Figure 18. Additionally, in this model the bucket wheel boom, the counterweight boom and both masts (fixed and mobile) was discretized, therefore in the simulations they will be treated as deformable part. The bucket wheel was assumed to be a rigid body. The model also uses elements replacing structural strands and hoist ropes of the bucket wheel boom.

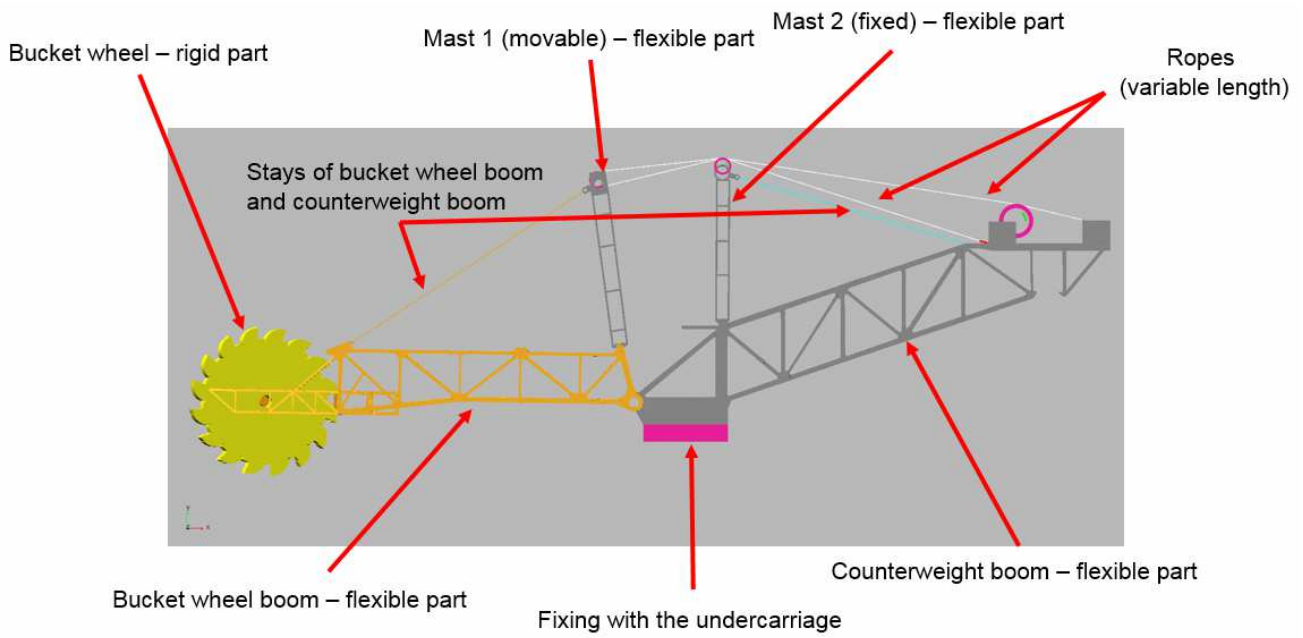


Figure 18 Physical model of the bucket wheel excavator's body

Figure 19 shows the rotational constraints used in the physical model. The use of such constraints allows to simulate rotation of the bucket wheel, as well as to lift or lower the bucket wheel boom. In addition, it is possible to rotate the entire body, which allows to simulate rotation of the excavator's body relatively to its chassis.

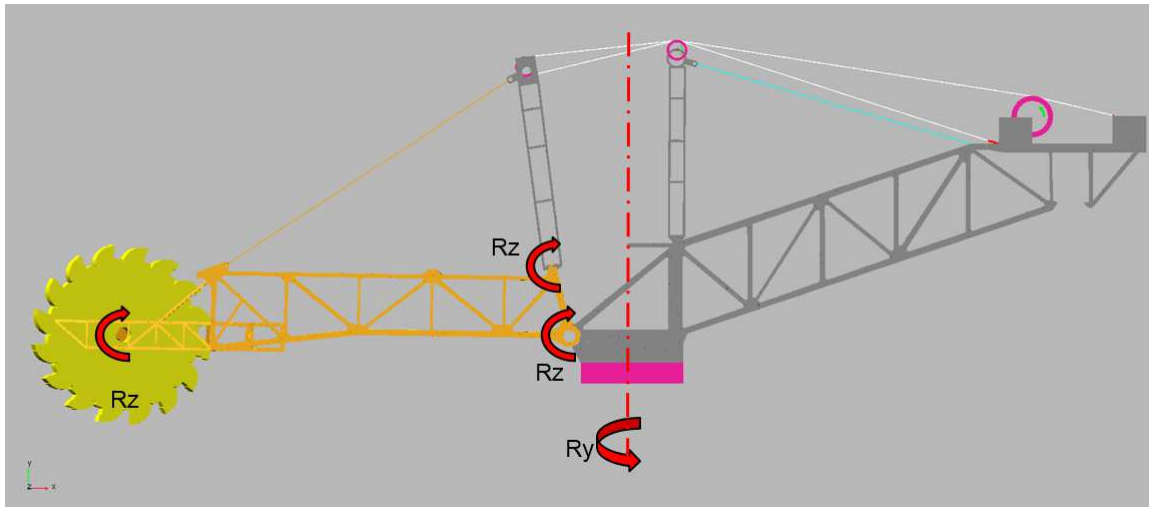


Figure 19 Physical model of the bucket wheel excavator's superstructure

The method of modelling the hoist ropes for the bucket wheel boom and the drums on which ropes are wound when lifting the boom, is shown in Figure 20. The cylinders to which the ends of boom hoisting rope are attached were modelled by means of elastic-attenuating components with properly selected characteristics.

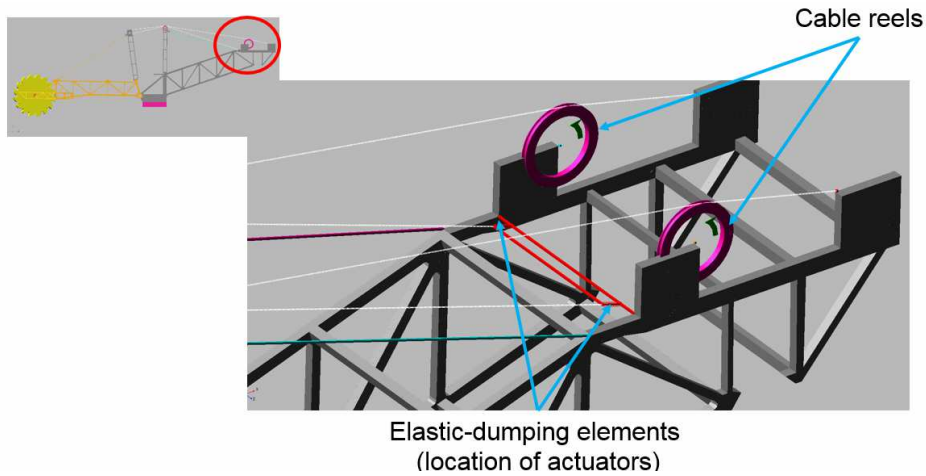


Figure 20 The method of attaching the bucket wheel hoisting ropes

Additional simulation possibilities are provided by applying the co-simulation techniques that enable integrating the different computing environments. As a result of using this technology, it is possible to model the driving motors or control algorithms, as well as the method of measuring the load to the bucket wheel using a separate software. This allows to carry out load analysis of electric motors, check the correct functioning of the developed control algorithms or change the character of the load of individual buckets during the simulation. In order to carry out simulation in the physical model of the bucket wheel excavator's body, the vectors of forces loading the bucket wheel and the torque vector, setting the bucket wheel into a rotational motion were defined.

Electric motors that drive the bucket wheel can be modelled in various ways and at various levels of simplification. The best results are achieved when modelling the engine by implementation of all characteristic features of the components delivered by a manufacturer in dedicated modules for modelling electric motors. However, if there is no access to the required data, the engine operation method can also be described in a simplified manner by means of the torque relationship generated by a given engine as a function of its rotational speed. A sample relationship of the torque value expressed in the function of the rotational speed of the bucket wheel (including reducers) is shown in Figure 21. The value determined on the basis of this relationship was the value of the torque vector driving the bucket wheel in the physical model.

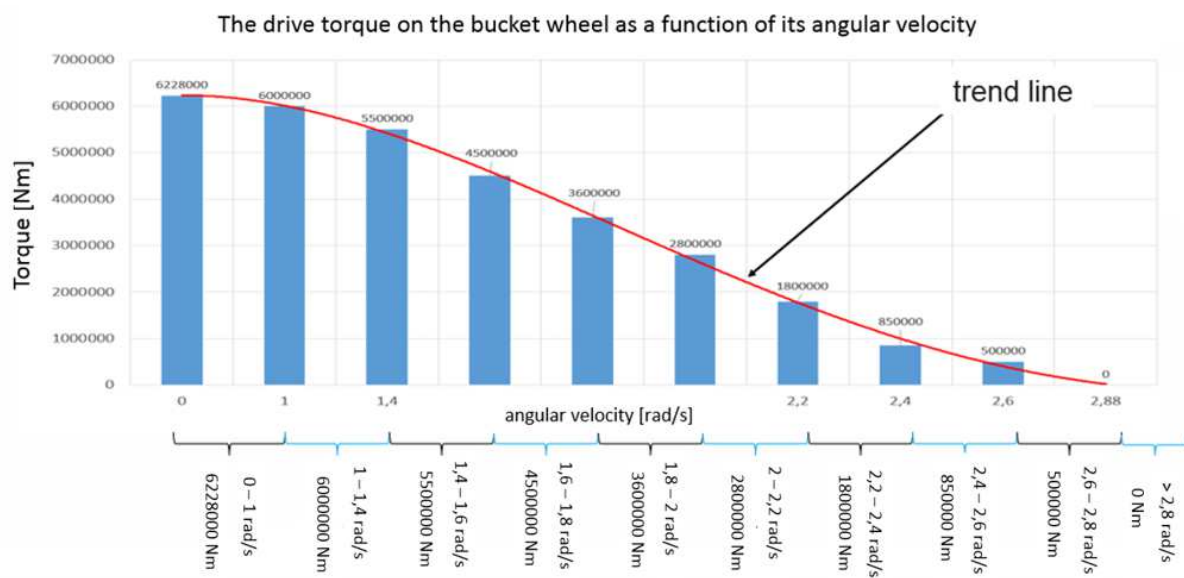


Figure 21 Value of the driving torque of the bucket wheel as a function of its rotational

The load to bucket wheel can also be modelled in various ways. One of the methods of modelling the load of the bucket wheel is to define the vector that will "brake" the bucket wheel. This moment can be calculated in accordance with the accepted mathematical correlation. However, it is also possible to define any number of vectors loading the individual wheel dumps. The vectors of these forces can have different operational directions, thus, it becomes possible to distinguish the load from the run-of-mine weight or forces from the bucket wheel cutting into the rock mass, connected with e.g.: the gravitational acceleration of the Earth, friction forces or forces resulting

from the rotation of the excavator's body in relation to the wall. Additionally, the consideration of the direction of loading forces can be related to the rotation angle of the bucket wheel.

In the presented example, the load of one fourth of the bucket wheel weight was assumed by defining a series of vectors of both vertical and horizontal forces, by means of which the external load, resulting from the process of mining and transportation of the run-of-mine was simulated. Dependences describing the ratio of vertical force to horizontal force constituting the components of the resultant loading force of the bucket is shown in Figure 22.

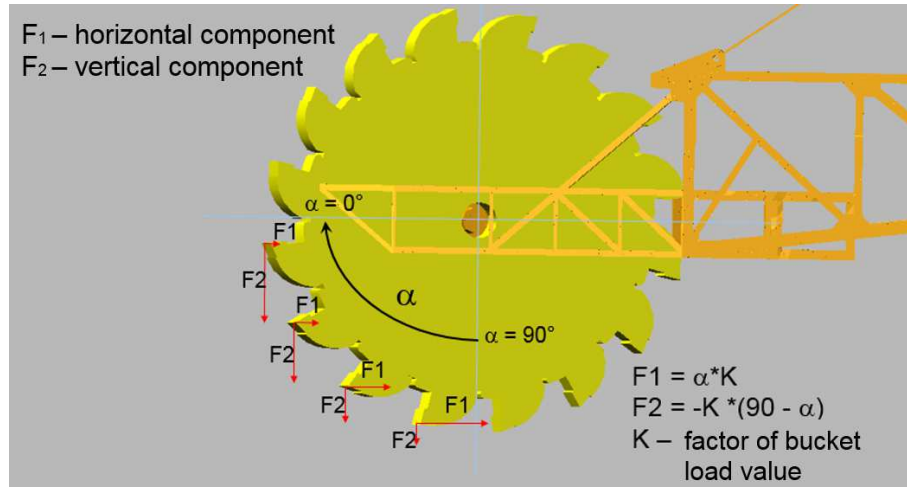


Figure 22 The method of loading the bucket wheel

A sample computational model of the excavator body consisted of a physical model of a multi-bucket excavator body and a model of mapping the operation of driving motors of the bucket wheel and the excavator's control. In order to carry out the simulation, co-simulation technology was used to integrate individual components of the computational model developed in various software environments. Structure of the computational model is shown in the figure below.

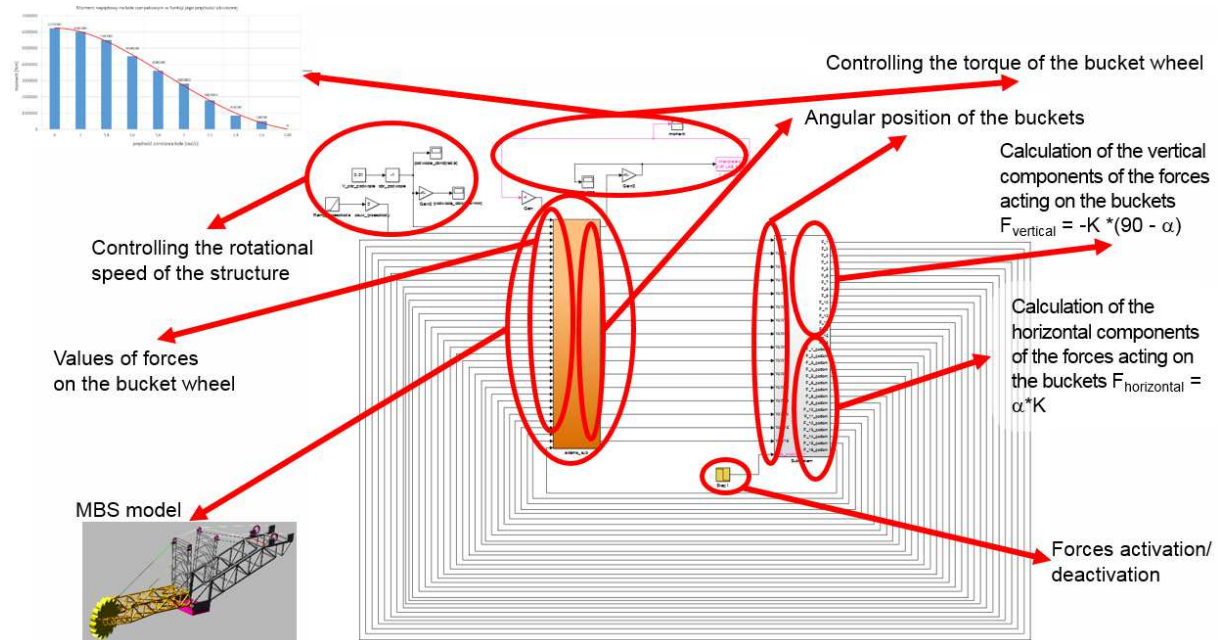


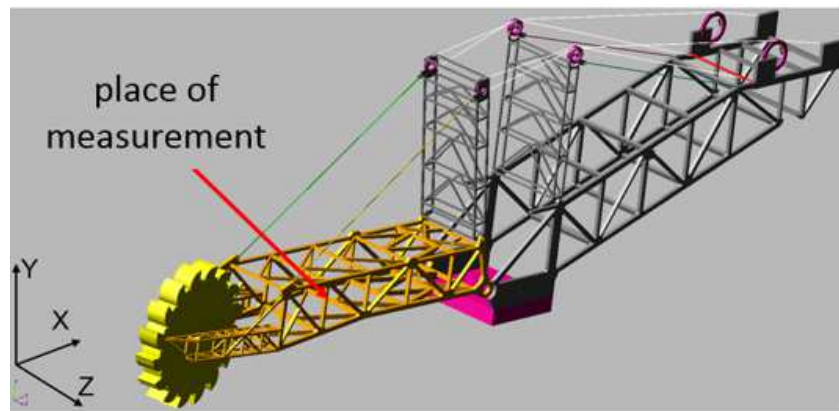
Figure 23 Computational model of a multi-bucket excavator

The presented computational model of the multi-bucket excavator body after the validation, can be subjected to any loads, and then basing on the results of numerical simulations, one can draw conclusions about the behaviour of the structure body.

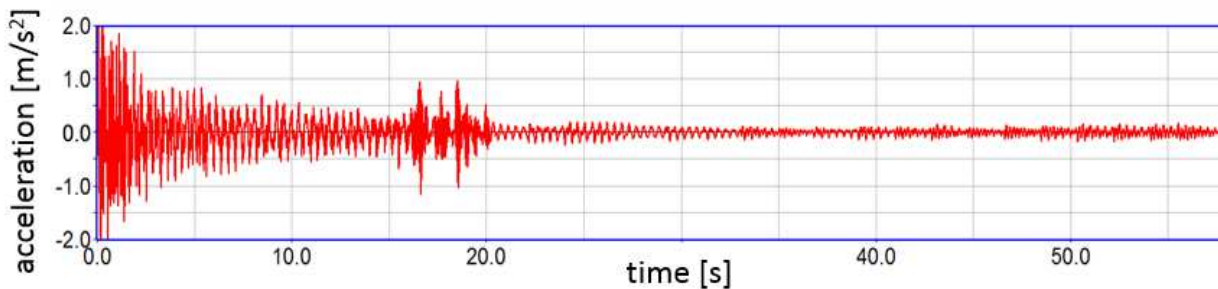
The presented computational model can be used to analyse the vibrations of the multi-body excavator body structure resulting from the mining process, excavator torques, as well as caused by external factors such as wind. In order to analyse the vibrations of individual subassemblies of the body at specific locations of the structure, it is possible to add to the model virtual accelerometers measuring the acceleration at a given point in a given direction. Figure 24 presents an example of acceleration measurements in the Z axis at the indicated point, along with their Fast

Fourier Transform (FFT), recorded during numerical simulations. The Fast Fourier Transform (FFT) allowed the presentation of accelerations in the frequency domain, recorded during simulations.

a)



b)



c)

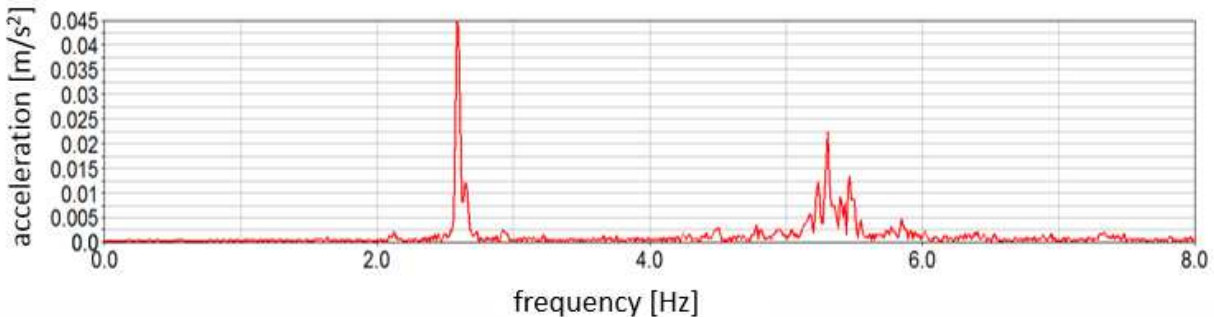


Figure 24 Measurement of vibrations by numerical simulations

- a) place of measurement,
- b) recorded accelerations in time domain,
- c) fast Fourier transform of registered vibrations

Comparison of the acceleration results recorded from accelerometers on the real object, and virtual accelerometers in the computational model can be one of the validation points of this model. Then, any number of virtual accelerometers can be built in the computational model to analyse vibrations in any place on the structure and in any criterion states, e.g.: during lifting and lowering of the bucket wheel boom, during mining when the buckets are loaded or during the excavator travel.

In addition, in the case of deformable bodies, the natural frequency and deformation form are calculated for each of these frequencies. Figure 25 shows samples of deformations at four natural frequencies in relation to mast 1.

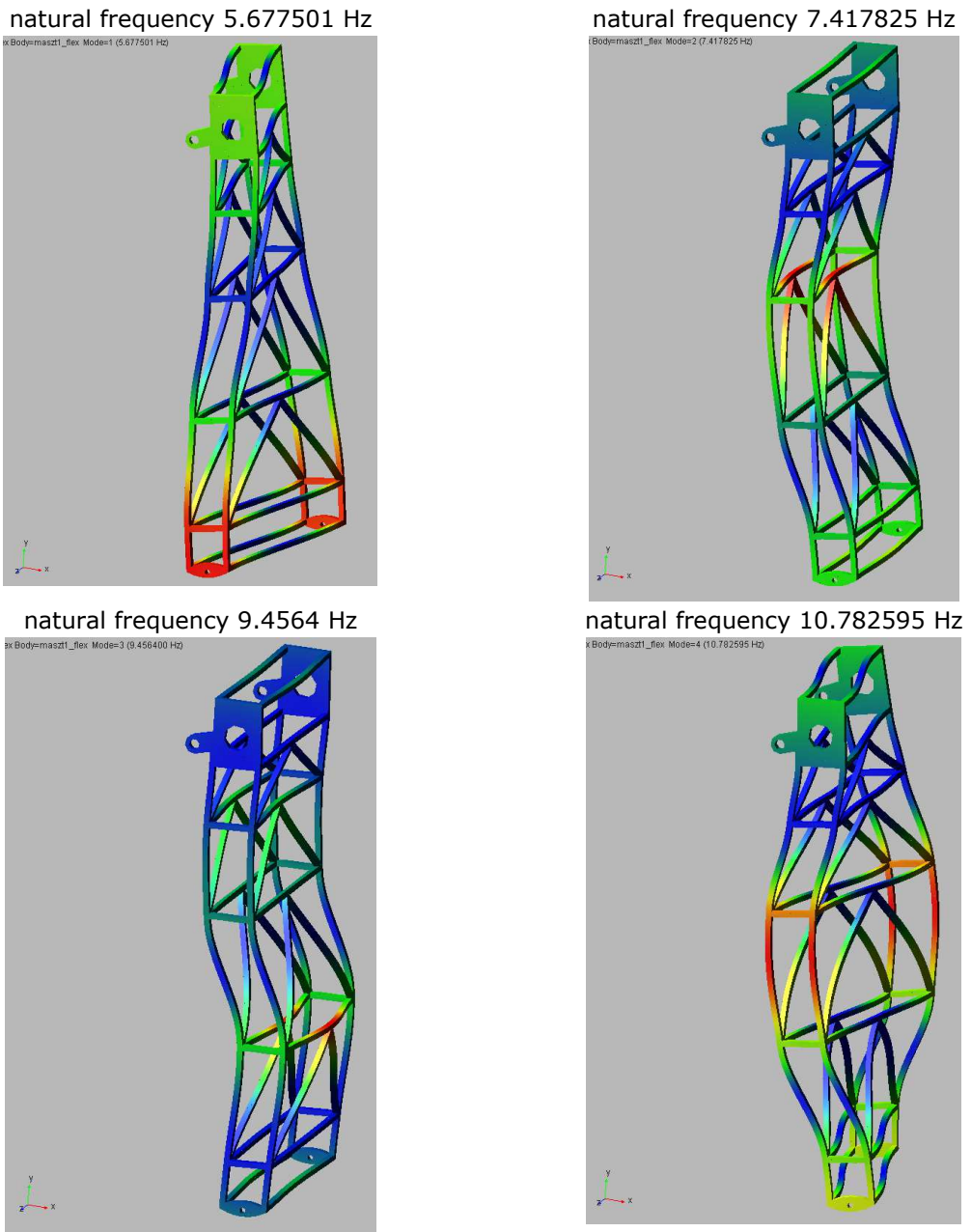


Figure 25 Mast 1 deformation forms in relation to selected natural frequencies

In the same way, one can determine and present the natural frequencies and deformation form of all deformable bodies in the computational model.

During simulation of the excavator's operations, the forces and torques are calculated in all nodes of the body structure. Recording these forces allows the analysis of force distribution through the structure during operation and identification of the most strained places in the body structure. Figure 26 presents the forces recorded during a sample simulation at the point of fixing the rope, that supports and lifts the bucket wheel boom and in an elastic-attenuating element representing the actuator holding the rope.

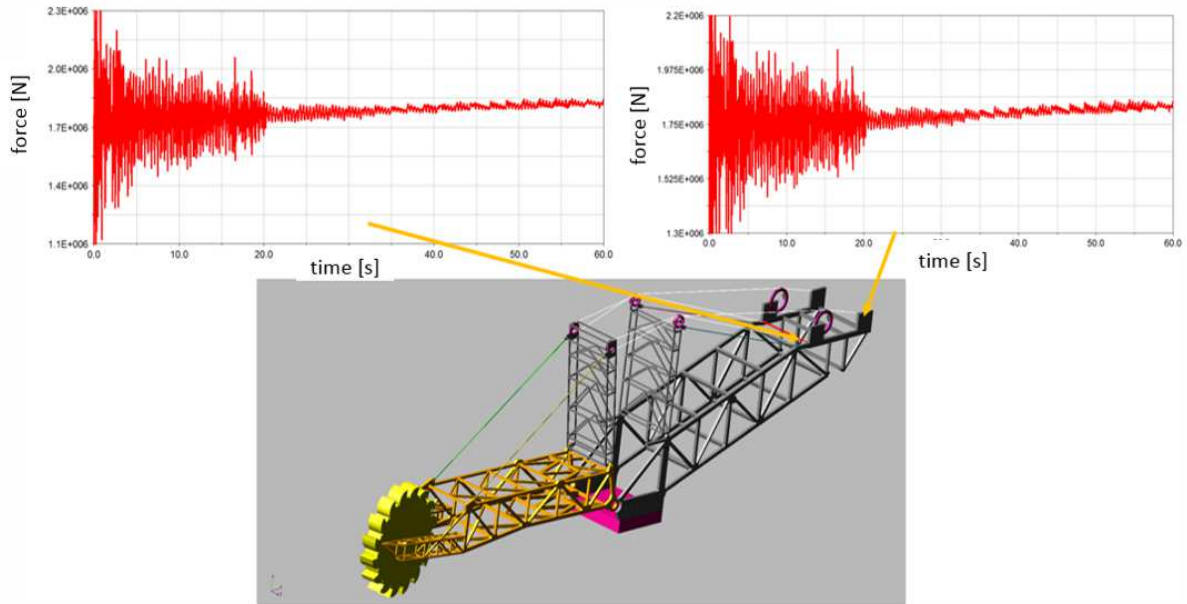


Figure 26 Forces at the point of fixing the rope, that supports and lifts the bucket wheel boom

Determination of boundary conditions for MES type strength analyses is another application of numerical simulations, in which forces are determined at given nodes of the structure. Such conditions can be determined with any setting of the bucket wheel boom and with any method of loading this wheel. On this basis, strength calculations may be carried out in relation to the most unfavourable operational conditions of the entire structure.

Another possibility of using a computational model is to perform simulations in emergency criterial states. During such situation, significant dynamic overloads are often observed, resulting in danger of structural damage. An example of emergency condition simulation is the simulation of the bucket wheel hitting an obstacle during mining, this situation can take place in the case of a bucket wheel collision with the inclusion in the excavated deposit. Figure 27 presents the simulation of a dangerous collision situation, where the bucket wheel hits an obstacle. The red element in front of the bucket wheel is an obstacle which was hit by one of the wheel buckets, while lifting the boom.

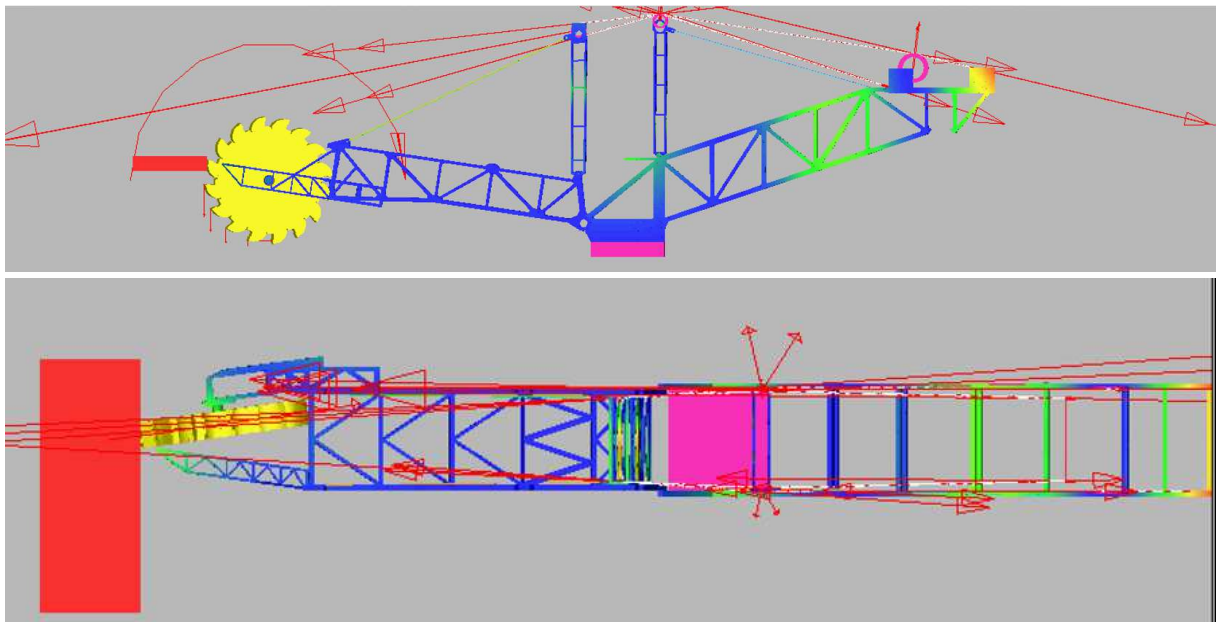


Figure 27 Visualization of the collision situation of the bucket wheel hitting an obstacle

During the simulation, just like in the previous case, forces and accelerations are recorded in individual construction nodes, which may be the starting point for strength analyses in emergency situations.

The advantage of using the co-simulation technique is that it allows simulation of the correctness of the operation of the newly developed machine control algorithms. After the control algorithm is implemented, a virtual controller is built to change the parameters of the computational model

during simulations. The force and torque vectors, the speed and rotation of the excavator body or the degree of lowering the bucket wheel boom may be the subject to changes and adjustment. This approach allows to detect imperfections of new algorithms and their maximum refinement before their implementation on the real object.

Experimental verification of correctness of selection of calculation values of load factors resulting from vibrations of load carrying structure during operation in selected conditions was realised on excavators KU 800 a K2000.

During experimental verification 2 methods were used during preparation of the methodology for calculation of loading and torque moment from drive vibrations

The first, direct method is based on measuring in the same moment acceleration and deflecting of vibration in the site with known moment of inertia.

The second, indirect method is based on application for measurement working in the central office BEWEXMIN - 3x DS-NET. This system consists of three modular components and evaluation computer. Three measure switchboards are equipped by 20 tensometric channels, 12 vibration channels, 20 analogue input ports, 16 digital input ports and indication of measurement from rotate shaft.

The measurement was realised during mining operation of excavator K2000. The electrical input of the drive of bucket wheel was measured in the same time as vibration acceleration. The vibration was measured in admission of down electromotor of gearbox. The values of vibrations (acceleration and deflecting) were measured by Brüel and Kjaer equipment. That was done for checking of transformation formula and obtaining more data.



Figure 28 Preparing of sensors for loading measurement

According to vibration diagnostics, curves of vibration time for rotation machinery nodes were obtained. These curves are very important for characterization of wearing out development. These curves are characteristic primarily for machines working in continuous conditions (loading, working, digging slewing). It means that operational situation of every bucket wheel excavator is different. The results of the work package showed that for proper evaluation of the topic, a matrix of these curves respecting specific load of excavator is needed.

All results of measuring, formulas and figures are shown in the Deliverable D1-4.

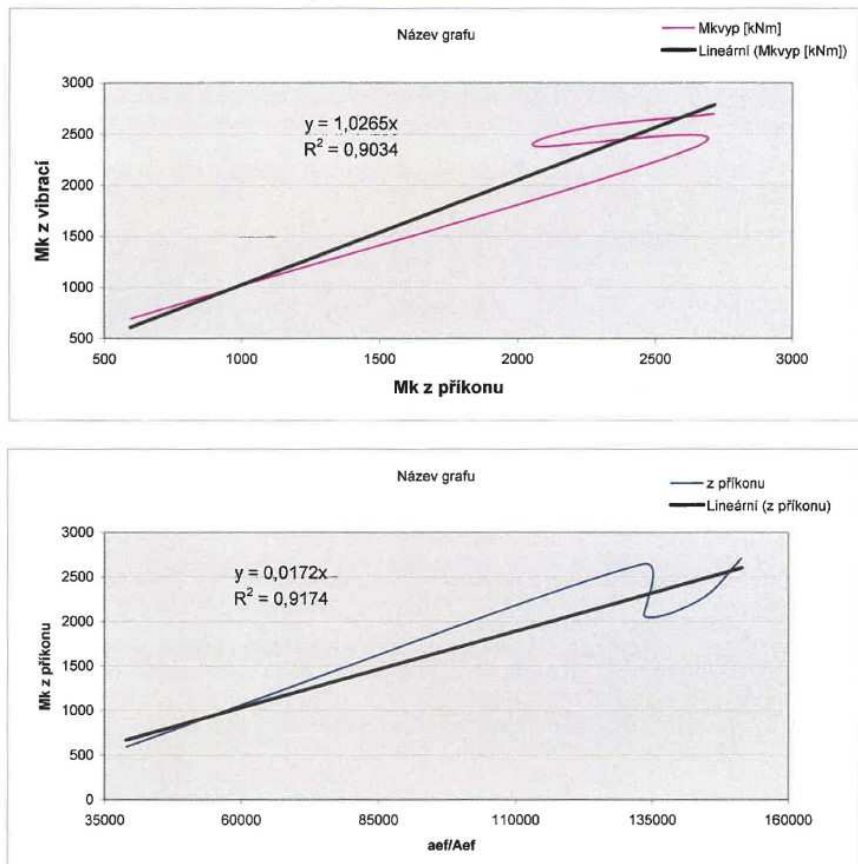


Figure 29 Example of vibration curve

WP 1.4 Major achievements:

- computational model MBS (Multi-Body System) of BWE,
- integration with the external software,
- co-simulations including normal operating conditions and emergency ones,
- experimental verification of correctness of selection of calculation values of load factors resulting from vibrations of load carrying structure during operation in selected conditions realised on excavators KU 800 a K2000.

2.2.1.5 WP 1-5 Assessment of selected excavator adjustment for operation under conditions including unmineable inclusions and geological structures with excessive mining resistance as well as definition of possible changes introduction increasing adjustment to operation in such conditions

For the assessment the excavator SchRs 4000 was chosen. The purpose of the work was to verify the design and modification of the bucket wheel for the SchRs 4000 excavator and to present the form and value of effort in specific regions of the wheel. The works were carried out based on the criteria set for this type of objects by the PN-G-47000-2 standard.

As part of the work, strength verification of the bucket wheel, which is currently used on excavators, was carried out taking into account the loads from the mining process. The details of the analysis are provided in the first chapter of the Deliverable D1-5. This chapter also presents the state of effort and the deformations. The results of calculations of the variant currently used in the mine on SchRs 4000 excavators indicate local exceedances of stress values in which operational problems are observed. These areas are mainly located in the vicinity of the bucket mounts.

In order to carry out numerical calculations of the bucket wheel, a shell geometric model was constructed that faithfully reproduces the structural form of the analysed object. Because the wheel is made up of 16 identical parts, the geometric model is 1/16 of the actual object. During the construction of the surface, the principles of their creation in the middle of the thickness of the plates were kept, whose colours closely corresponded to the thicknesses of the modelled elements.

This procedure was intended to significantly simplify the physical properties of finite elements during the creation of a discrete model.

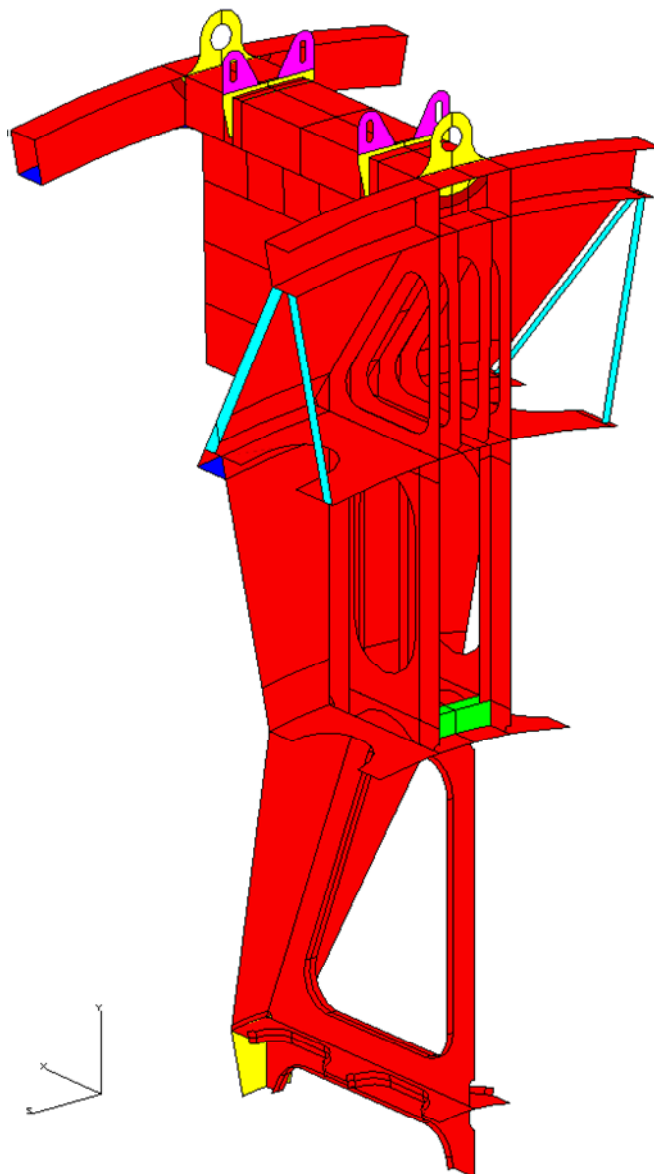


Figure 30 The geometric model of the bucket wheel

Discretization of the geometric model was carried out. The discrete model shown in Figure 31 consists of 319 280 nodes and 332 656 finite elements, which gives the total number of degrees of freedom of about 1.91 million. They are mainly quadrangular lower-order shell elements. Other elements in the model are: beams, mass elements, rigid elements, constraints elements as well as volume elements Penta-6 and Heksa-8. During the discretization, finite elements with an average size of 50 mm were used. The size was chosen so that at least two finite elements were created on the narrowest plates. In places of construction notches, this size was reduced, which led to the compaction of the netting.

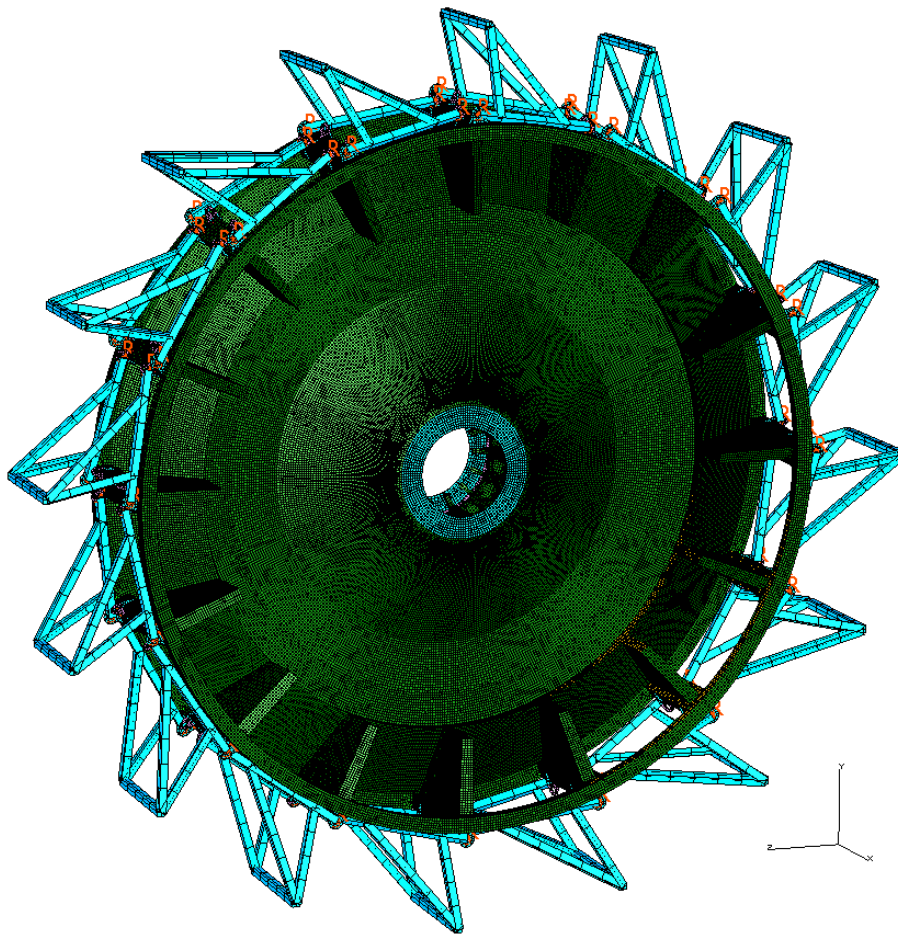


Figure 31 Discrete model of the bucket wheel

High stress values were also observed in the vicinity of the connection of the rim part of the bucket wheel to the central part in the chute area, for which additional comparative analyses of several modernization solutions were carried out. The results of these calculations are presented in the second chapter of the Deliverable D1-5. Calculations showed that the best is concept 4. A decrease in maximum stresses was recorded by approx. 30% for immediate strength and about 15% for fatigue strength. **Much more important for this variant is that the maximum stress values occur outside the zones of welds (as opposed to the original version), whose fatigue strength is at least twice as high.**

WP 1.5 Major achievements:

- verification of the design and modification of the bucket wheel for the SchRs 4000 excavator.

2.2.2 WP-2. Monitoring system of bucket wheel excavator load carrying structure efforts and method of diagnostic signals analysis for current assessment of threats of load carrying structure damages as well as constant control of residual strength of the structure

The aim of WP-2 was a technical development of the system for monitoring operation of the bucket wheel excavator load-carrying structure based on tensometric measuring systems. The system enables registration of abnormal excavator's loads occurring during mining of hard or unmineable materials. The results of our long-term observation of machines operation indicate that bucket wheel excavator load-carrying structures are increasingly more often subjected to loads affecting the safety of construction. The abnormal loads are temporary loads occurring during machine operation which exceed values taken into account while dimensioning load-carrying structure at the design stage of the machine. As a result of the implementation of WP-2 activities, a system of monitoring the effort of bucket wheel excavator load-carrying structure was created, based on continuous analysis of the operating parameters of the main mining unit drive mechanisms, in correlation with current stress level measured in sensitive sections of the machine construction. According to adopted guidelines, the system can analyse diagnostic signals on a continual basis and assess potential threats of load-carrying structure damage, resulting from temporary abnormal loads that may occur during operation.

2.2.2.1 WP-2.1. Method of monitoring of load carrying structure stresses along with selected parameters of excavators' operation as well as methods of load carrying structure efforts assessment on the basis of registered signals

Bucket wheel excavator belongs to a group of machines for continuous operation. The behaviour of continuous cutting process requires the use of three basic movements of the tool and the material to be cut. These basic working movements are as follows:

- the main movement that causes the penetration of the blade of the bucket into the cut material,
- advancing movement (advance), which causes a change of cutting place necessary to ensure continuity of the process,
- in-feed movement (in-feed), which renews the contact with the material after cutting a lot of the material contained within the blade range.

A characteristic feature of the excavators is that the tool (bucket) performs all these three basic working movements. Mined material (i.e. ground) is stationary with respect to the substrate, on which the excavator is located. In each of the individual movements, the translational and angular components can be distinguished. Due to this, a large number of combinations of these movements can be obtained. In practice, the number of combinations of the excavator working movements is only reduced to a few, namely:

main movement:

- rotary motion – wheel excavators (bucket wheel rotation),
- straight motion – chain-and-bucket type excavators (movement of the excavating chain along the boom),
- involute – single-bucket excavators (resultant of the bucket rotary and translational movements).

advancing movement:

- advance – longwall system operation,
- angular – shortwall system operation.

in-feed movement:

- advance:
 - wheel excavators – excavating with vertical chip,
 - chain-and-bucket type excavators – work with a permanent boom tilt, in parallel strips,
- angular:
 - wheel excavators – excavating with horizontal chip,
 - chain-and-bucket type excavators – work with variable boom tilt working, in V-shaped strips.

All operating resistance loading the supporting structures are overcome by the operation of the following drives:

bucket wheel drive

- circumferential component of the resistance to mining,
- bucket filling resistance,
- resistance to the excavated material lift.

body rotation drive

- lateral component of the resistance to mining,
- resistance to operate on a slope.

traction drive

- radial component of the resistance to mining,
- resistance to operate on a slope,

bucket wheel boom lift drive:

- resistance to the bucket wheel boom lift.

In addition, all drives overcome resistance that do not affect the change of the bearing structure load:

bucket wheel drive

- electrical loss (in motors),
- mechanical loss (in gears),
- characteristics mismatch loss (multi-drive systems),

slew drive overcomes

- electrical loss (in motors),
- mechanical loss (in gears),
- loss associated with movements,

traction drive

- electrical loss (in motors),
- mechanical loss (in gears),
- loss associated with movements,

bucket wheel boom lift drive

- electrical loss (in motors),
- mechanical loss (in gears),
- loss in sheave blocks (wire rope pulley blocks) (or hydraulic system).

Another subject within the Work Package 2.1 is method of determining stress distribution in the selected sections on the basis of measurable parameters of the excavation system during the machine operation. The task of the load-carrying structure is to transfer loads to the support points. Loss of ability to perform the task is equivalent to the depletion of its life reserve and entering into a condition preventing its normal operation. Depleting the structure reserve is associated with its operation. In general cases, depleting the structure reserve may be due to its excessive strain or load capacity depletion. Excessive strains are associated with the occurrence of unacceptable deflections, horizontal deflections and vibration of structural components. Load capacity depletion is associated with reaching the critical effort or fatigue of structural components or loss of stability or transformation of the structure into a geometrically variable system. For a correctly designed structure with components in normal condition, there should be no depletion of its reserve as a result of excessive strains. This can happen as a result of the loss of load capacity by its components. The load-carrying structure is protected at the design stage by suitable selection of the structure design, the profiles used and the selection of material prior to the occurrence of excessive deflection and deformation. Therefore, the occurrence of such phenomena during the operation will be associated with the degradation of structural components or combinations thereof, or occurrence of oversize loads (despite the activation of means of overload protection). The situation is similar in the case of vibration of the structure. Vibration is the result of the structural resonance due to cyclically variable loads. Therefore, adequate analysis of proper vibration is carried out at the design stage. Variation of the proper vibration of the structure is the result of changes in its stiffness or weight of its assemblies or components. Therefore, the occurrence of this type of phenomenon is also related to the degradation of structural components

or combinations thereof. This does not include the upgrading changes that may interfere with the existing structure or its rigidity and require repeating the strength calculations. When designing the structure, its designers use the available calculation methods specified in the standards and studies as well as calculation supporting tools. Although these methods are improved, aiming to make the most accurate reflection of reality, they do not specify precisely the impact of loads on structural components and the possibility of mutual excitation of the structural assemblies. This is due to the current state of knowledge, computational tools available and various kinds of simplifications and approximations applied. Moreover, there is no precise information on the presence of abnormal loads during operation and the intensity of mining process available at the design stage. For this reason, it is impossible to estimate the effort and fatigue life of the structure accurately at the design stage.

For the load-bearing structure, loss of stability is associated with the loss of ability to transfer external loads through the support. Such an event could take place in case of occurrence of loads abnormal to the work of the structure (in specific types of support through the exiting of the centre of gravity beyond the tipping edge). Such an event may also take place in case of degradation of structural components or connections at the points of support or in their vicinity or the occurrence of abnormal external loads.

Transformation of the structure into the geometrically variable system is the result of changes in its structure. This may occur in case of destruction of certain structural components from the degradation of some components or combinations thereof.

As discussed above, the structure reserve depletion is largely the result of degradation of the structural components or combinations thereof. It can result from deterioration of the technical condition of individual components, fatigue processes occurring in them or exceeding the critical stress. These processes will result in changes in load capacity of the components. Therefore, *monitoring of stresses* seems to be the most appropriate.

Stress condition in the most effort components of the load-bearing structure is measured using the extensometer method. The measurement and estimation requires the construction of the measuring circuits, and a data acquisition and processing system. The central unit is provided with a module for the analysis of the test results obtained in the extensometer method.

The following data are stored:

- signal envelopes,
- signal static values, including the maximum value,
- statistic values for the calculated envelopes, including the standard deviation.

Dependence of the influence of the excavation forces on the stresses in the structural bars can be used to measure these forces. In the non-extendable wheel excavators, both lateral and circumferential components of the excavation force affect stress changes in the structural bars. Radial force can be omitted (a non-extendable excavator does not perform any operating motions in the radial direction).

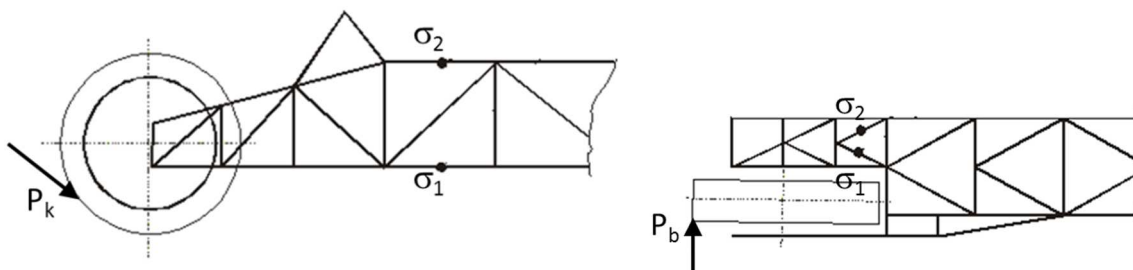


Figure 32 Examples of stress measurement points

Examples of stress measurement points are presented in Figure 32 in order to determine:

- a) circumferential excavation force, P_k
- b) lateral excavation force, P_b

$$S = C_1 \cdot \sigma_1 + C_2 \cdot \sigma_2$$

S – Excavation force

C_1 C_2 – coefficients

σ_1 σ_2 – stresses

Bars on which the stresses induced by excavation forces are measured should be selected so that the measured stress values caused by one component (e.g. circumferential) would be totalled, and the stresses caused by the second component (e.g. lateral) would be subtracted. In such a way, one obtains an increase of one component and decrease the effect of the other component of the excavation force for the sum of the stresses.

In order to determine the value of the selected excavation force component, S , the coefficients C_1 and C_2 should be selected so that the result would only depend on this one component.

All above topics and methods of monitoring them are presented in detail in Deliverable D2-1.

WP 2.1 Major achievements:

- Identification of the nature of the structure load on the basis of the mining system drive load parameters
- Method of determination of stresses distribution in selected sections depending on measurable parameters of exploitation system during excavator operation
- Method of monitoring of load carrying structure stresses along with selected parameters of excavators' operation as well as methods of load carrying structure efforts assessment on the basis of registered signals

2.2.2.2 WP 2.2 Definition of experimental methods of correlation of stresses in load carrying structure in measured points with the stresses in the areas of their concentration

The load-bearing structure of wheel excavators is complex and complicated in its construction. Due to its large size and changes in loads associated with the operation of the machine, theoretical determination of the actual effort of individual components is encumbered with substantial errors resulting from some generalizations used in the calculation process. In the proposed monitoring method, the evaluation of construction's effort is performed based on limited number of measuring points. The measuring point should be understood as a spot in which a sensor (strain gauge) is fixed. Whereas, the monitored spot is an area or a part of a construction in which – based on the preliminary assessment and the calculative analysis – a fatigue damage is likely to occur. It is not possible to indicate one (precise) spot where a damage will occur first; it is, however, possible to indicate – with calculation methods – areas of construction exposed to more stress. In the design process, during the dimensioning of the construction, taken into account are standard loads and the occurrence of their maximum combination. These generalizations have been verified by years of operation of the excavators. Spots particularly vulnerable to damage are indicated depending on the type of structure and design solutions, as well as gained experience regarding construction's behaviour.

Monitored spots are indicated in the following stages:

- identification of the most stressed parts based on static and dynamic strength calculations for load-bearing structures,
- indication of stress concentration areas based on structural analysis of a part (node) of load-bearing structure.
- analytical estimation of the impact level of the dynamic load on fluctuation of the average level of stress in inspected parts (nodes) vulnerable to fatigue damage, based on measurement and analysis at measurement points.

The first stage of identifying the parts vulnerable to fatigue breakdown is selecting (indicating based on calculations) the spots of the highest effort. This stage is carried out based on a FEM structural analysis, depending on the requirements of the whole construction or basic assemblies of load-bearing structure. The aim of calculations is to determine the parts under the greatest stress. For technical reasons, the strain gauge measurements can therefore be performed only for a limited number of spots. Assuming the continuity of a medium, the perfect elasticity and homogeneity of the material, and the linear relation between deformations and stresses, the values measured in such measurement points can be interpolated to monitored spots. Such an assumption allows for estimation of effort in areas of expected stress concentration. Indication of

stress concentration areas is the next stage of identifying the parts vulnerable to fatigue breakdown. Areas are indicated by structural analysis of a separated part or structural node.

The goals of the experiment and the expectations related to the results of the measurements of a structural node model were:

1. verification of theoretical FEM calculations for the selected node,
2. validation readings and recorded values of strain gauge measurement systems and the possibility of using the obtained readings to monitor the value of the loading force,
3. experimental comparison of deformation in the area where a strain gauge is attached with areas of expected stress concentration, taking into account the occurrence of a notch,
4. in the final stage – recording the number of load cycles before the occurrence of a fatigue damage to node's structural parts,
5. testing of procedures for counting the number of cycles in specified value ranges under laboratory conditions.

Due to the frequency of variable external loads, the most vulnerable to damage is the boom of the bucket wheel. Node selection is based on our observations and experience relating to the occurrence of damage to the real object. In the inspected excavator, it is a point of connection between the boom and the excavator's turntable (Figure 33). The nature of the clevis fastener and the damages occurred lead us to the conclusion, that the damage results from a combination of external loads and deformations arising from construction's vibrations in the horizontal plane. The laboratory tests should therefore be able to subject the model to a bending moment and a torque moment (simulating the effect of a lateral force).

Figures below presents strain gauges mounted on SchRs 4000x37.5

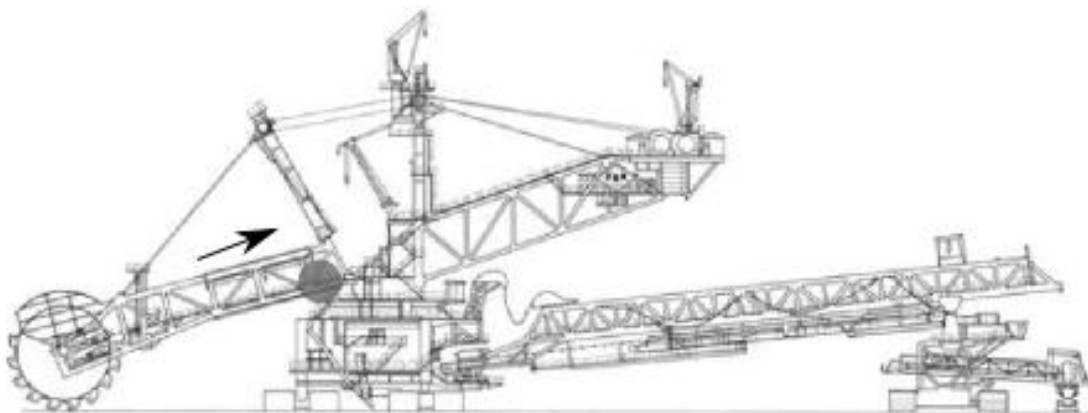


Figure 33. Selected structural node



Figure 34. Deformation measurement point on the boom – left side



Figure 35. Deformation measurement point on the boom – right side

More information about experimental methods of correlation of stresses in BWE's superstructure with areas of their concentration can be found in Deliverable D2-2.

One of the activities was determination of the notch coefficient, β_k , using the INVENTOR software, for a simpler (engineering) analysis using the finite element method, and determining the shape factor, a_k with it, and then determining the notch coefficient, β_k . Both coefficients combine very common relation (below) on the material susceptibility to notch, η_k ($\eta_k = 0.5 \div 0.9$ for raw steel).

$$\alpha_k = \frac{\sigma_{max}}{\sigma_n}; \quad \alpha_k = \frac{\tau_{max}}{\tau_n}$$

$$\beta_k = 1 + \eta_k(\alpha_k - 1)$$

Basing on the slightly inflated (in accordance with the assumptions of the method) values of the shape factor and selecting a slightly lower sensitivity of the material to notch effect ($\eta_k = 0.6$) and modelling the actual shape of the weld specimen, a reliable estimation of the desired notch coefficient was obtained.

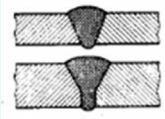
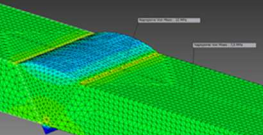
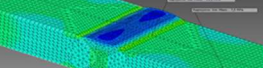
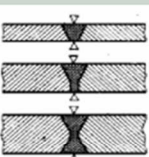
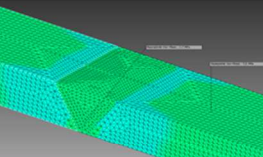
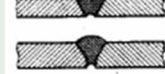
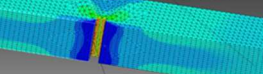
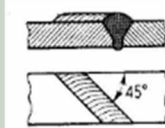
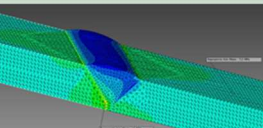
	Opis złącza spawanego	Schemat złącza spawanego	Wartość współczynnika działania karbu β_k przy obciążeniach zmiennych przy rozciąganiu	Model MES
1.	Jednostronne złącza czołowe z podspawaniem (nie obrabiane)		2,0	
2.	Dwustronne złącze czołowe (nie obrabiane)		2,0	
3.	Jedno i dwustronne złącza czołowe (z podspawaniem) obrabiane		1,55	
4.	Jednostronne złącza czołowe bez podspawania (nie obrabiane)		2,8	
5.	Jednostronne złącza czołowe podspawane, nie obrabiane, ukośne		1,75	

Figure 36 Examples of modelled welds

POLISH	ENGLISH
Opis złącza spawanego	Description of the welded joint
Schemat złącza spawanego	Welded joint diagram
Wartość współczynnika działania karbu β_k przy obciążeniach zmiennych przy rozciąganiu	Value of the notch coefficient, b_k , at variable loads under tension
Model MES	FEM model
Jednostronne złącza czołowe z podspawaniem (nie obrabiane)	Single V-butt weld with backing run (not machined)
Dwustronne złącze czołowe (nie obrabiane)	Double V-butt weld (not machined)
Jedno i dwustronne złącze czołowe (z podspawaniem) obrabiane	Single and double V-butt weld (with backing run), machined
Jednostronne złącza czołowe bez podspawania (nie obrabiane)	Single V-butt weld without backing run (not machined)
Jednostronne złącza czołowe podspawane, nie obrabiane, ukośne	Single V-butt weld with backing run, not machined, slant

A specification included in the literature, which directly determines the values of the searched coefficient, was comparatively adopted to the research. Similar cases have been modelled and analyzed. The results of the finite element analysis with the assumptions made, show some underestimation of the notch coefficient when considering the results obtained directly from the calculations – it is lower by an average of 25 %.

A parameter named a correction factor was adopted for further analysis, and its value was set to **0.51**. This treatment improves the results in a significant way, because they are only inflated by an average of 2 %. The values of the notch coefficients are summarized in the diagram below. Only the comparative analysis of the value of shape coefficients and the correction made, allowed modelling of monitored excavator nodes.

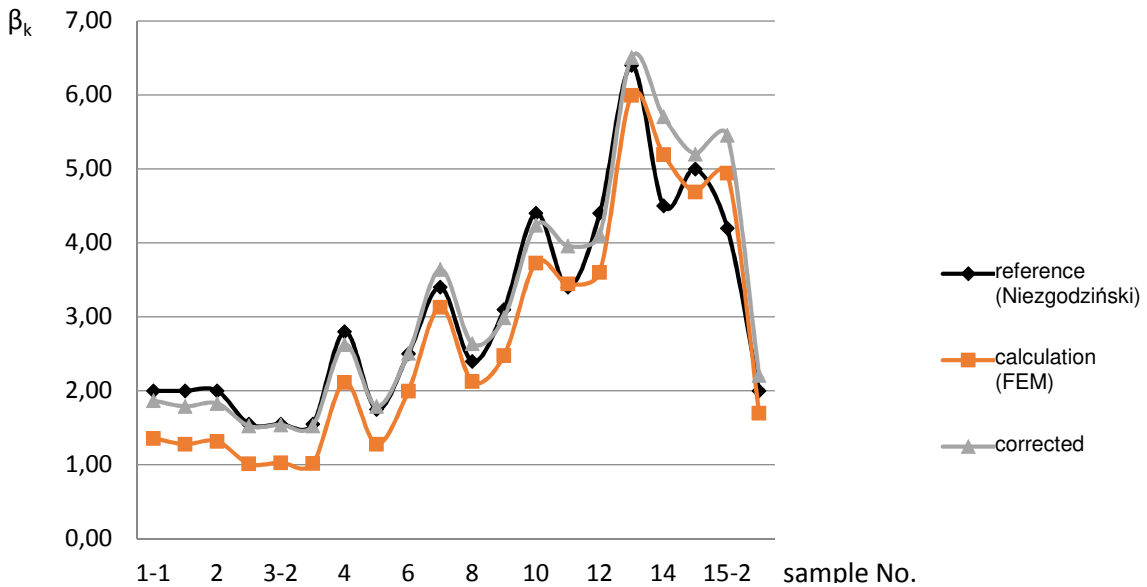


Figure 37 Diagram of notch coefficient values

In order to determine the effect of changes in the magnitude of stresses in machine structure elements from external loads, it was proposed to monitor simultaneously stress changes in the load-carrying structure elements and basic excavator operation parameters, i.e. a power of a bucket wheel drive, a power of the body rotation drive, a rotational speed of a body, and a bucket wheel boom angle. For this purpose, output of electrical signals corresponding to aforementioned values has been taken from the excavator automatic systems, which are introduced to the system of monitoring of the effort of the structure.

Another aim of the WP 2.2 was stand tests on a model of construction nod using extensometer measurement systems in order to define instructions for construction of functional measurement systems enabling measurement of complicated stresses and monitoring of areas of construction nods.

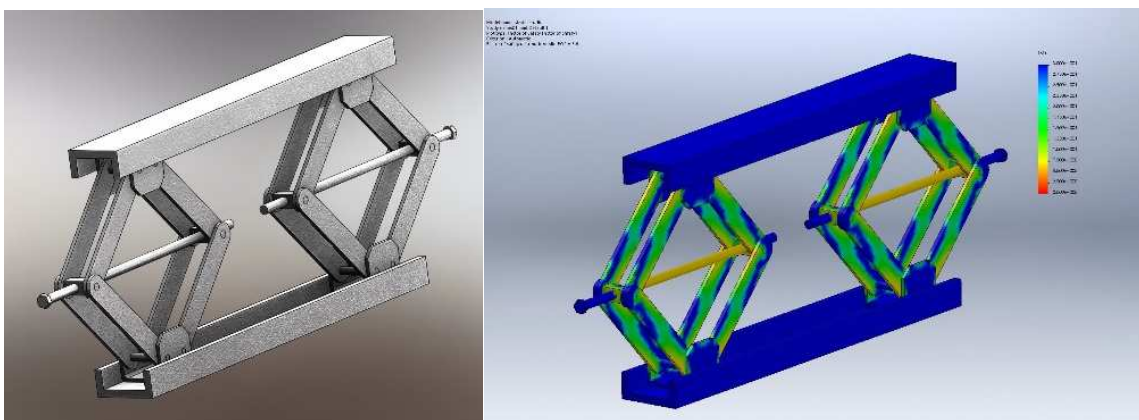


Figure 38 Testing rig

The devised and embodied rig is a versatile tool for experimental tests in view to respond to the main question: how to translate the multipoint values to the most vulnerable one, in which is no practical possibility to set measuring sensors. Designed rig is also versatile because it is a reduced scale model of a truss section and in same time a quite real scale a model of a bolted or welded node (joint).

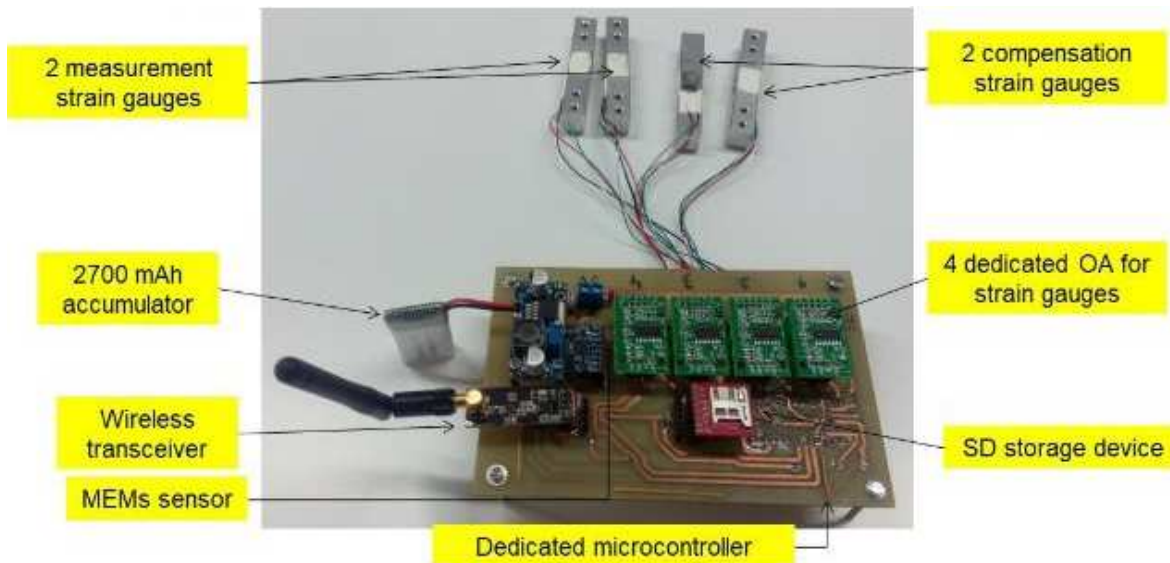


Figure 39 Rig measurement system prototype

WP 2.2 Major achievements:

- correlation of stresses in load carrying structure in measured points with the stresses in the areas of their concentration,
- determination of the notch coefficient,
- development of the testing rig for measurement of complex stresses and testing of monitoring of construction nod areas.

2.2.2.3 WP-2.3 Definition of parameters of stresses distribution in bucket wheel excavator load carrying structure for different properties of mined materials on the basis of tests on real machines in exploitation conditions

Strength analysis of KU 800.7 bucket wheel body, bucket wheel shaft and bucket

The main steel structure of the chamberless one wall bucket wheel has a form of the disc with the ring on external diameter. The disc include two cone surfaces, that are opposite to each other. Internal cone disc is connected to the flange by screws. The flange is a part of the carrier. This one is fixed on the hollow shaft with rings Dobicon. The external ring has buckets on external diameter.

Main characteristics:

Diameter of the bucket wheel	D_k	12750 mm
Diameter of the bucket wheel disc	D_d	10400 mm
Number of buckets	Z_k	15
Revolution per minute	n_k	3 - 5.6 1.min ⁻¹
Peripheral speed (velocity)	v_k	2 - 3.7 m.s ⁻¹
Capacity of the bucket	V_f	1000 dm ³
Theoretical output – excavated ground	Q_{th}	7390 m ³ .h ⁻¹
Output of the bucket wheel driving motor	P_{ck}	4x400 kW
Minimal circumference power	P_{min}	428 kN
Nominal circumference power	P_{jm}	486 kN
Maximal circumference power	P_{max}	800 kN
Length of the shaft between bearings		7500 mm
Max. diameter of the shaft		720 mm
Diameter of the shaft in the bearing		500 mm

The Material

- External and internal cones and the ring are welded from steel of the class S355 J2 G3 (11523.1).
- Internal diameter of the internal cone is welded with flange, that is connected with carrier by screws
- The material of the carrier is cast steel 42 2709.6

- The shaft is forging from steel 16 431.6
- The bucket is from cast steel 42 2712.5 (socket) and from rolled steel S355 (container).

Reliability coefficient of material	$\gamma_{M0,1} = 1.15$ dle ČSN EN 1993-1-1
Characteristics of material	according to ČSN EN 1993-2:
Yield point of the steel S355	$f_y = 355$ MPa for thickness < 16 mm
Yield point of the steel 16 431.6	$f_y = 569$ MPa
Breaking strength of the steel 16 431.6	$f_u = 686 \div 834$ MPa
Yield point of cast steel 42 2712.5	$f_y = 280$ MPa
Breaking strength of cast steel 42 2712.5	$f_u = 500$ MPa
Coefficient of the strength of the weld	$\gamma_r = 1.00$
Deformation of the shaft under ring DOBICON	max. 10 mm.

Used documentation

- ČSN 27 7008:2007 „ Design of steel structures of excavators, loading machines and overburden dumping machines“
- ČSN EN 1993-1-1:2006 „ Design of steel structures, General rules....“
- 3D model of the bucket wheel with shaft and buckets – inventor v. 20

The model:

The bucket wheel is fixed against rotation.

The shaft is supported by hinges located in two places - bearings - of the boom.
The length between supports - 7500 mm.

Permanent load

Buckets	$9.2 \cdot 15 = 138$ kN
Hopper	98.10 kN
The part of belt conveyor	68.67 kN
Driving mechanism	750.47 kN
Cover of the driving mechanism	29.43 kN

Random load (dynamic)

Material on cutting element. Included in cutting force.

Material adhesived in the bucket wheel. It is in ring of bucket wheel. The all - 11 kN.

Material on chute. It is localized on the hopper and on part of the disc of the bucket wheel next to the hopper

1.4 kN.

Material on the belt.

20 kN.

Digging force - extremal operation

Nominal value of the digging force (df) is calculated from power of the driving mechanism 2x800kW.

Revolution of the bucket wheel	3 min^{-1}	4.9 min^{-1}	5.6 min^{-1}
Peripheral component df	800 kN	486 kN	28 kN
Side component df	400 kN	243 kN	214 kN
Radial component df	800 kN	486 kN	28 kN

Distribution of the df to two cuttings buckets:

bucket 1 73%

bucket 2 27%

Place of operation of the df is on wheel radius

$R = 6375$ mm.

Static load from side wind was ignored.

Forces on teeth

The forces are calculated in work „Strength analysis of the shaft and deformation of the axis of the bucket wheel of the excavator KU800“ archival N. 4-00-20663.

Horizontal force..... $F_x = 2308$ kN/1402 kN for max./nominal peripheral force

Vertical force $F_y = 152$ kN/92 kN for max./nominal peripheral force

The transfer of forces from bucket wheel to the shaft is via the carrier. The effect of forces is in connection carrier – the ring Dobicon.

The support of the bucket wheel

Table 8 The load of the bucket wheel axis is in direct up.

Load Num.	Load/Loads Combinations	LCC 51 Extremal L	LCC 52 Extremal P	LCC 56 Critical L	LCC 57 Critical P	LCC 60 Extraordinary mode
1	Weight of the structure	1.1	1.1	1.1	1.1	1.1
2	Digging force - right	2.25		1.22		
3	Digging force - left		2.25		1.22	
4	Material on the belt	1.25	1.25	1.25	1.25	
5	Weight of the technology	1.1	1.1	1.1	1.1	1.1
6	Material on chute	1.25	1.25	1.25	1.25	
7	Weight of the epithelium of the disc	1.1	1.1	1.1	1.1	1.1
8	Forces in toothing	1.13	1.13	1.22	1.22	
9	Pretension on rings Dobicon	1	1	1	1	1
10	Supporting of the bucket wheel					1.1

Stress check

Stress check was conducted using the program DesignStar providing values of the effective stress by theory HMH (von Mises).

Extremal operating mode

Condition for cone wall of the disc of the bucket wheel

$$\sigma_{\text{ef}} \leq f_y / \gamma_{M0} = 308 \text{ MPa} \quad \text{and} \quad \sigma_{\text{ef}} \leq f_u / 1.6 / \gamma_{M0} = 276 \text{ MPa} = \sigma_{\text{Lim}}$$

σ_x, σ_y normal stress
 T shear stress

Conditions for carrier of the bucket wheel

$$\sigma_{\text{ef}} \leq f_y / \gamma_{M0} = 375 \text{ MPa} \quad \text{and} \quad \sigma_{\text{ef}} \leq f_u / 1.6 / \gamma_{M0} = 338 \text{ MPa} = \sigma_{\text{Lim}}$$

Critical operating mode

The loads combinations are identical with extremal operating mode. Maximal value of the peripheral digging force is 900 kN + 22% = 1100 kN with limiter.

The shaft – effective stress σ_{ef} [MPa] is under a value of 150 MPa. Local maximal stress has value 200 MPa in contact with ring Dobicon – a diameter of 720 mm.

Internal cone of the wall - effective stress σ_{ef} [MPa] has max. value of 226 MPa in the area of the connection – the wall of the thickness of 20 mm with the flange for fixation of the bucket wheel to the shaft.

External cone of the wall - effective stress σ_{ef} [MPa] has max. value of 125 MPa in the area of the connection – the wall of the thickness of 20 mm with the ring of the bucket wheel. There are cuttings buckets there.

The ring of the bucket wheel - effective stress σ_{ef} [MPa] has max. value of 410 MPa on peripheral diameter in the area of pin connection of cuttings buckets. This local stress rapidly descent to value of 200 MPa in distance of 100 mm.

Check usability

There are two deformation conditions:

- The wall of the bucket wheel must not to be in contact with wiping ring, it means limit deformation is 50 mm in direct of the axis of the bucket wheel
- The deformation of the shaft has max value of 10 mm under DOBICON ring.

The ring of the bucket wheel. Maximal deformation has a value of 44 mm by left cutting forces.

The axis of the bucket wheel. Maximal deformation has a value of 6.3mm in distance of 3540mm - 4420mm from bearing on the side of the driving mechanism.

The deformation under rings DOBIKON under bucket wheel	$\varnothing 720\text{mm}$	max 3.9 mm
on bearing	$\varnothing 540\text{mm}$	max. 1.0 mm

Application of complex measurement system in the excavator KK 1300

Situation during complex measurement of KK 1300 excavator

During project realization complex measurement of the excavator KK 1300 parameters have been realized.

- Complex measurement in the excavator KK 1300.1 started on 28.11 2017, at 10:00 a. m. The excavator started mining of selected and defined rock block.
- The time interval of mining and complex measurement - **48:00 hours**

start – Monday 28.11. 2017 – 10:00 a. m.

finish – Wednesday 30.11. 2017 – 10:00 a. m.

- The time of mining of block $T_b = \mathbf{27.44 \text{ hours}}$

Full load test and measurements finished on 30.11.2017 at 10:00 a. m. It was evaluated the real volume of mined overburden rocks was equal of **61 631 m^3** . Geodesic survey of this block occurred before the start of the test and after the test.



Figure 40 Excavator KK 1300.1-CZ/K111

Geological situation of the mined rock block

The excavator was situated in second overburden cut during the measurement. The geological situation was quite simple. The overburden cut consisted of one horizon – Tertiary brown clays. The position is shown in the Figure 40, the results of the laboratory analyses are shown in the Table 9. The main minerals were: quartz, montmorillonite, illite and kaolinite. The content of siderite was about 3-4%. No hard rock structures were discovered. Six typical samples were taken for laboratory tests.

Table 9 Laboratory analyses of the samples (position No 3)

rock type	density (kg/m³)	moisture W_v (% capacity)	penetrometer test (N.cm⁻¹)	compressive strength (MPa)
grey clay	2000	39.4	135	1.85
grey clay	2050	37.9	143	2.05
grey clay	1990	40.1	155	2.25
grey clay	2030	37.5	149	1.65
grey clay	2020	36.8	175	1.55
grey clay	2040	37.1	168	1.95

Geological parameters of the mining block were considered as good.



Figure 41 Clays in mined block

Long term complex testing – loading test

The measurement of mechanical and electrical quantities was the very important part of the complex testing of the excavator KK 1300.1-CZ/K111.

During the loading test the following activities were realized:

- measurement and evaluation of digging resistance
- measurement and evaluation of bucket wheel drive input
- measurement and evaluation of slewing gear drive input
- measurement and evaluation of lateral force in the bucket wheel
- measurement and evaluation of the volume of mined rock
- measurement and evaluation of the tooth warming
- measurement and evaluation of the tooth wearing out

Measurement and evaluation of the digging resistance

During this task realization the „indirect method“ was used. It consists of the measurement of main parameters of mining cuttings (depth, height, thickness) and corresponding bucket wheel drive input. Parameters of cuttings were evaluated according to data in operator's cockpit.

A notebook was used for registration of engine input, bucket wheel drive input and turning of excavator upper part slewing gear.

Measurement and evaluation of bucket wheel drive input

The bucket wheel drive of the KK 1300.1-CZ/K111 excavator consists of reduction gearbox ABN KK1300 2X1150kW with 2 electric motors 1LA4 502-6CMOO-Z, 2X 580A, general input 2x1150 kW.

Also measurements with analysers ENA 500 a BK 550 in engine room and switching station were realized. Electric current and voltage of the bucket wheel were obtained from the switchboard RM 10.

The quantities of the input ranges were between 0.4 MW and 1.1 MW (good geological parameters of the rocks). $\cos \varphi$ ranges between 0.40 a 0.70.

Measurement and evaluation of the general input of the excavator KK 1300

The measurement was realized in the switching station. The voltage was detected by measuring transformer in the switchboards RM 1.2 a RM 1.3. The analyser BK 550 MULTI was used for this purpose. The quantities of the input ranges were between 0.60 MW and 3.30 MW.



Figure 42 Switchboard RM 10

Measurement and evaluation of slewing gear drive input

The drive input of HS KK 1300 slewing gear consists of 6 engines 1LGA-316-5ZZ64-Z, capacity 55 kW (source – alternators situated in switchboards RM 7.13 (engine modules 25M1-3) and RM 7.14 (engine modules 25M4-6)).

Measurement and evaluation of lateral force in the bucket wheel

For the measurements tensiometric sensors fixed in diagonal of bucket wheel construction were used.

The lateral force of KK 1300.1-CZ/K111 bucket wheel was measured in switching room on the switchboard DT27.2 (system ČASO company DAP Brno, measuring card DAQCard-AI-16E-4 and with measuring computer ASUS A6Jc with software FlexPro 5.0).

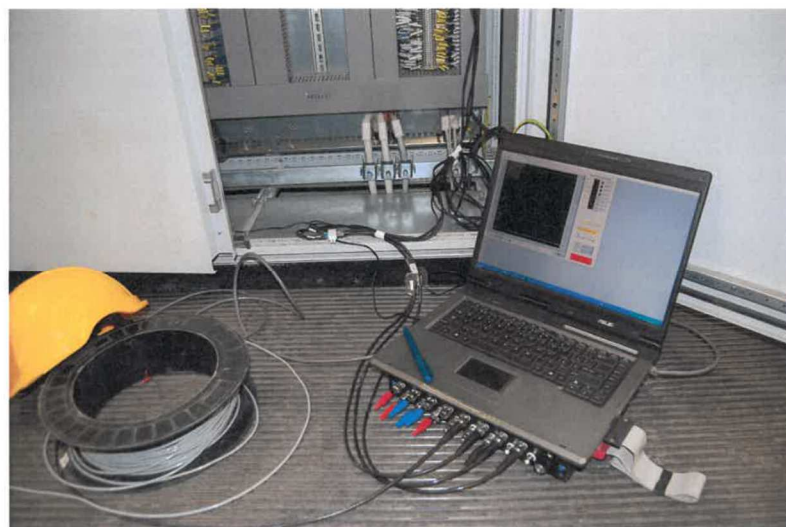


Figure 43 Measurement of bucket wheel lateral force

Measuring of the volume of mined overburden rocks

The volume of mined material was registered as a result of the measurement of weighing machine (part of the belt conveyors system). Driving system DPD, software FlexPro 5.0.

The second method was geodesic survey of the mined rocks block occurred before the start of the test and after the test.

Measuring of the cuttings depth

The registration of the cuttings depth was realised from the driving system. Non – contact, laser telemeter was situated in the probe, 5 meters from the belt of the caterpillar carriage.

Thermovision measurement

The realisation of thermovision measurement of electrical equipment and transformers during mining was the important part of the test. Second part of this measurement was detection of the tooth warming. The temperature changes are shown in Figure 44.



Figure 44 Thermovision measurement of teeth and buckets

Progress of the measurement

The measurement of mechanical and electrical quantities was realised in the second overburden cut with five benches. The measurement of digging resistance started 29. 11. 2017 at 10.10 a. m. and finished 29. 11. 2017 at 11.12 a. m. The measurement was realised in the third bench. The digging resistance ranged between $103 - 155 \text{ kN.m}^{-1}$.

Measurement of the lump size of the mined rocks

The measurement of the lump size of the mined rocks was realised with the use of snaps methodology. All pieces with the edge longer than 400 mm were evaluated. The results are shown in the Table 10

Table 10 The lump size of mined rocks (KK 1300.1 CZ, 29.11.2017)

Size (mm)	400 450	450 500	500 550	550 600	600 650	650 700	700 750	750 800	800 900	900 1000	1000 1100	1100 1200	1200 1300	1300 1400	general size
Number of pieces	45	18	11	10	9	3	8	3	6	6	2	3			124
Number of pieces/100 bm	150	60	37	33	30	10	27	10	20	20	7	10			414
Number of pieces/100 bm (%)	36.3	14.5	8.9	8	7.3	2.4	6.5	2.4	4.8	4.8	1.7	2.4			100%

Vibration measurements

Vibration measurement was realised in repose (no operation of the excavator). We realised necessary force impulse for vibration by breaking of the experimental steel pole (between bucket wheel boom and bulldozer situated on the overburden cut surface). Because of movement of bucket wheel boom started stress and breaking of the steel pole and vibration of the machine. The dimension of the experimental pole breaking was 150kN.

3 measurements were realised. (2 measurements in insert position of boom, 1 measurement in lowered position of the boom. Measured value of mechanical vibration was acceleration [m.s⁻²] of movement in concrete direction.

Measured values were detected with sampling frequency 50 samples/1 s (10 series), it was stored as txt files in notebook.

Situation of the sensors is shown in the report.

3 – axis sensor was situated on the left side of bucket wheel on the upper surface of drive gearbox. First axis is vertical to the axis of bucket wheel, second axis is parallel to axis of wheel and the third axis is parallel to axis of bucket wheel.

1 – axis sensor was situated in the right girder of bucket wheel. The detected direction of vibration was vertical to the bucket wheel axis.

The last 1 – axis sensor was situated on the right side of the end of the balance bucket wheel. It detected vibrations in vertical direction.

Measured data of mechanical vibration were detected by measure card and uploaded to the hard disk of computer. The conversion of these data to measured physical values follows.

Average values of vibration own frequency of the upper excavator construction according the table follows:

Insert bucket wheel boom	bucket wheel boom	$f = 0.793 \text{ Hz}$
	balance bucket wheel boom	$f = 0.792 \text{ Hz}$
Lowered bucket wheel boom	bucket wheel boom	$f = 0.668 \text{ Hz}$
	balance bucket wheel boom	$f = 0.681 \text{ Hz}$

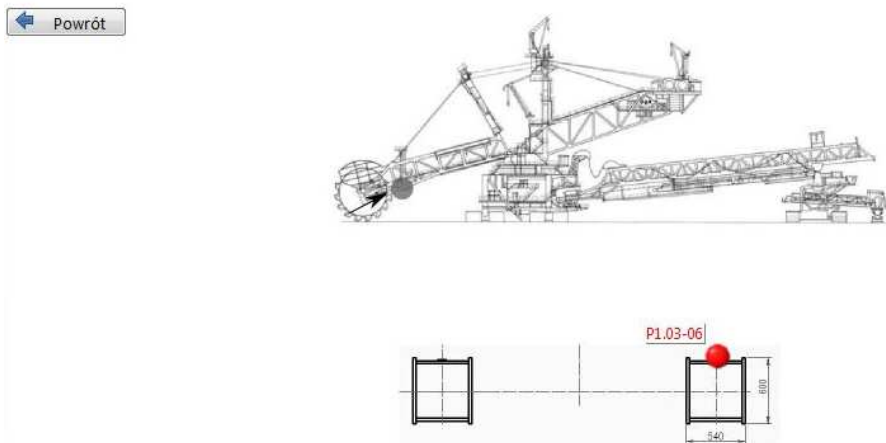
WP 2.3 Major achievements:

- strength analysis of KU 800.7 excavator;
- application of complex measurement system in the excavator KK 1300;
- frequency measurement (definition of parameters of stresses distribution in bucket wheel excavator load carrying structure) in the excavator KU300.30/K9102.

2.2.2.4 WP-2.4 Experimental verification of obtained results through tests of the monitoring system in exploitation conditions

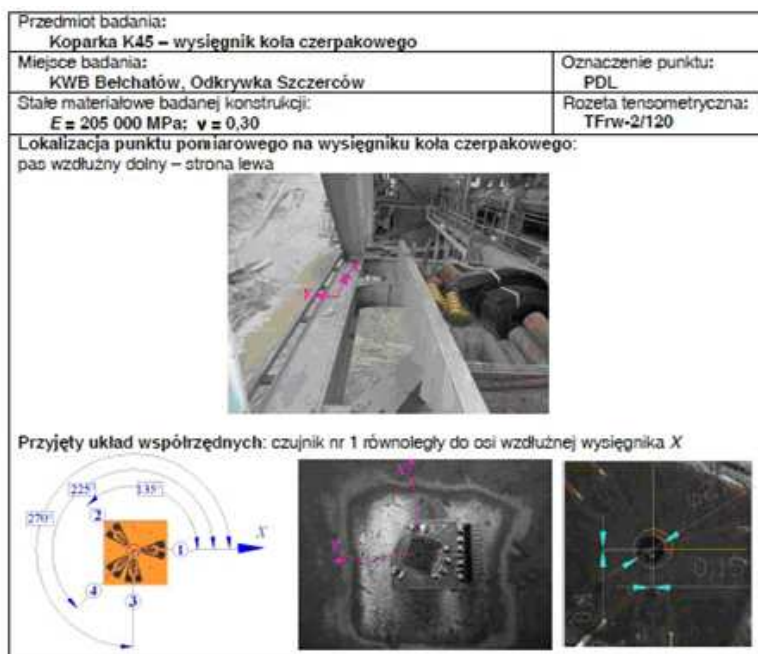
After starting the monitoring system at the excavator, experimental studies commenced. The tests were carried out during the normal operation of the excavator. It operated at the overburden of the III-IV class of workability. The tests were performed in a continuous manner, measuring the increments of dynamic stresses originating from the excavator loads due to the mining process. An indication of the extensometer sensors during the stoppage of the excavator was taken as a so-called zero level.

Before starting the measurements of dynamic stresses, a value of static stresses was measured, derived from the excavator's own loads (mainly its own weight). Due to specific construction of basic machines, these loads may account for up to 80% of all loads affecting their load-bearing structures. Although their impact on the fatigue process is not significant, they obviously have a decisive influence on the level of stress values derived from immediate loads. A drill hole method was used to measure static stresses. Figure 46 Measurement report of static stresses. A lower left girder of the bucket wheel boom gives an example of a report on static stresses measured at one of the elements of the bucket wheel boom. The tests were performed for the same elements of the load-bearing structure, which were then subjected to dynamic stress tests.



NATIONAL INSTRUMENTS
 LabVIEW™ Evaluation Software

Figure 45 Measuring points at the bucket wheel boom - boom hanging area, lower left girder point P1.03.06



Średnica i położenie otworu odciążającego oraz zmierzone odkształcenia:

$D_0 [\text{mm}]$	$\epsilon_x [\text{mm}]$	$\epsilon_y [\text{mm}]$	$\epsilon_z [\text{mm}]$	$\epsilon_{11} [\%]$	$\epsilon_{22} [\%]$	$\epsilon_{33} [\%]$	$\epsilon_{44} [\%]$
2,04	-0,15	-0,1	-0,101	0,018	-0,007	-0,134	

Kierunki i wartości naprężeń ekstremalnych:

Rozeta	$\alpha [^\circ]$	$G_1 [\text{MPa}]$	$G_2 [\text{MPa}]$	$G_{12} [\text{MPa}]$
R 1-2-3	-24	51	-25	67
R 1-2-4	-24	51	-25	67
R 1-3-4	-24	56	-30	75
R 2-3-4	-24	51	-25	67
Srednia	-24	52	-26	69
95% PU	0	4	4	7
Badający:		Sprawdził:		

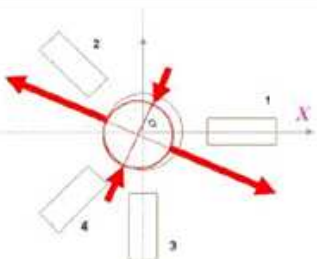


Figure 46 Measurement report of static stresses. A lower left girder of the bucket wheel boom

During tests, the following up to date information is provided to the user:

- Residual time (residual fatigue life). Calculated on the basis of a total number of Nc cycles at individual measuring points with reference to a number of the registered cycles N or Np. The presentation of the calculation results refers to the estimated time left until a possible fatigue failure at the monitored point.
- Maximum stress recorded in the stress spectrum table for the entire monitoring period.
- Maximum stresses occurring in a time interval of 150 s for a period of 1h during the last hour's operation to the system, mean stresses calculated from all indications in a time interval of 150 s for a period of 1h.
- Maximum stresses occurring in the interval of 1h for a period of 24 h, average stresses calculated from 24 mean indications of every 150 s for a time interval of 1 h over a period of 24 h.
- Information on exceeding certain warning levels of stresses (above 170 MPa, above 240 MPa), for 30 days back.

During 8 months of system operation at the selected measuring points of the bucket wheel boom and feeder bridge of the tested excavator the fatigue strength threshold for S 355 JO steel was not exceeded.

With regard to static stresses, it was found that their values in the measured points at the bucket wheel boom and the feeder bridge did not exceed 100 MPa. Therefore, the value of total immediate stresses at these points, even for occasional values of the registered maximum amplitude increments of about 175 MPa, will be 275 MPa, which is lower than the yield strength Re for S 355JO steel equal to 360 MPa. Of course, it can always happen that during further exploitation of the excavator there will be short-term local exceedances of the allowable immediate stress values, which may cause, for example, damage to the surface layer of the load bearing structure elements, and thus create conditions for fatigue concentration and its further development. Then, fatigue cracks can appear and develop at the values of dynamic stresses far below the fatigue limit Zg0. Hence, the system level values were set at: the warning level at 170 MPa and the alarm level at 240 MPa, so that the possible occurrence and development of fatigue cracks could be prevented. In both cases, the indicated elements of the load bearing structure should be particularly supervised and controlled as potential outbreaks of fatigue.

The system presented above, after designing and construction, was subjected to laboratory tests and after confirming its operational correctness, it was mounted at the load bearing structure of the SchRs 4000.37.5 excavator at KWB "Bełchatów". Then, it was subjected to operational tests during the normal operation of the excavator. The tests included continuous measurements of dynamic stress increments recorded during 8 months of operation of the excavator that mined overburden of the second and fourth class of workability, and one-time measurements of static stresses.

The obtained test results allowed for the following statements:

- the system works properly both in terms of fatigue strength and immediate strength assessment,
- during the testing period, the thresholds of fatigue strength and immediate strength for all tested components of the load bearing structure were maintained,
- the most loaded components of the tested load-bearing system include the elements of the bucket wheel boom and two elements of the feeder's bridge,
- selected elements of the mining boom and feeder bridge due to the relatively high rate of increase in the value of dynamic stresses and static stresses should be carefully controlled as potential sites of the occurrence of fatigue cracks.

The novelty of the mounted system includes continuous effort monitoring of the load-bearing structure, on line processing and analysis of measurement results, determination of the fatigue life and immediate transmission of the resulting information to a user.

In addition, an important novelty is a possibility to determine a current number of fatigue stress cycles that have been transferred by the load-bearing structure, which then allows the assessment of fatigue life with regard to machines subjected to long-term use. This is very important due to the fact that such machines constitute the majority in brown coal opencast mines. Continuous monitoring will be used simultaneously for an ongoing assessment of immediate strength, which has not been applied before in the studies concerning load bearing structures of open cast mining machines.

The above mentioned actions will enable a relatively accurate assessment of effort and, as a final result, an answer to a question which has not yet been answered, i.e. **how long the load bearing structure of the tested machine can be safely exploited**.

The answer obtained in this way results in many advantages related to the application of the above system in the current operation of opencast mining machines, which may include:

- taking measures preventing fatigue failures of the load-bearing structure in the form of appropriate early planning of renovations or exchanges of specific elements and assemblies,
- taking urgent actions preventing the load bearing system failure due to exceeding the immediate strength thanks to alarm signals sent to the user and machine operation team, which then allows, for example, quick switching off the mechanisms, etc.,
- receiving information on various local exceedances of permissible level of immediate strength of the load-bearing structure by machine users, e.g. during various types of machine collisions with escarpments with regard to individual operational sets, etc.,
- achieving an increase in durability of load-bearing systems of basic machines and a reduction of costs related to their operation (e.g. reduction of costs and time of repairs, reduction of duration and a number of stoppages due to failures) on a mine scale,
- obtaining information about real stress level in the load-bearing structure, which can be used for various types of technical condition assessments, upgrades, reconstructions, etc., as well as for planning technologies and future machine operation fronts,
- increasing operational safety of opencast mining basic machines.

WP 2.4 Major achievements:

- development of experimental system of monitoring of stresses in load carrying structure of the excavator body which is installed on SchRs 4000 excavator in Bełchatów mine;
- development of software for monitoring of measurement systems, as well as collection and processing of data and their presentation;
- development of instructions for monitoring system construction, determination of measured parameters and method of analysis and data distribution.

2.2.3 WP-3 Real-time mine-face inspection system, based on geophysical methods, capable to detect hard rock inclusions and geological formations which are difficult to be excavated by bucket-wheel excavators

2.2.3.1 WP-3.1 Collection and analysis of geological information for geophysical methods selection.

Implementing Task-3.1 a literature review on the geophysical methods used in geo-engineering applications and especially for the assessment of properties and characteristics that affect the digability of geological formations has been conducted. The review focused on formations that are commonly associated with lignite deposits, like clay, sandstone and conglomerates, occurring as overburden or intercalations.

In order to clearly define the requirements, specifications and limitations of the geophysical methods and equipment on the basis of specific data, a questionnaire was prepared by NTUA and the consortium partners were asked to provide data of operating lignite mines. The requested data were grouped in eight Sections pertaining respectively to general mine data, geological data, mine configuration, installed monitoring infrastructure, excavated material data, material difficult to excavate, bucket wheel excavators, and prior geophysical projects. Two additional Sections were provided for submitting in free text format typical excavation problems encountered in the mine, additional information that the partner considered important, and comments regarding the submitted data.

All industrial partners provided the requested data they had available. Table 11 lists the mines for which data were submitted. The main findings are given in tables below.

Table 11. List of lignite mines

No.	Country	Mine	Coordinates (degrees)	Data provided by
1.	Czech Republic	Bílina	N50.5703544 E13.7110790	VUHU
2.		ČSA	N50.5488439 E13.5345258	
3.		Vršany	N50.4918986 E13.5552111	
4.	Greece	South Field	N40.4180833 E21.8378000	PPC
5.	Poland	Szczerów Field	N51.2466667 E19.1186111	PGE
6.	Romania	Husnicioara	N44.6702778 E22.7600000	CEO

Table 12. Environmental conditions

Mine		Bílina	ČSA	Vršany	South Field	Szczerów Field	Husnicioara
Elevation (m)		200-300		660	180	320	
Climate		Cool to temperate continental		Humid continental	Humid continental	Humid continental	
Annual temperature (°C)	min	-15		-1	-24	-28	
	mode	15		N/A	N/A	12	
	max	35		29	38	41	

Table 13. BWE characteristics

Mine	Bílina	ČSA	Vršany	South Field	Szczerów Field	Husnicioara
Service mass (t)	5560	4360	4360	3886	8107	1452
Inverter (units x kVA)	2×1150	2×800	2×800	No	6×400	No
Motor (units x kW)	2×1150	2×800	2×800	3×700	6×200	2×630
Motor RPM	993	993	993	N/A	990	980
Motor frequency (Hz)	8.26-19.84/ 50	8.26-19.84/ 50	8.26-19.84/ 50	50	N/A	50
Motor voltage	400-690V	400-690V	400-690V	20kV	500-690V	6kV
BW diameter (m)	13.5	12.6	12.6	17.5	17.5	11.5
Bucket capacity (m ³)	1.3	1.3	1.3	3.7	4.6	1.8
Pre-cutters	No	No	No	Yes	Yes	Yes
Chain back	No	No	No	Yes	Yes	No
Rock deflectors	No	No	No	No	No	Yes

Table 14. Inverters on BWEs.

Mine	Bílina	ČSA	Vršany	South Field	Szczerców Field	Husnicioara
BWEs with inverter	12	9	9	-	5	-
BWEs without inverter	26	26	26	9	6	5
Total BWEs	38	35	35	9	11	5

Table 15. Excavation characteristics.

Mine	Bílina	ČSA	Vršany	South Field	Szczerców Field	Husnicioara
Multi-layer	Yes	No	Yes	Yes	No	Yes
Selective mining	Yes	No	No	Yes	Yes	Yes
Max block height (m)	35	32	32	33	50	22
Max block width (m)	81	75	75	57	110	50
Working method	Terrace	Terrace	Terrace	N/A		Terrace
Minimum height of cut (m)	0.6	0.6	0.6	N/A		N/A
Max typical height of cut (m)	6.7	6.3	6.3	(8.75)		4.7
Max depth of cut (m)	0.62	0.5	0.5	N/A	1.6	0.81
Max cutting speed (m/s)	3.9	3.7	3.7	3.02	5.0	2.81
Max slewing speed (m/s)	1.06	1.06	1.06	0.58	0.58	0.5
Max boom vertical speed (m/s)	0.15	0.07	0.07	0.08	0.12	0.1
Max BWE travel speed (m/s)	0.6	0.6	0.6	0.17	0.17	0.1

Table 16. Availability of data relevant to geophysics.

Mine	Bílina	ČSA	Vršany	South Field	Szczerców Field	Husnicioara
Water table depth	✓	✓	✓	✓	✓	✓
Layer thickness	✓	✓	✓	✓	✓	✓
Clay minerals content	✓	✓	✓			✓
In-situ apparent density	✓	✓	✓		✓	✓
Porosity						✓
In-situ moisture	✓	✓	✓		✓	✓
Permeability	✓	✓	✓			
Grain size distribution	✓	✓	✓			✓
Texture	✓	✓	✓			✓
Color	✓	✓	✓	✓	✓	✓
Reflectance	✓	✓	✓			
Relative permittivity	✓	✓	✓			
Resistivity	✓	✓	✓			
Attenuation						
Prior geophysical surveys	✓		✓		✓	
Geophysical reports	?		✓		In Polish	

Table 17. Formations hard to excavate.

Mine	Bílina	ČSA	Vršany	South Field	Szczerców Field	Husnicioara
Continuous layers	Yes	Yes	No	Yes	Yes	No
Boulders	Yes	Yes	Yes	No	Yes	Yes
Boulder material	Quartz Siderite Ankerite Kaolinite	Clayey siderites	Quartz Ankerite Siderite Kaolinite		N/A	Sandstone
Matrix material	Claystone Sand	Claystone	Claystone Sand		Sand Gravel Clay Loam	Claystone Sand
Size	0.2-15 m	0.1-1 m	0.2-3 m		0.1-10 m ³	0.5-15 m
Shape	Spherical	Slab	Spherical	Irregular	Oval	Irregular
Density (kg/m ³)	2200	2300	2200	2400- 2700	N/A	2340
Compressive strength (MPa)	15-20	10-35	15-25	15-143	N/A	40-45

Table 18. Installed monitoring infrastructure.

Mine	Bílina	ČSA	Vršany	South Field	Szczerów Field	Husnicioara
Optical fiber	No	No	No	Yes	Yes	No
Wireless	Yes	Yes	Yes	Yes	Yes	No
Stress	Yes	Yes	Yes	Yes	Yes	No
Strain	Yes	Yes	Yes	Yes	Yes	No
Acceleration	No	No	No	Yes	No	No

Taking into account the reported geologic setting, the specifications of the excavating equipment used in the mines and the employed working methods bibliographic research have been conducted.

The evaluated geophysical methods were: ground penetrating radar, geoelectric, electromagnetic, combined electromagnetic and electrical resistivity, infrared detection and optical sensors, seismic reflection, gravity, magnetics, x-ray fluorescence, natural gamma radiation, and body sound analysis.

The evaluation indicated that in the generally similar geologic environment of the examined mines the electromagnetic induction and resistivity methods are able to outline lateral inhomogeneity, while the GPR method can do so if the signal can pass through the conductive clayey materials before facing the hard formations.

Infrared detection and optical sensors cannot be used to see ahead of the face. However, they could be used for assisting material detection and calibration of other methods based on the optical properties of the excavated materials.

The seismic reflection method is good for detecting layer interfaces. In a quite environment it can be used for detecting layer boundaries. The detection of bodies is dependent on depth. However, the echo signal is severely influenced in noisy environments, thus the method cannot be applied by any technique with a device attached on a BWE.

Gravity and magnetics are reconnaissance methods for surveying wide fields of mining interest. They cannot accurately focus in a certain depth in the conditions of an operating opencast mine or when attached on a BWE.

X-ray fluorescence devices require firm placement on the target and cannot be used remotely, which makes them inappropriate for the given purpose.

Natural gamma radiation is limited to mines with shale as host rock and needs frequent calibration.

Like infrared detection and optical sensors, body sound analysis cannot be used to see ahead of the face. However, it could be used for assisting material detection and calibration of other methods based on characteristic vibration frequencies that may be associated with certain materials.

Positioning technologies, data transmission technologies, signal processing/analysis, and visualization techniques were reviewed in addition to the geophysical methods, in order to highlight critical issues in the development of the real-time hard inclusions detection system.

Probably the major challenge in the development of the system is the implementation of the visualization subsystem. The output of geophysical measurements may be comprehensible in the eyes of an experienced geophysicist but provides little or no information to the layman.

The ultimate objective of BEWEXMIN's WP-3 was to develop a prototype that would be able, based on continuous geophysical measurements, to provide in real-time and in a visually meaningful way information on the materials anticipated to be encountered in the next few cuts of the face. This information would ideally be displayed on a monitor installed in the BWE's operator cabin.

In this regard, each geophysical method has a certain type of output that defines and confines what can be done.

Measurements with the apparent resistivity, resistance with resistivity, and apparent electromagnetic conductivity methods actually are a single numerical value for each surveyed point and therefore can be easily overlayed on a map. If the measured numerical value is stored in a database record along with its spatial coordinates (xyz absolute or relative to some predefined coordinate system) the data records can be used to provide a colour coded layer on an image or drawing of the excavated face. For example, colouring according to the conductivity values could indicate the presence of rigid formations, coarse material, fine grained material or clayey loose material. If such a layered image is refreshed in real-time or near-real-time (e.g. every 5 s) a change in conductivity colour could indicate to the BWE operator the presence of hard formations or local features.

The presentation of GPR data has a higher complexity. On color-coded slice maps or 3D cubes high amplitude reflection signals can accurately indicate interfaces of closed shapes, like boulders, or layers. If GPR is combined with electric or electromagnetic methods the boulder or layer material can be identified lithologically. Here, as in the previous case, colour change on the display could indicate the presence of hard formations or local features.

It becomes obvious that the visualization subsystem has to integrate images and measurements of various modalities and fuse them in one consistent image of the 2D projection of the cut face. This concept is illustrated in Figure 47.

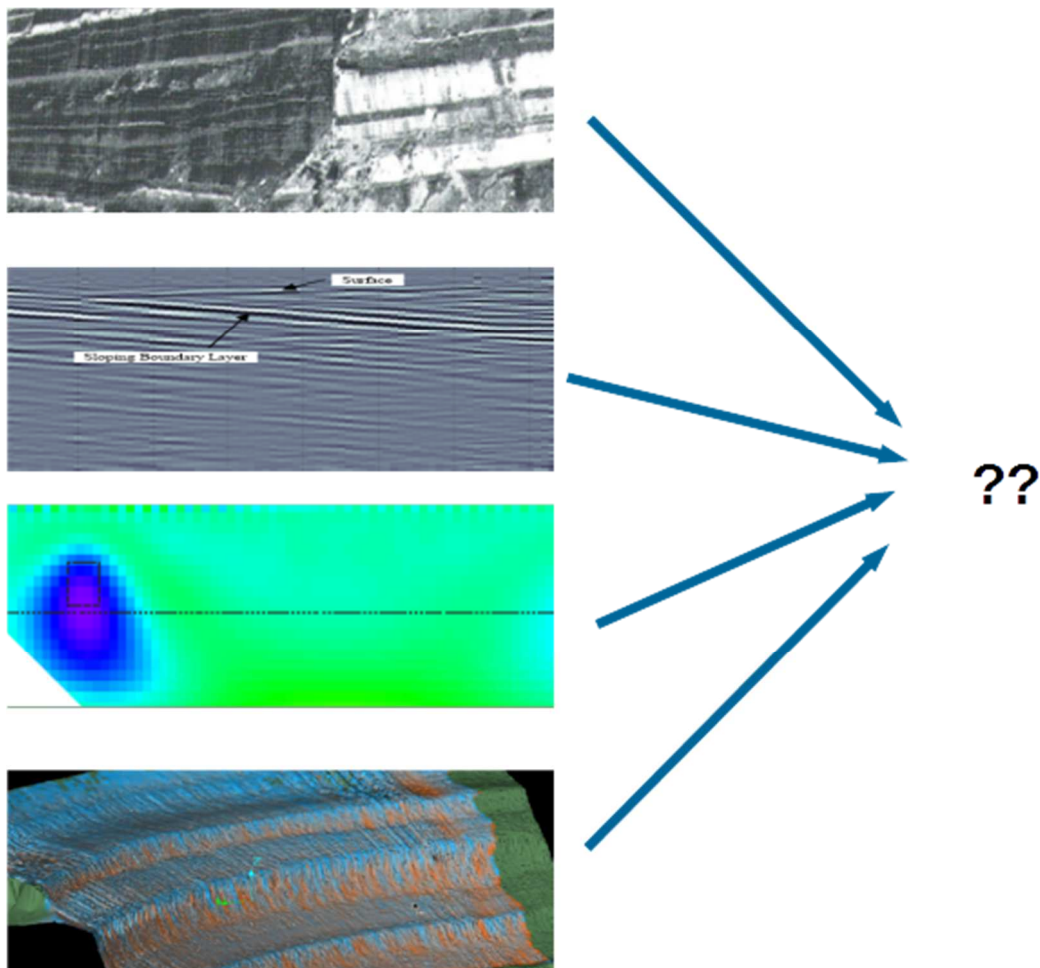


Figure 47. Integration of images and measurements of various modalities.

The scope of the system is conceptually illustrated in Figure 48. The approach is to focus on the area where the actual problem of digging into hard inclusions may take place, namely the excavation face of the BWE. The goal is to extract and visualize useful information on the existing ground conditions from geophysical data for a few cutting depths ahead of the face, typically in the range from one to three meters.

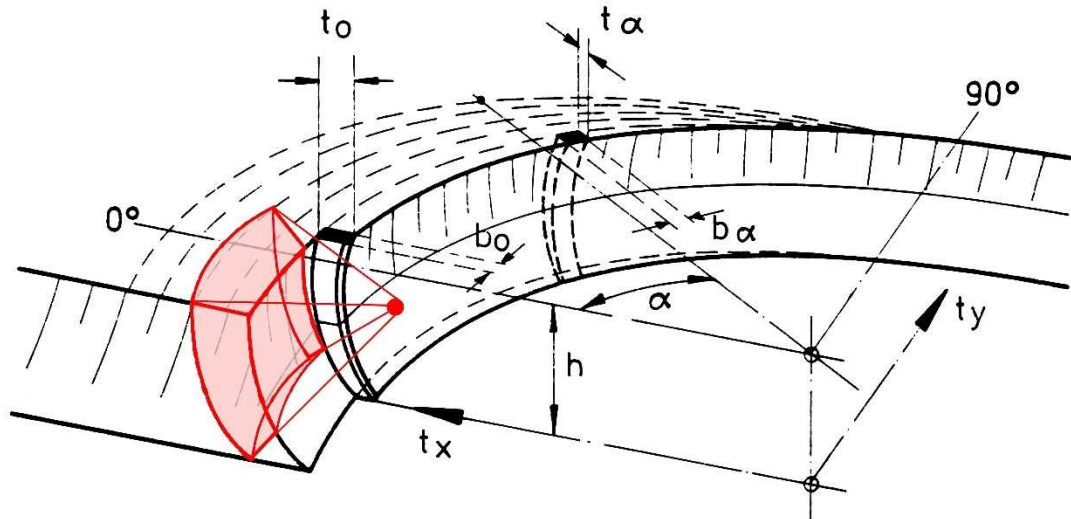


Figure 48. Scope of the hard inclusions detection system

Several critical issues have been identified in Task-3.1, such as:

- the harsh mining environment. Extreme temperature variations in the range of -30 to 45 °C, humidity and precipitation, dust, machine vibrations, massive steel structures, and electromagnetic interferences impose the need for rugged equipment that can withstand these conditions and remain operational and reliable;
- high data volume and transfer rates have to be managed;
- high computational throughput is needed for processing the raw data by using high-complexity algorithms in a relatively short amount of time;
- precise positioning is required for minimizing the margin of error.
Different data modalities have to be fused into spatially located information and simple, comprehensible visual and audio messages.

WP 3.1 Major achievements:

- review on the geophysical methods used in geo-engineering applications and especially for the assessment of properties and characteristics that affect the diggability of geological formations;
- taking into account the reported geologic setting, the specifications of the excavating equipment used in the mines and the employed working methods, limitations of the evaluated geophysical methods have been identified, requirements were defined, and a plan for developing the real-time hard inclusions detection system was set up.

2.2.3.2 WP-3.2 Report on field tests for the selection of the most appropriate geophysical method.

As presented in Deliverable D3-2, WP 3.2 deals with the geophysical field tests conducted at the South Field mine Kozani Greece (PPC), at the Szczerbow Field, Belchatow mine, Poland (PGE) and at Husnicioara Field and Rociuta Mines, Romania (OLTENIA). The most extensive and detailed field test program was carried out at the Power Public Corporation (PPC) coal mine. The geophysical investigation involved the following methods: Electrical Resistivity Tomography (ERT), Seismic Tomography (ST), Slingram (EM) electromagnetic method and Ground Penetrating radar (GPR). The assessment of four different methods in the PPC mines instead of two, as was initially proposed, was decided after the completion of the literature review. The implementation of two additional geophysical methods increases the confidence of the final decision about the most appropriate geophysical method.

GPR simulations

Simulations were performed in 2D and 3D, in order to examine the response of GPR in a stratified geological structure consisting of four layers, which exhibit the same conductivity, and boulders of various sizes. Two scan setups, against the mine face and below the bucket wheel, as well as GPR antennas of 100 and 250 MHz were used in the simulations.

The resulting radargrams (Figure 49) showed that in all examined scenarios the presence of boulders was detected at depths less than four meters. More realistic but time consuming 3D simulations are preferable for imaging the boulders. Thus, the simulations verified the potential of

the GPR method and justified further investigation through field tests that were performed in the context of developing a real-time hard inclusions detection system.

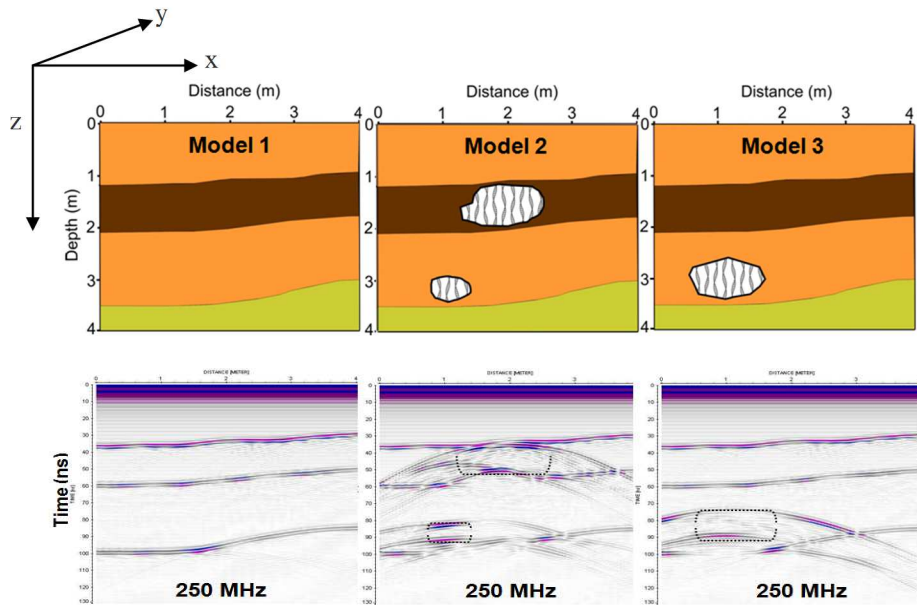


Figure 49. Simulated 2D models with the resulting radargrams using the GPR 250MHz antenna.

Collection and evaluation of the existing geophysical data

Existing geophysical data are from the lignite open-cast mine "Bełchatów" in Poland and the PPC open pit mines in Western Macedonia, Greece. Three geophysical surveys conducted at lignite open-cast mine "Bełchatów" employed gravity, electrical, seismic and GPR methods. Bouguer maps were generated from conventional gravity and microgravity surveys. Regarding the electrical methods, the resistivity profiling and sounding employed the Schlumberger and Wenner arrays. The seismic survey employed the seismic refraction and reflection methods. GPR cross-sections were carried out on mining levels from the lignite surface towards the expected occurrence of the Mesozoic hard rocks. GPR data were compared with geological information obtained from drilling. The electrical tomography was recently employed in an effort to locate boulders. Drilling data superimposed on the electrical resistivity sections at area IV indicate that high resistivity anomalies are related to sands and quartzites.

The available information for open pit lignite mines in the Western Macedonia consists of data and sections from geophysical surveys. The geophysical investigation at Aminteon field mine employed electrical and seismic tomography but could not image very thin layers of hard rock formations attributed to conglomerates. The geophysical survey at South Field mine employed the vertical electrical sounding and the GPR methods. The average resistivity values of the formations of interest at PPC open pit mine were deduced from the geo-electrical survey. The resolution with an 80MHz antenna is not adequate to provide information about small targets like hard rock inclusions.

Borehole data and laboratory tests

Several samples originated from the mines of the participating companies (PPC, PGE, OLTEANIA) were collected and analyzed in the laboratories of the TUC. The mineralogical composition of all samples was determined and their moisture, electrical conductivity and compressive strength (for hard rock samples) were also measured. The obtained laboratory data were also compared with the existing data, which were provided by the companies, to confirm and enhance our knowledge about the excavated materials regarding their interactions with electromagnetic and seismic waves used in the investigated geophysical methods.

Laboratory results indicated that the hard rocks formations of South Field mine (PPC) consist mainly of calcareous and minor of siliceous conglomerates, breccia and sandstones. The surrounding soft formations are mostly clays and lesser sands. The uniaxial compressive strength of hard formations varies from 15 to 35 MPa, the moisture ranges from 4 to 6% and the electrical resistivity from 0.9 kΩm to 5.0 kΩm. The surroundings clays indicate considerable lower resistivity ranging from 11.2 to 29.8 Ωm. The electrical properties of the examined samples are highly affected by the moisture content. The collected hard rock boulders from the Szczerbow Field, Belchatow mine, Poland (PGE) are limestone and siliceous rocks (granites) exhibiting high

compressive strength (30-60 MPa) and low moisture (<2%). Their electrical resistivity ranges between 53-260 kΩm while the surrounding formations consist mainly of sands and clays with considerably lower conductivity. Examined hard boulders from Husnicioara Field and Rociuta mines, in Romania (OLTENIA), were characterized as compacted sandstones, siltstones and volcanic rocks. Their compressive strength varies from 24.0 to 46.6 MPa and their electrical resistivity from 0.40 to 240 kΩm.

The examined samples were classified according to their moisture and resistivity values as shown in Figure 50. Classification of the examined samples according to their moisture and resistivity valuesSoft surrounding formations, like clays and argillaceous marls, are clearly distinguished from the included hard rock formations such as conglomerates, breccia layers and boulders of varying lithology (limestone, granite, sandstone, volcanic rocks).

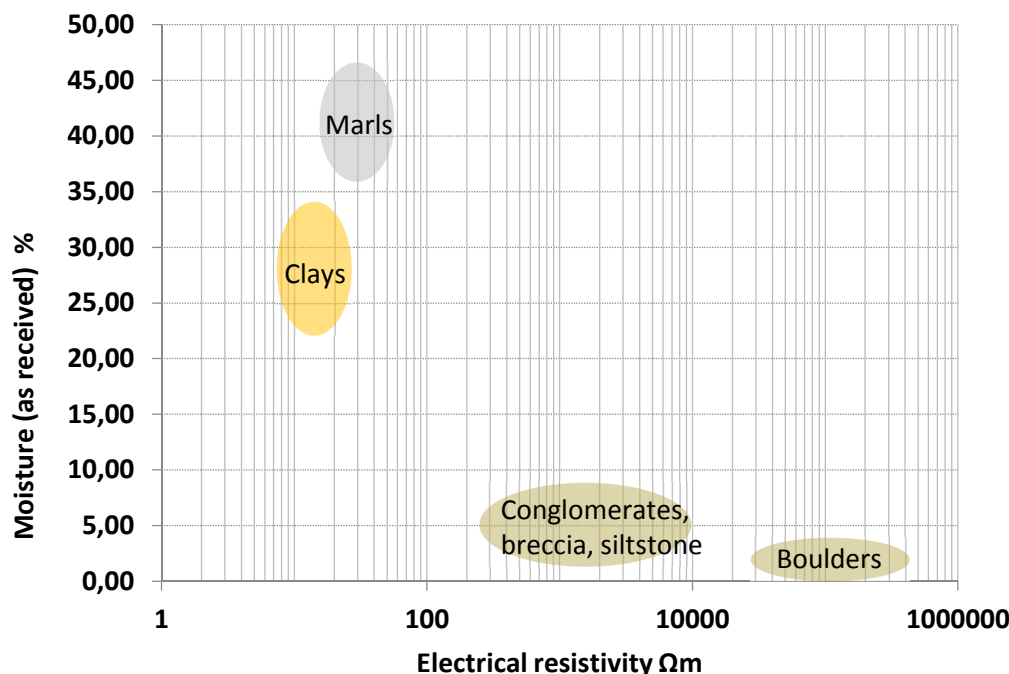


Figure 50. Classification of the examined samples according to their moisture and resistivity values

Geophysical survey at South Field mine Kozani Greece

The geophysical survey at South Field mine Kozani Greece, employed electrical, seismic and GPR methods. The electrical tomography employed two types of electrode arrays namely the Dipole-Dipole (DD) and the Wenner-Schlumberger (WS). The DD array enhances lateral variation of the electrical resistivity, while the WS array is more suitable to describe the vertical variation of the electrical resistivity. Electrical tomography detects two higher resistivity layers, attributed to conglomerates. The Slingram electromagnetic (EM) method was employed using the CMD from GF Instruments in order to measure apparent conductivity at two slopes. For comparison reasons the data from the bigger slope were coded using a color scale and were displayed next to the photo of the slope, indicating that hard rock layers consisting of conglomerates exhibit lower apparent conductivity values (Figure 51). GPR measurements, using a Mala Ramac system with two antennas (250 MHz and 100 MHz) were collected on two benches and two slopes at the overburden of the PPC South Field mine. The GPR sections at the slopes show changes on the direct wave arrival time and shape between the hard and soft rock layers. The 250 MHz GPR section at one of the benches images properly the hard rock inclusion which is seen at the smaller slope at a depth of 1.8m.

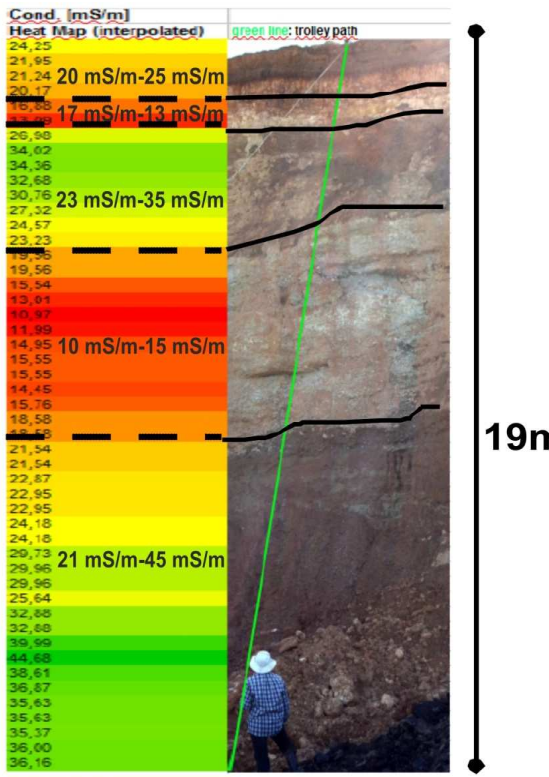


Figure 51. Range of apparent conductivity values deduced from the EM survey on the slope, next to a photo of the mine front. Lower apparent conductivity zones in red are observed next to hard rock layers.

Geophysical survey at the Szczerów Field, Belchatow mine, Poland

The multi-frequency Slingram electromagnetic (EM) method was employed in order to collect data at Szczerów Field using the EMD-400 Profiler and station spacing 0.25m. An artificial site was constructed at a location in the mine where the sub-ground material is the same with the material surrounding the hard boulders. A boulder whose size is approximately 1.5m x 1.5m x 1.5m was placed in an excavation larger than the dimensions of the boulder and covered with the excavated loose material. Then we made a trench around with special access ramp which provides the best research condition (Figure 52).

The artificial site was scanned along four lines using five frequencies namely 1kHz, 5kHz, 7kHz, 10kHz and 15kHz. The profiles of the apparent conductivity values along line in the radial direction show lower values at the limits of the excavated trench. Local minima, additionally observed both on the several profiles as well as on the apparent conductivity map at 15 kHz, are attributed to the buried boulder. Another small lower apparent conductivity anomaly attributed to the buried boulder is present on top of it at the flat part of the site.

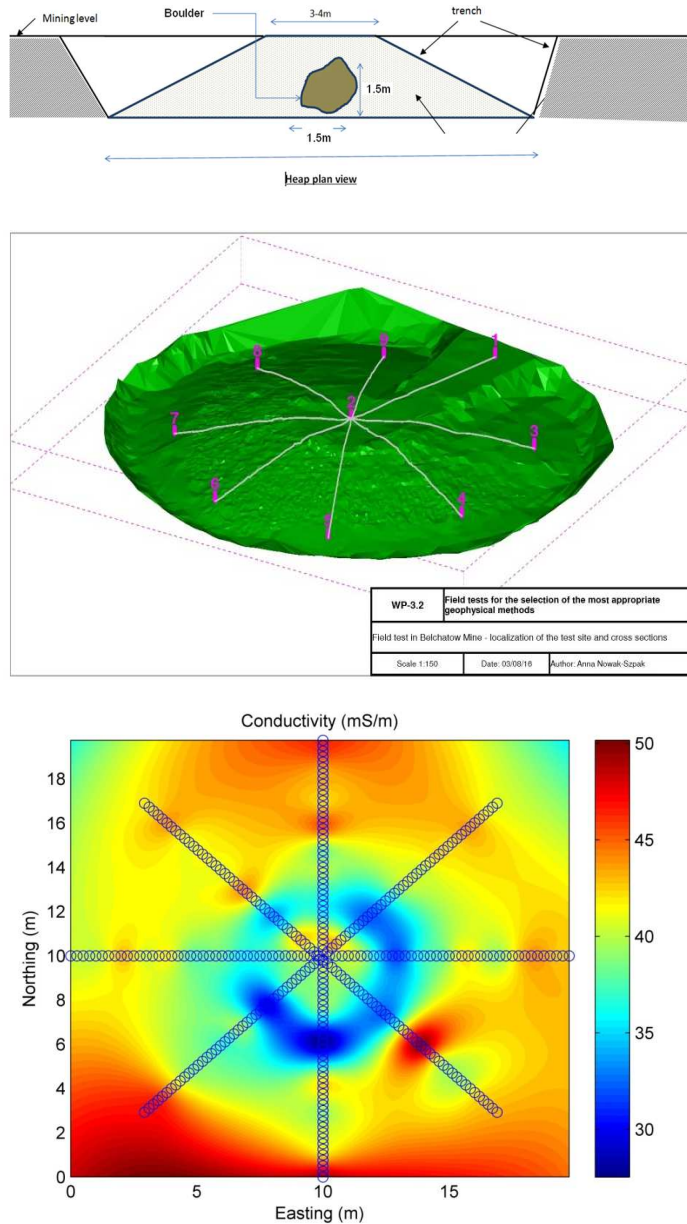


Figure 52. Apparent conductivity maps for measurements at the artificial site created at Szczerów Field Mine

Geophysical survey at Husnicioara Field and Rociuta Field Mines, Oltenia, Romania

The multi-frequency Slingram electromagnetic (EM) method was employed in order to collect data at three artificial sites two at Husnicioara mine and one at Rociuta Mine using the EMD-400 Profiler and station spacing 0.25m and 0.5m. For the artificial sites we chose an easily accessible flat site in the mine whose sub-ground material is the same with the material surrounding the hard boulders. We then placed a boulder whose size is approximately 1.5m x 1.5m x 1.5m in an excavation larger than the dimensions of the boulder and covered it with the excavated loose material. The burying depth is as close as possible to 1m. At Husnicioara Mine more than one smaller boulders were placed inside the excavation and covered by clay (clay site) and sand (sand site).

At Husnicioara Mine, the sand site was scanned along four lines with line spacing 2m using three frequencies namely 5kHz, 10kHz and 15kHz and the clay site was scanned along four lines with line spacing 2m using five frequencies namely 1kHz, 5kHz, 7kHz, 10kHz and 15kHz. The profile of the apparent conductivity show lower values on top of the excavated area indicating the limits of the excavation as well as the pile of boulders. The corresponding profile from the clay site show a less pronounced low apparent conductivity anomaly attributed to the pile of boulders but fail to indicate the limits of the excavated area.

At Rociuta Mine, the site was scanned along three lines with line spacing 0.5m and station spacing 0.5m using three frequencies namely 1kHz, 7kHz and 15kHz. The profile of the apparent conductivity exhibits a low conductivity anomaly at a distance of 14m which is more pronounced at frequency 1kHz. This anomaly attributed to a 1.5m x 1.5m x 1.5m boulder also present at the apparent conductivity maps and several pseudo-depth sections at frequencies 1kHz, 7kHz and 15kHz.

Selection of the most appropriate method

The selection of the most suitable geophysical methods for the detection of hard formations via real-time mine face mapping was based on Analytic Hierarchy Process (AHP). AHP is a multi-criteria decision technique that can be applied for the selection of one alternative from a given set of alternatives or for ranking the alternatives. The criteria used involved performance of the specific geophysical method in detecting boulders and hard layers, required geophysical and electronic equipment, data processing and evaluation, ability to work in harsh environment and ease of installation of the equipment on the boom of the bucket wheel excavator. The four investigated geophysical methods (alternatives) were ranked according to AHP methodology. AHP ranking indicated that GPR and Slingram (EM) are the most promising methods for real-time detection of hard rock during mining by BWE.

WP 3.2 Major achievements:

- Geophysical field test in South Field, Bełchatów, Rociuta and Husnicioara Mines.
- Selection of the most appropriate methods for real-time detection of hard mineable obstacles during BWE operations.

2.2.3.3 WP-3.3. Hardware development and installation on the BWE.

In order to examine the hardware setup in the relevant environment of a BWE operating on an actual excavation face, the EM instrument and a differential GPS receiver were mounted by means of a 6m long fixed wooden beam on one of PPC's BWEs in the South Field mine. The material and length of the beam kept the EM instrument at a distance sufficient to minimize any Electromagnetic Interference (EMI) due to the massive steel structure and electric motors of the BWE (Figure 53).

A series of conductivity measurements was taken with this setup on a face with hard inclusions. In the resulting conductivity map (Figure 54) the layer of hard material, which has a low conductivity value, is clearly detected. However, the variation of conductivity cannot be solely attributed to the different materials present at the face. During the test it was observed that the air gap between the EM instrument and the face was varying due to the undulations on the face surface, acting as an irrelevant source of conductivity variation.

Moreover, it was observed that the fixed geometry of the beam was suitable only when the BW was engaging the face at a specific cut height. In order to adjust to all possible cut heights, the mounting setup must be able to rotate across an arc, corresponding to the lower front quadrant of the BW, and point the EM instrument towards the face.

For finalizing the specifications of the mounting setup, a series of measurements was taken for determining the minimum safe distance between the EM instrument and the BW with respect to EMI. The findings showed that no significant EMI was observed for distances greater than 4m (Figure 55). The concept of the new mounting setup is shown in Figure 56 and Figure 57.

In addition, a series of reliable conductivity measurements was taken manually by utilizing a bucket truck (Figure 58). These measurements are used for the development and validation of the data processing and expert systems.

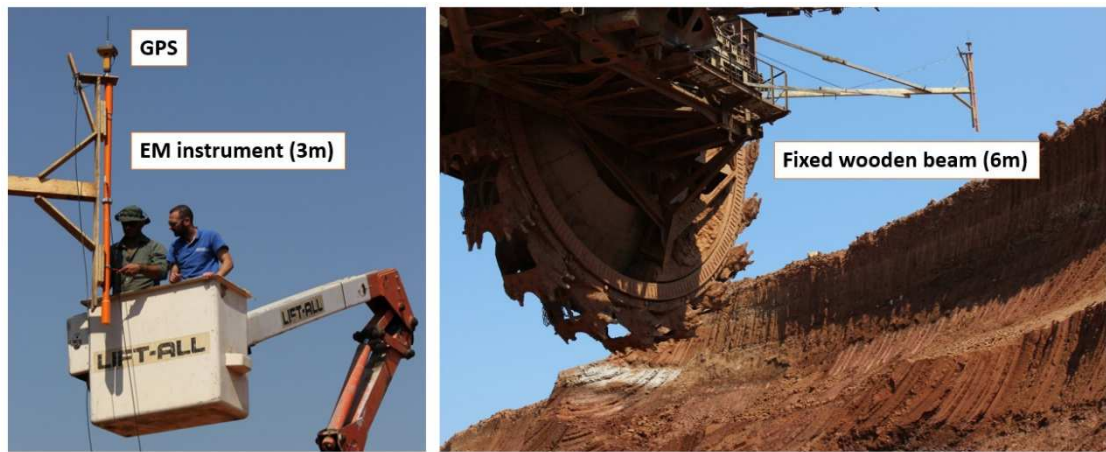


Figure 53 Mounting of EM instrument and differential GPS on the 6m long fixed wooden beam on one of PPC's BWEs in the South Field mine.

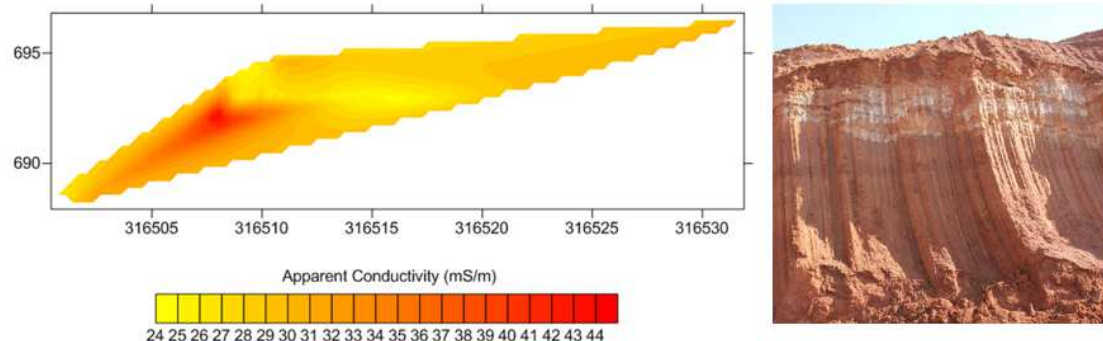


Figure 54 Conductivity map of the mine face surveyed by the EM instrument mounted on the BW. The layer of hard material, which has a low conductivity value, is clearly detected.

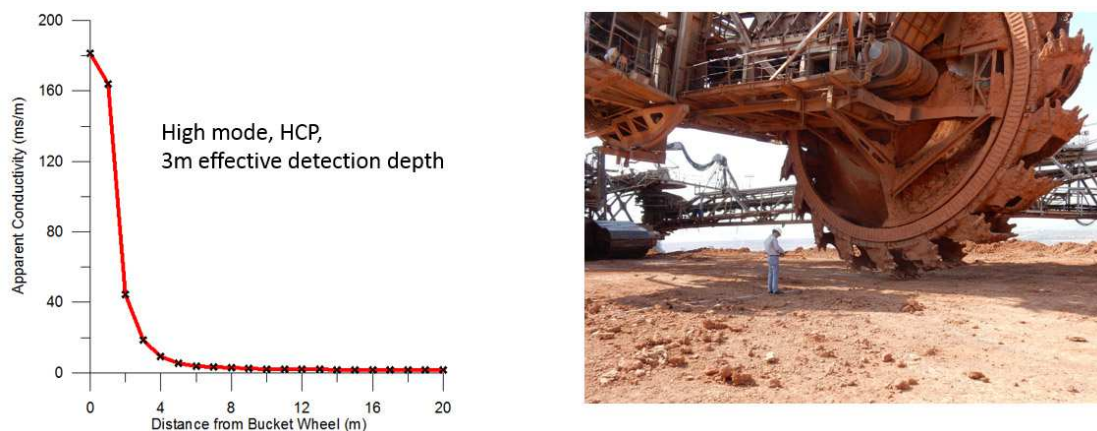


Figure 55 Determination of the minimum safe distance between the EM instrument and the BW with respect to electromagnetic interference.



Figure 56 The concept of the new mounting setup

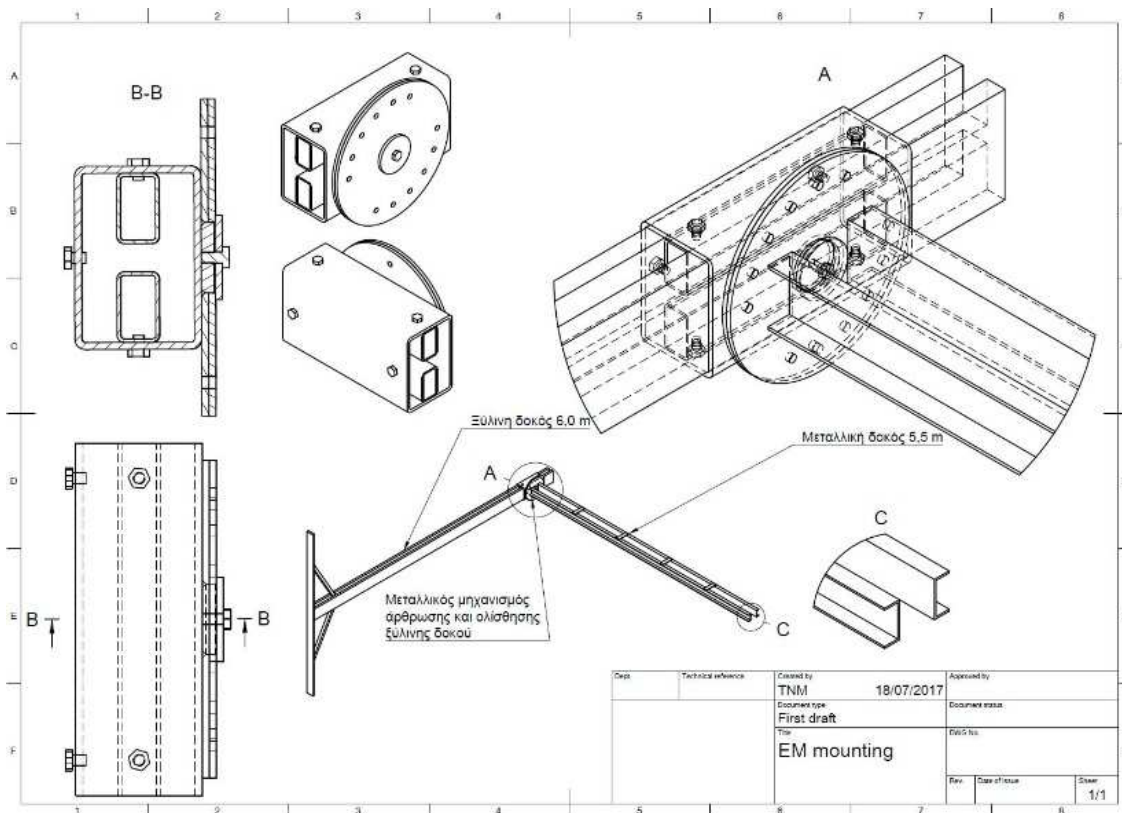


Figure 57 Design details of the new mounting arm.

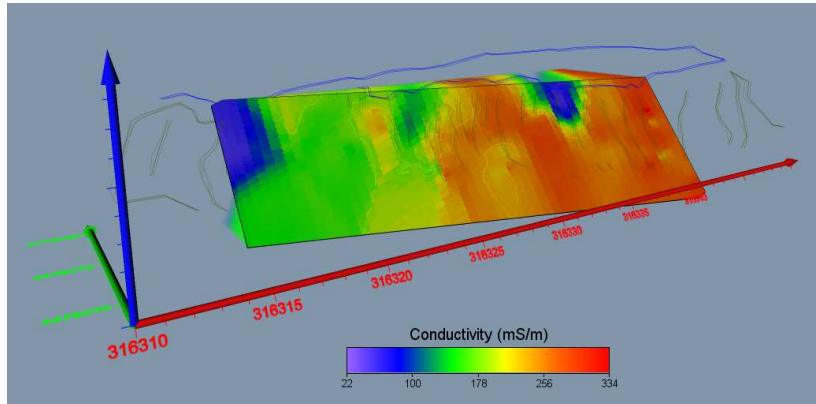


Figure 58 3D conductivity map of the mine face surveyed by the EM instrument using the bucket truck. The inclusions of hard material, which has a low conductivity value, are clearly detected

WP 3.3 Major achievements:

- Manual conductivity measurements using a bucket truck for validation of the data.
- Development of the first version of mounting arm.
- Design of the second version of mounting arm for purposes of WP 3.5 and WP 3.6.

2.2.3.4 WP-3.4 Development and testing of an automated algorithm for geophysical data processing and evaluation.

WP 3.4 involved the development of the algorithm for automatic processing of data obtained from the geophysical sensor (Electromagnetic conductivity-CMD2) and positioning system (Differential Global Positioning System, DGPS). First the overall system for data collection, pre-processing and evaluation was designed (block diagram). Subsequently, existing evaluation methods and algorithms were examined and the creation of the synthetic data required for the first phase of the development was completed. Several numerical, statistical and neural network models were created and tested with synthetic data as well as with data collected from the field test carried out in the coal-mines of the PPC and CEO. Two different evaluation approaches were investigated, a relative simple one (Simple Mode) based on statistical process control and a more sophisticated one (Advanced Mode), based on PPI (Position Prominence Index) and on NNPR (Neural-Network based Pattern Recognition). The respective algorithms (software) were developed within Matlab programming environment. Both methods (simple and advanced) were tested extensively, first with synthetic data and then with real data, collected using bucket truck as well as, with the EM sensor mounted on the bucket wheel of an excavator. The integration of the operating parameters of the excavator and the optimal processing algorithm settings were performed in WP3.5 (Expert system development) and WP3.6 (Integration phase).

System for data collection, processing and evaluation

The measurement and data processing system, as shown in Figure 59, consists of three subsystems. The first subsystem includes the measuring devices (EM sensor, differential GPS and CCD camera) installed on the bucket wheel and the boom of BWE. The second subsystem is the EM control unit which collects, stores, transmits data and controls the operation of the EM sensor. GPS is connected and synchronized with EM sensor. Thus, the positioning and resistivity data from EM

are transmitted simultaneously to control unit. The data, recorded in continuous mode at predefined sampling intervals, are: time (UTC, coordinated Universal Time), coordinates (Latitude, Longitude, Altitude) and conductivity of the surveyed part of the mine face by the EM instrument. Finally, the third subsystem is the developed software, installed on a fully rugged laptop, hosted in the control cabin of the BWE, consisting of four modules. The first module receives data from EM control unit, performs the required pre-processing, and sends the corrected data to automated algorithm module. Automated algorithm module predicts the probability of occurrence of a hard rock formation at a specific position, and sends this information to expert system module. Expert system estimates the probability of collision (between excavating buckets and hard rock formation) and if necessary, generates alarms. The last module of the third subsystem is the visualization unit, which provides the machine operator with all required information as well as with real-time video for the visual inspection of the mine-face.

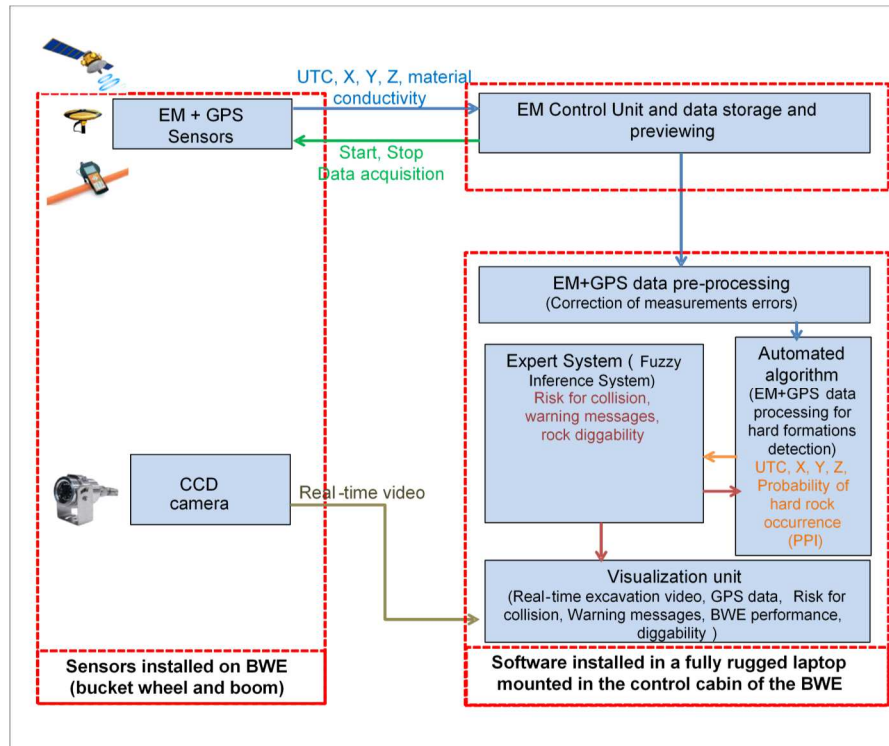


Figure 59 Block diagram of measurement and data processing system.

Pre-processing of collected data

The original data collected from EM sensor (CMD2) contain the GPS data (Latitude, Longitude, Altitude and Time) and the measurements of CMD2 (Conductivity and Inphase). The first pre-processing step is to convert the coordinates from Latitude - Longitude (WGS84') to UTM Cartesian (X, Y, Z) geodetic system, as shown in the table below.

Table 19 Part of original data, collected from CMD2 electromagnetic instrument in June 2017 at South Field open pit mine, Ptolemaida, Grece. The last three columns deduced after the coordinates conversion from Lat.-Long. (WGS84') to Cartesian (UTM) geodetic system

Latitude	Longit.	Altitude	Time	Cond. [mS/m]	Inphase [ppt]	X (UTM)	Y (UTM)	Z
40.43720 58667	21.83863 90967	696.801	09:10:01 .97	28.50	5.90	571127.7 48	4476622. 280	696.801
40.43720 58633	21.83863 90867	696.794	09:10:02 .87	28.54	5.91	571127.7 48	4476622. 279	696.794
40.43720 57417	21.83863 90167	696.816	09:10:03 .92	28.65	5.90	571127.7 42	4476622. 266	696.816
40.43720 57583	21.83863 90233	696.793	09:10:04 .97	28.91	5.90	571127.7 42	4476622. 268	696.793
40.43720 58933	21.83863 91583	696.670	09:10:06 .92	29.19	5.87	571127.7 54	4476622. 283	696.670

Both coordinate and conductivity (or the equivalent resistivity) values are subjected to pre-processing. UTM coordinate data (X, Y, Z) are smoothed (using moving average filters) and checked for outliers, which are removed. Resistivity data are subjected to smoothing and negative - outliers (extremely high) values removal as well.

Advanced Mode operation of the automated algorithm for real-time data evaluation requires the obtained data organized in profiles, resulting from the slewing operation of the bucket wheel. Since CMD2 instrument is mounted next to the bucket wheel at a certain distance (approximately 4m), its trajectory is cyclic as it follows the movement of the bucket wheel. To calculate the coordinates (X, Y, Z) of the individuals trajectories of CMD2 corresponding to slewing operation of the bucket wheel we have modelled the excavation of a block by a BWE when terrace cutting is applied (Figure 60).

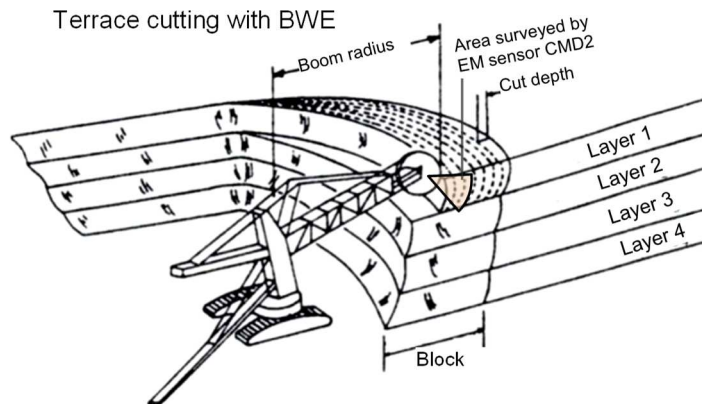


Figure 60 Excavation of a block by terrace cutting. The CMD2 instrument follows the slewing movement of the bucket wheel.

An example of X, Y and elevation coordinates from CMD2 synthetic instrument trajectories are shown in Figure 61 and Figure 62, respectively. Subsequently, taking into account the above mentioned excavation process, the collected data were organized in blocks, layers and cuts in order to form the resistivity profiles which are essential for the algorithms used in Advanced Mode operation. Finally, the data of each resistivity were de-trended and the cut advance depth was estimated from the coordinates of the successive profiles.

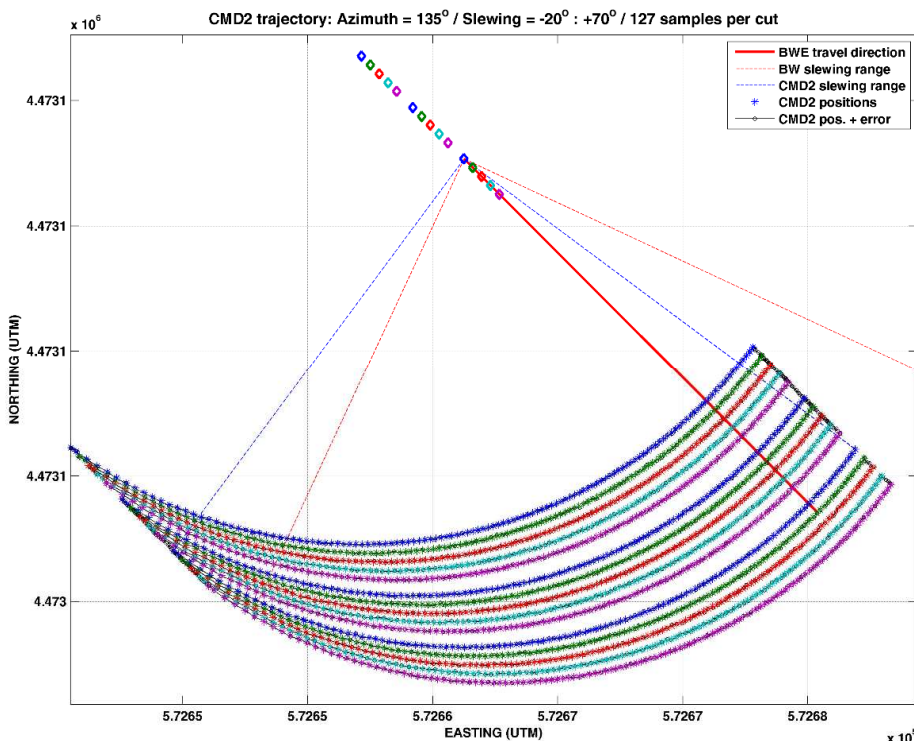


Figure 61 EM sensor (CMD2) trajectories in X-Y coordinates (UTM) during the excavation of a block by terrace cutting.

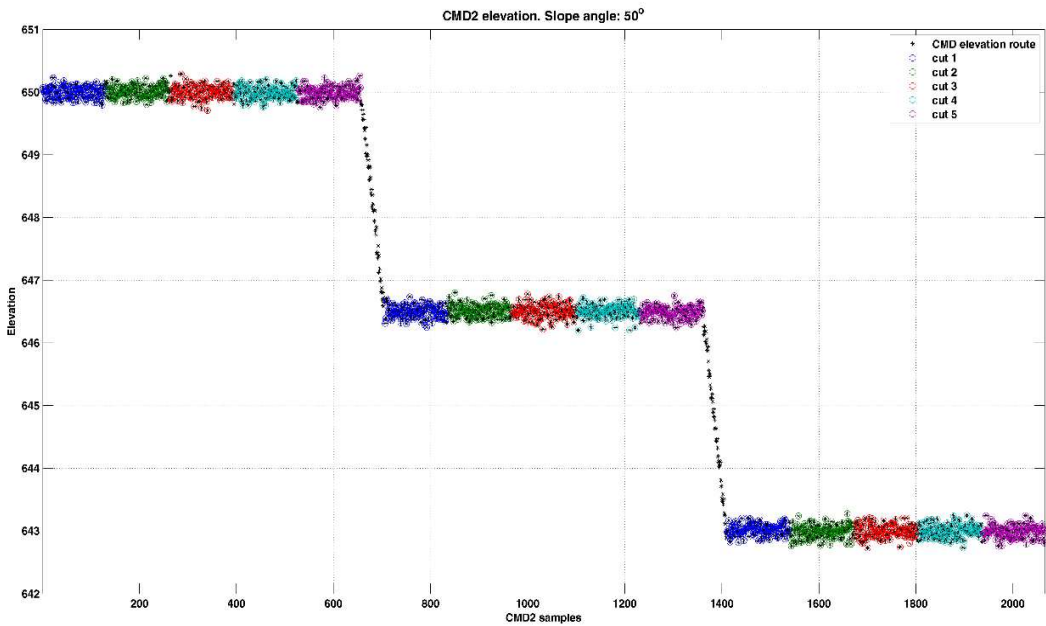


Figure 62 EM sensor (CMD2) elevations during the excavation of a block by terrace cutting

Development of automated algorithm

Existing methods for EM data evaluation

Existing methods for EM data evaluation are mainly based on the inversion to provide information about the size and location of hard rock inclusions based on the estimation of the conductivity spatial distribution ahead of the front. This inversion method though, is currently utilized as a post processing technique, since it is computationally expensive and requires the complete dataset along one or more profiles. Up to date it was impossible to reduce computational time of the most computationally intensive part of the inversion namely, the synthetic apparent conductivity calculation which involves finite differences EM wave propagation simulations.

Numerical models

Modelling of ground conductivity measurements from EM instruments requires the numerical solution of the quasi-static Maxwell's equations, since analytical solutions exist only for limited cases (free space or at the surface of the earth for half space). It is common practice to numerically solve an equivalent quasi-static differential equation in the frequency domain for the unknown secondary electric field in case of heterogeneous earth. Here, the electric and magnetic fields of the free space are necessary for the simulation of the loop-loop configuration source. These homogenous medium fields, so called primary fields, can be explicitly described. Alternately, one can calculate by numerical integration the primary or background fields for a horizontally layered medium. For a magnetic susceptibility free heterogeneous earth, the above mentioned differential equation does not require the primary magnetic field in the so called source term.

The problem to be solved is a boundary value problem with Dirichlet conditions at the edges of the model. From the calculated secondary electric field one can evaluate the vertical component of the secondary magnetic field at the receiver position. This is added to the vertical component of the primary magnetic field which is explicitly known as a function of frequency. The resultant vertical component of the magnetic field is employed for the generation of apparent conductivity synthetic data.

Apparent resistivity synthetic data

The ground conductivity instruments use a phase sensitive measurement between the transmitter (Tx) and the receiver (Rx) magnetic fields to obtain the apparent conductivity, with σ_a in S/m or equivalent the apparent resistivity ρ_a in Ωm ($\rho_a = 1/\sigma_a$). Synthetic data have been generated both for the design of the geophysical experiment using the EM method and testing the automated algorithm for the detection of hard rock inclusions. A simple way of predicting the instrument reading on an arbitrary layered earth, as long as the coil spacing is much less than the skin depth in all of the layers, is to add the contribution of each layer independently. Namely, the synthetic apparent conductivity is equal to the weighted average of the conductivities of each layer. The above mentioned approach in the case of laterally varying medium, will not predict the instrument's σ_a profile. Thus, 2D effects must be taken into account.

2D weights which are modifications of the 1D ones were proposed. These 2D weights called cumulative sensitivity, were tested using analytical profiles (Telford et al., 1979). For coil separation of 1.89m (which applies for the CMD2 instrument), low depth range mode and maximum depth of penetration 7m, the cumulative sensitivity is depicted in Figure 63. The corresponding synthetic $p_a=1/\sigma_a$ for both the 1D and 2D approaches are shown in Figure 64, over a conductive half space containing two non-conductive bodies.

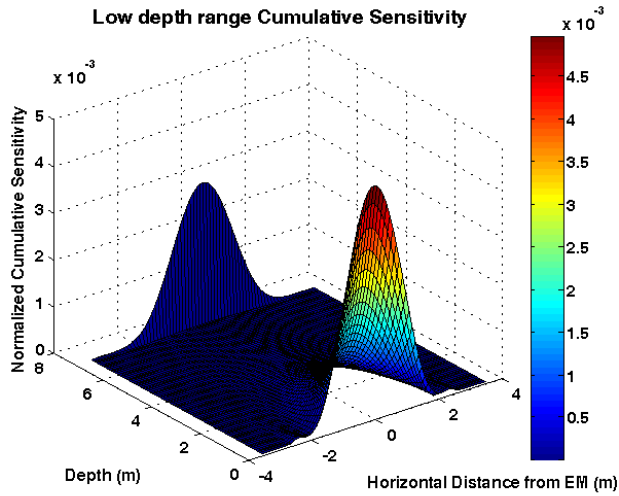


Figure 63 Low depth range 2D cumulative sensitivity for intercoil separation 1.89m and maximum depth of penetration 7m. The instrument is located at horizontal distance $x=0$ m, where maximum sensitivity values occur.

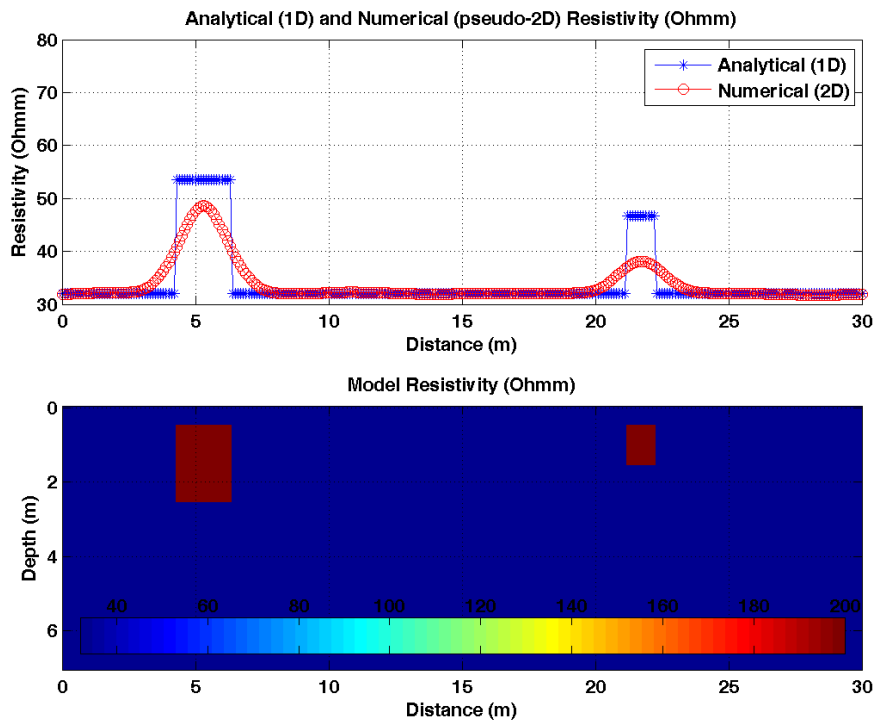


Figure 64 The apparent resistivity values as estimated by both analytical and numerical approach over a 30m x 7m model. Two relatively higher resistivity bodies are buried (their top surface) at depth of 0.5m from the surface within a conductive homogeneous half

Simple Mode operation algorithms

In the Simple Mode operation a relative simple algorithm called Simple Mode Hard Rock Detection (SMHRD) is used to issue alarms when bucket wheel is approaching a hard rock formation. It is based on statistical process control and uses data collected during the current BWE cut. According to this algorithm, first the real-time CMD2 conductivity data are transformed to resistivity values and simple pre-processing is applied (negative and extreme positive values excluded). Then SMHRD algorithm uses a moving data window containing the last 21 resistivity values to evaluate

its average (Long Term Average - LTA) and its standard deviation. A narrower moving data window containing 3 measurements is also used to estimate if its average value (Short Term Average - STA) lies within pre-defined limits. In addition, the Short Term Average (STA) to Long Term Average (LTA) ratio is calculated for the above mentioned data windows and is examined if exceeds a pre-defined limit, as well. Based on the above mentioned criteria, an alarm indicator is issued if the 3 measurements average exceeds both standard deviation and STA/LTA ratio limits.

Figure 65a shows an example of SMHRD algorithm when the synthetic resistivity data of the model shown on Figure 65b was used. Random noise of 10% of half-space resistivity value ($32 \Omega\text{m}$) was introduced in model resistivity values. The Long and Short Term data windows are set 21 and 3, respectively, while the standard deviation and STA/LTA ratio limits are set to 1.1 and 1.1, respectively. The best selected values of data windows and threshold limits are set after performance evaluation on synthetic resistivity data, using different sets of parameters combination. The above mentioned parameters combination resulted in 95% and 85% success rate on finding the boulders in last BW cut, when tested with 1 and 2 boulders models, respectively, while 5% and 23% in false alarms, respectively (Figure 66). An alarm is considered successful if, at least one alarm position lies within the area of the shallowest hard rock horizontal extend, while false alarm is considered if alarm is issued in a position where no hard rock exists or there is a deeper hard rock. Since the false alarms in the scenario of 1 hard rock models is quite low (5%), the false alarm in the case of 2 bodies' models is attributed to the detection of the deeper (and sometimes bigger) hard rock. Another issue of SMHRD algorithm is the high success rate in deeper slice cuts (cut1-cut3 in Figure 66) than the current (cut4) resulting to early warning alerts. This is one of the most important reasons for the necessity of the development of more advanced models such as employed in the Advanced Mode operation.

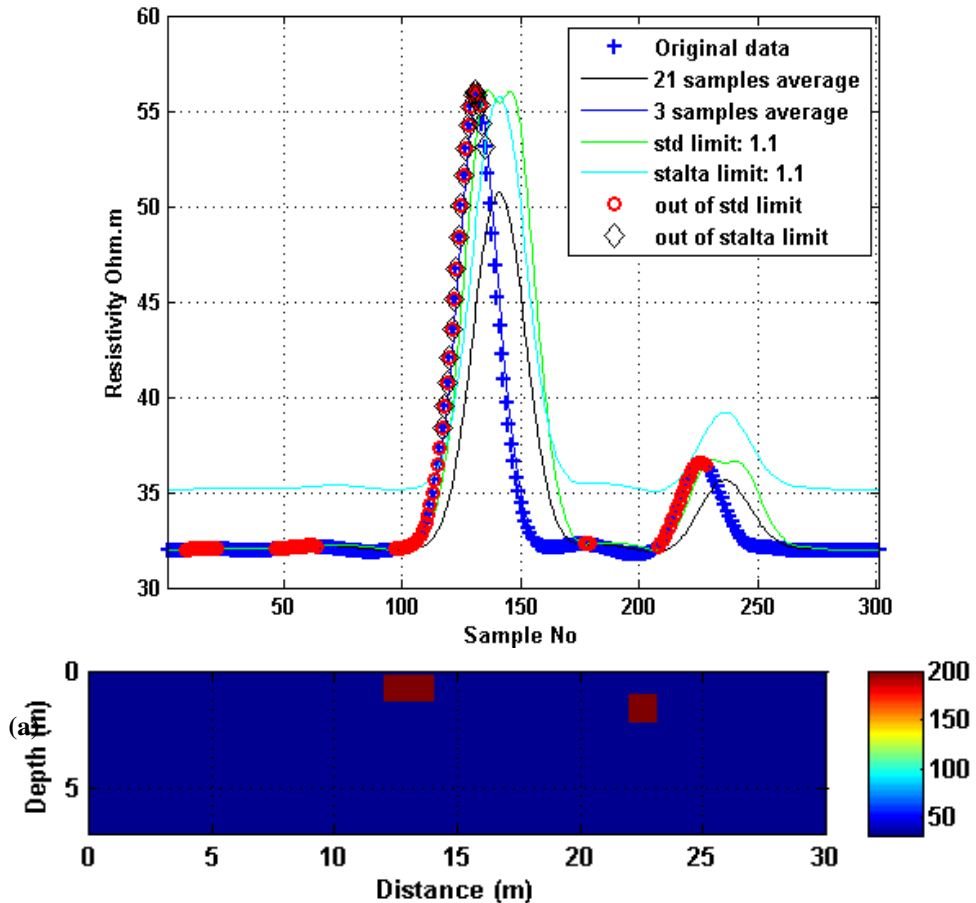


Figure 65 Application of Simple Mode Hard Rock detection algorithm to synthetic resistivity data. Simulation resamples the last BW cut before hitting the boulder, located at 0.2 m depth (the top of boulder) and 13 m (center) of model. The sampling interval in horizontal direction is 0.1 m and the colour scale corresponds to model resistivity in Ωm

(b)

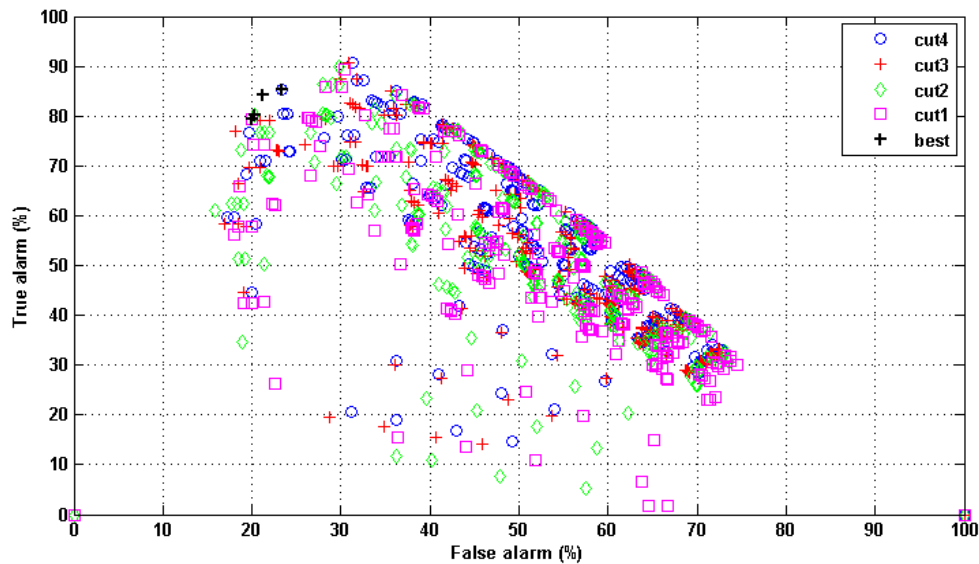


Figure 66 Performance evaluation of SMHRD process data windows and threshold limits, using synthetic resistivity data and successive BWE cuts. Cut4 correspond to the last BW cut before hitting on the boulder. Different BW cut depths (0.2, 0.6, 0.8, 1.0, 1.2 m) were examined in 100 different (randomly generated) 2 boulder models. The most successful parameter combination result for the 4 cuts is highlighted with crosses.

Figure 67 shows a map of experimental apparent resistivity values acquired by moving CMD2 instrument mounted on a bucket truck against a slope, in June 2017 from South Field open pit mine, Ptolemaida, Grece. Hard rock inclusions in form of layers and lenses lied within the clays. The map is the product of interpolation from apparent resistivity values acquired from the EM instrument CMD2 along the route marked with white crosses. High resistivity values correspond to an area where hard rock inclusion was observed (Figure 68). Separated data were extracted along 7 resistivity profiles with 0.5m spacing and then data for five successive cuts (1-5) were derived to be used for processing.

Figure 69 shows an example of Simple Mode Boulder Detection application along the 4th cut of the above mentioned experimental data. It shows an area marked with warning alerts (both out of standard deviation and STA/LTA limits), at the positions where steep increase of resistivity values is encountered.

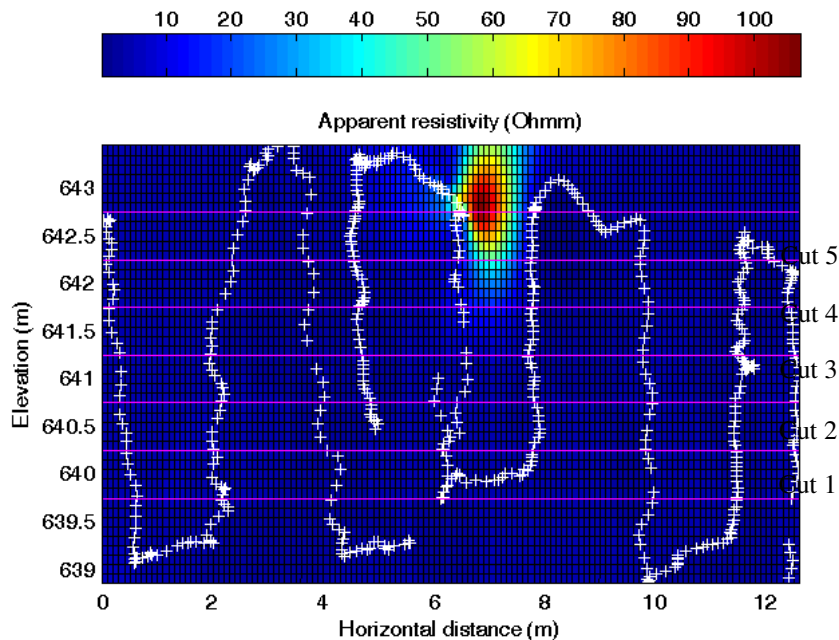


Figure 67 Apparent resistivity map deduced from experimental data interpolation, acquired by the EM instrument CMD2 along the route marked with white crosses. High resistivity values correspond to an area where hard rock inclusion was observed. Separated data were extracted along 7 resistivity profiles with 0.5m spacing and then data for five successive cuts (1-5) were derived to be used for processing.

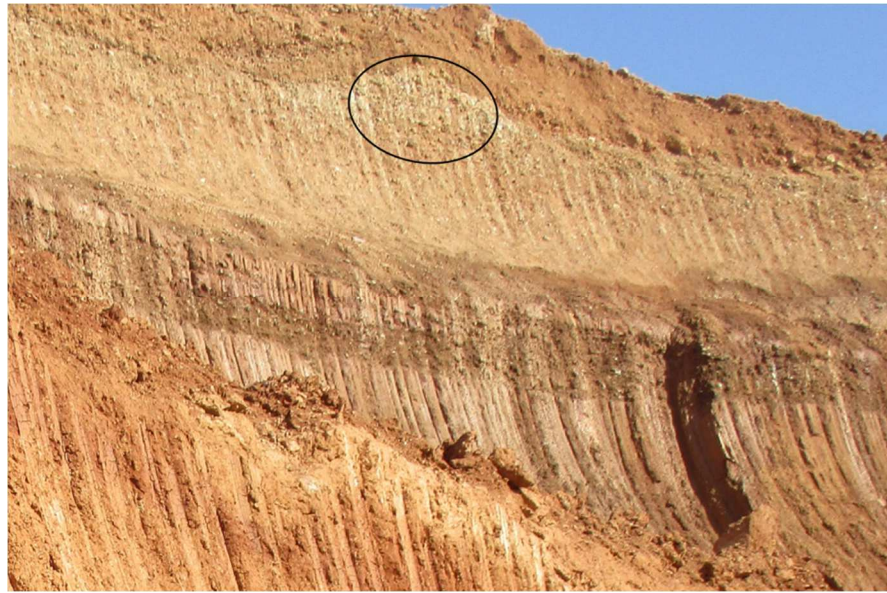


Figure 68 Part of the mine face surveyed with CMD2. It is located in the overburden bench of sector 7 of South Field mine of PPC. As shown in photo the hard rock inclusion is a lenticular conglomerate formation surrounded by brown-reddish clay layers

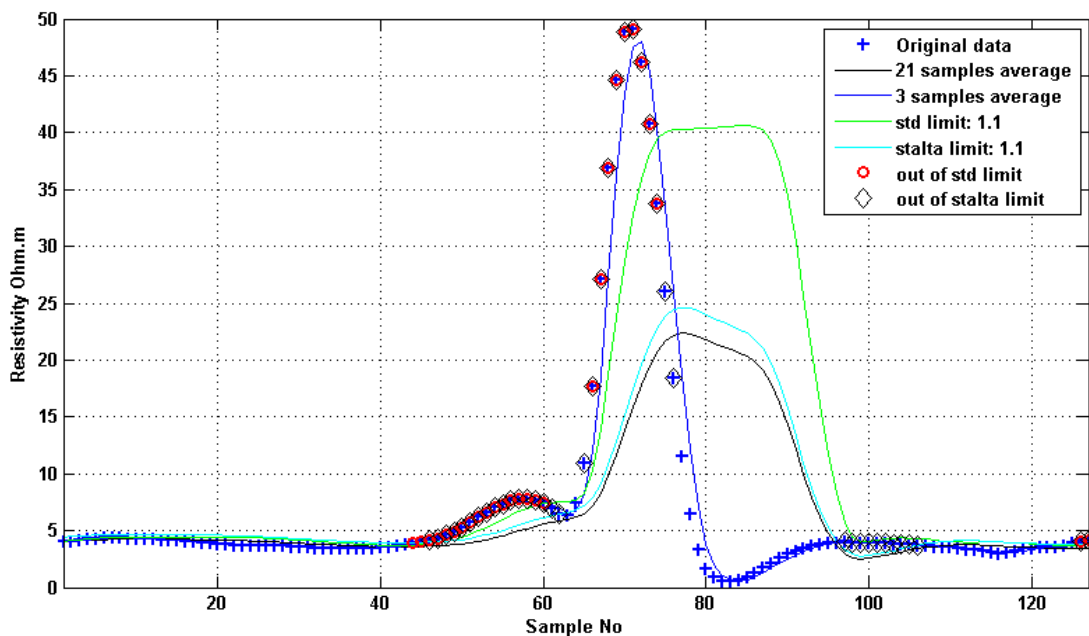


Figure 69 Example of Simple Mode Boulder Detection application on the 4th cut of the experimental resistivity data, shown in Figure 67. The area marked with warning alerts (both out of standard deviation -std- and stalta limits) at the positions where steep increase of resistivity values is encountered. The sampling interval along profiles is 0.1m.

Advanced Mode operation algorithms-Local maxima ranking and the Position Prominence Index

Hard rock inclusions are expected to increase the apparent resistivity within the EM profiles. Thus, local maxima detection is required in order to locate possible hard rock inclusions within the surrounding media. Within the Advanced Mode operation an algorithm for the detection of the most prominent peaks has been used. Peaks define a subset of the local maxima, since several local maxima may be closely located and the values in between do not change dramatically. In such case, only the higher local maximum is considered as peak. The algorithm is simple and exhibits the above mentioned qualitative description. An example is presented in Figure 70 where the 6 most prominent local peaks are selected on random data.

Since the excavation using a bucket-wheel excavator (BWE) is a repeated process along horizontal profiles, the high resistivity values caused by hard rock inclusions are anticipated: 1) at the same locations along profiles from the same front and 2) to be increased as the EM instrument (attached to BW) approaches the inclusion. The Position Prominence Index (PPI) is introduced to take into account the above mentioned criteria. Namely, the PPI value is increased in a specific position

when resistivity peaks are detected repetitively and their values are increasing. The PPI of a current BWE pass is defined at positions of local resistivity maxima and depends on the value of the peak, the Number of Local Maxima along a pass and the proximity of the prominent peak in successive passes. The apparent resistivity values (left axis) as well as the PPI values (right axis) calculated using the resistivity data from 3 successive cuts (2, 3 and 4) of the experimental data, are shown in Figure 71.

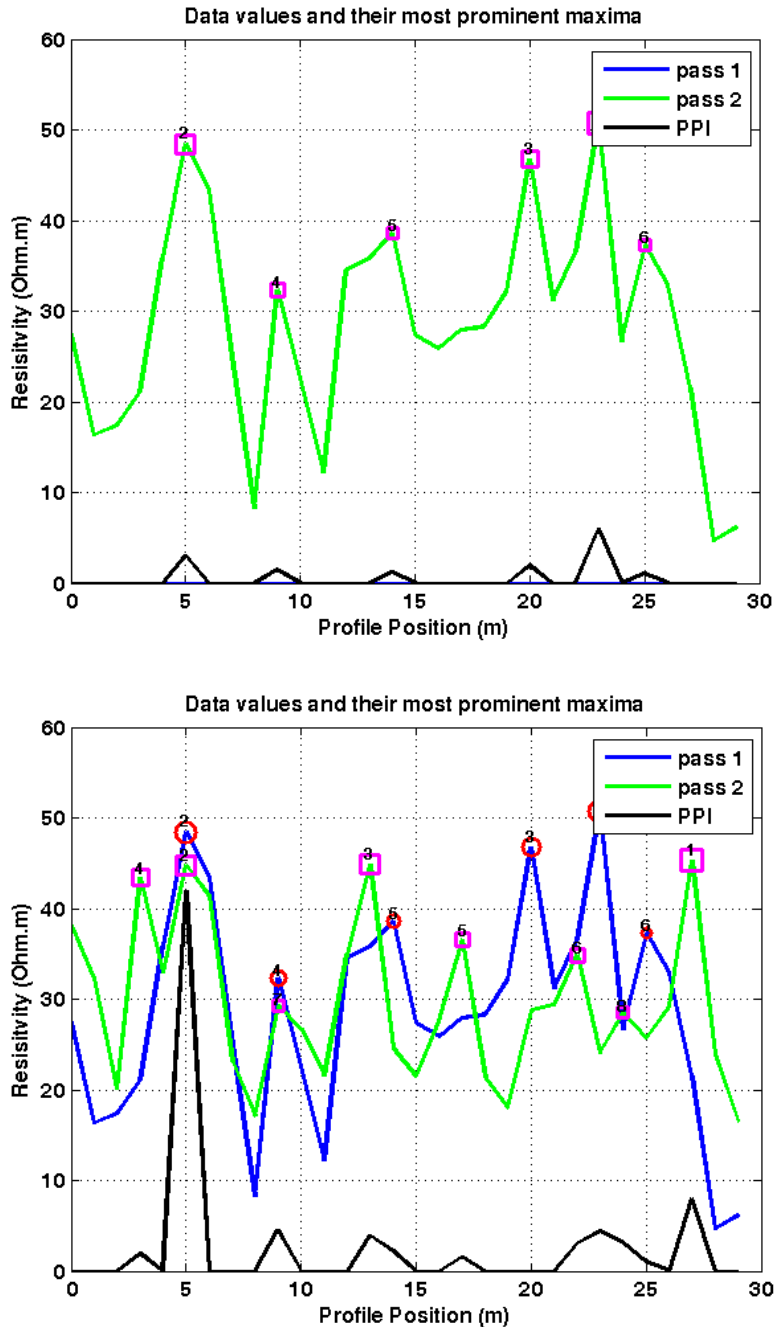


Figure 70 (Top) Random dataset and their 6 most prominent maxima. Numbers over the red circles indicate their rank. (Bottom) Prominent maxima at the same positions for both passes are detected at 5m. PPI value (black line) is accordingly increased

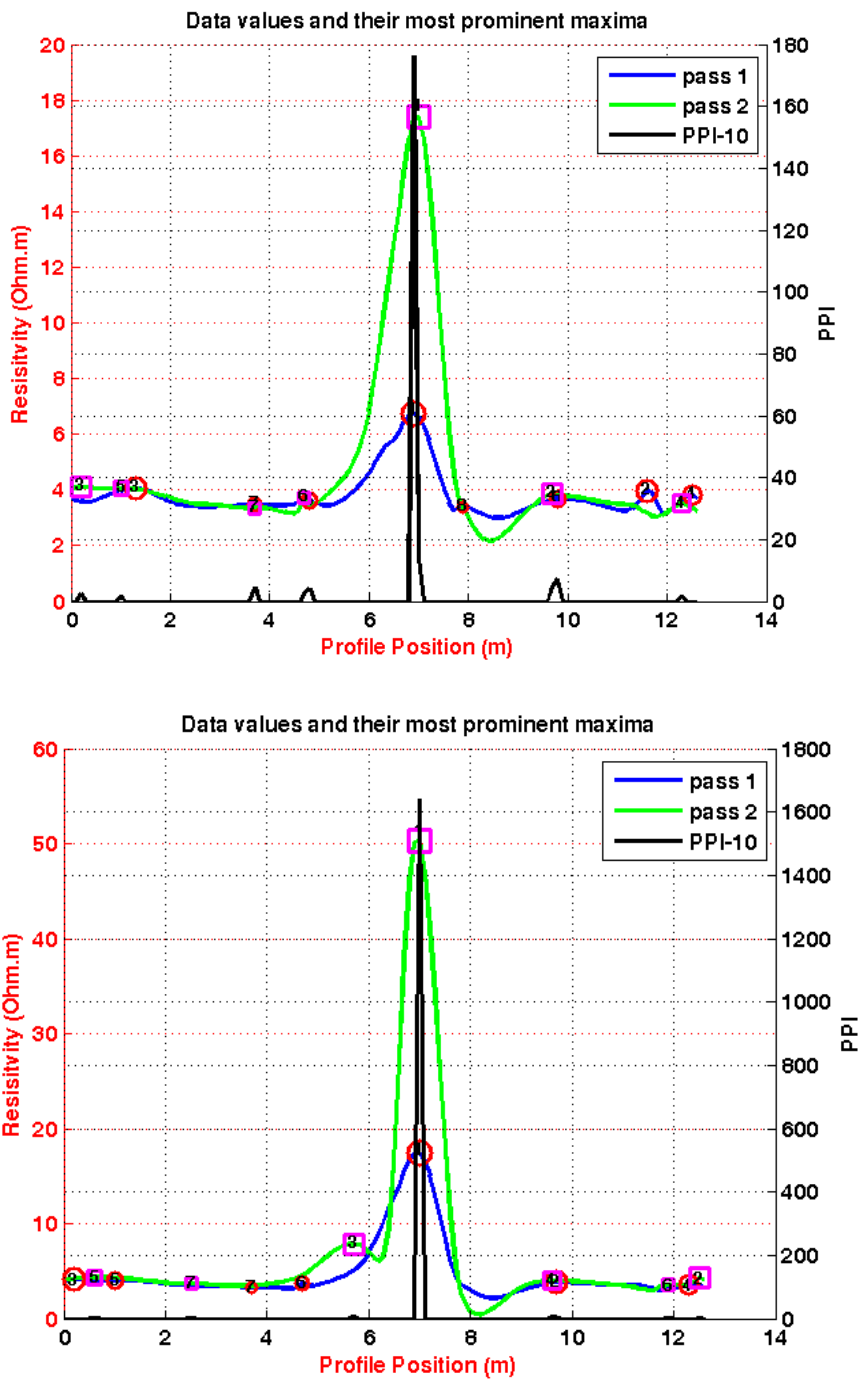


Figure 71 Apparent resistivity (left axis) and PPI values (right axis) calculated from 2 successive cut changes (up: cut 2 to 3, down: cut 3 to 4) of the experimental data

PPI is an excellent position boulder detector technique. However, suffers from 2 main drawbacks: a) is sensitive in measurement position errors and b) there are difficulties in establishing PPI threshold, since PPI is affected by the number of data points in profiles. However, it is anticipated to contribute positively in the expert system, by increasing the success rate of hard inclusion detection.

Advanced Mode operation algorithms-Artificial Neural Networks for Pattern Recognition

Artificial Neural Networks (ANNs) or simply Neural Networks (NNs) are nonlinear dynamic systems, composed of simple elements, operating in parallel, called artificial neurons. The operation of artificial neurons is inspired by biological nervous systems. Neurons are organized in hierarchical layers, with the output of one node serving as input to another. The way the neurons are interconnected and the number and kind of layers in a network result in varying types of NNs. A neural network can be trained to perform a particular function by adjusting the values of the connections between elements. Neural networks have been trained to perform complex functions in various fields of application including pattern recognition, identification, classification, speech,

vision and control systems. Among different type of NNs, multi-layer feedforward neural network models using the backpropagation learning method, have applied widely for pattern recognition and prediction and estimation problems.

The developed neural network model (Neural Network for Resistivity Pattern Recognition or NNRPR) is a feedforward NN with a hidden layer with 10 neurons that uses resistivity and positioning data from n successive cuts to estimate the probability of occurrence of a hard rock formation in the next cut ($n+1$) at a specific position x_o , y_o , z_o , as shown in Figure 71. The prediction is based on the examination of local changes of resistivity profiles created by the EM sensor (CMD2) mounted on the bucket-wheel during the excavation process. The considered excavation method was the terrace cutting, since this is the one used in the lignite mines of PPC. In terrace cutting the block under excavation is divided into layers and each layer is excavated by performing a series of cuts). As bucket wheel is approaching the hard rock formations, the resistivity values are increasing due to the presence of the hard rock formation. These patterns of resistivity profiles indicate the presence of a hard rock formation as shown in Figure 72. The developed neural network model NNRPR is capable, after training, to recognize these patterns (changes in the resistivity profiles) and to relate them with the position of the hard rock formation.

NNRPR examines local changes of the resistivity profiles of the n recent successive cuttings by using a moving window including k resistivity measurements from each cut. In addition, NNRPR uses as input the distance among the examined successive local resistivity profiles. This distance coincides with the cutting advance of the BWE at the position x_o , y_o , z_o . Thus, the number of the inputs of NNRPR is $kxn+1$, while the output of NNRPR is the probability of the occurrence of a hard rock formation at position x_o , y_o , z_o . Several different values of n and k were examined during training and testing of NNRPR and optimal values were determined to be, $n=3$ and $k=5$.

NNRPR was trained by using a large set of synthetic data (178200 cases). Synthetic data are vital for NNRPR training since they are derived from models that simulate various geological and mining conditions which cannot be observed in a specific mine during a certain time period. With synthetic data hard rock formations of different size, shape, number and position can be effectively represented by creating the respective digital models. The random variations occurring in real data were taken into account by adding noise to synthetic data.

Synthetic data were then randomly divided into three sets: the training (70% of the original data), the validation (15%) and the testing (15%) set. Validation data were used to validate that the network is generalizing and to stop training before overfitting (early stopping technique), while testing data were used as a completely independent test of network generalization.

The development, training and testing of NNRPR was performed within the Matlab programming environment. Figure 73 shows the structure of NNRPR consisting of 16 inputs, one hidden layer with 10 neurons and one output.

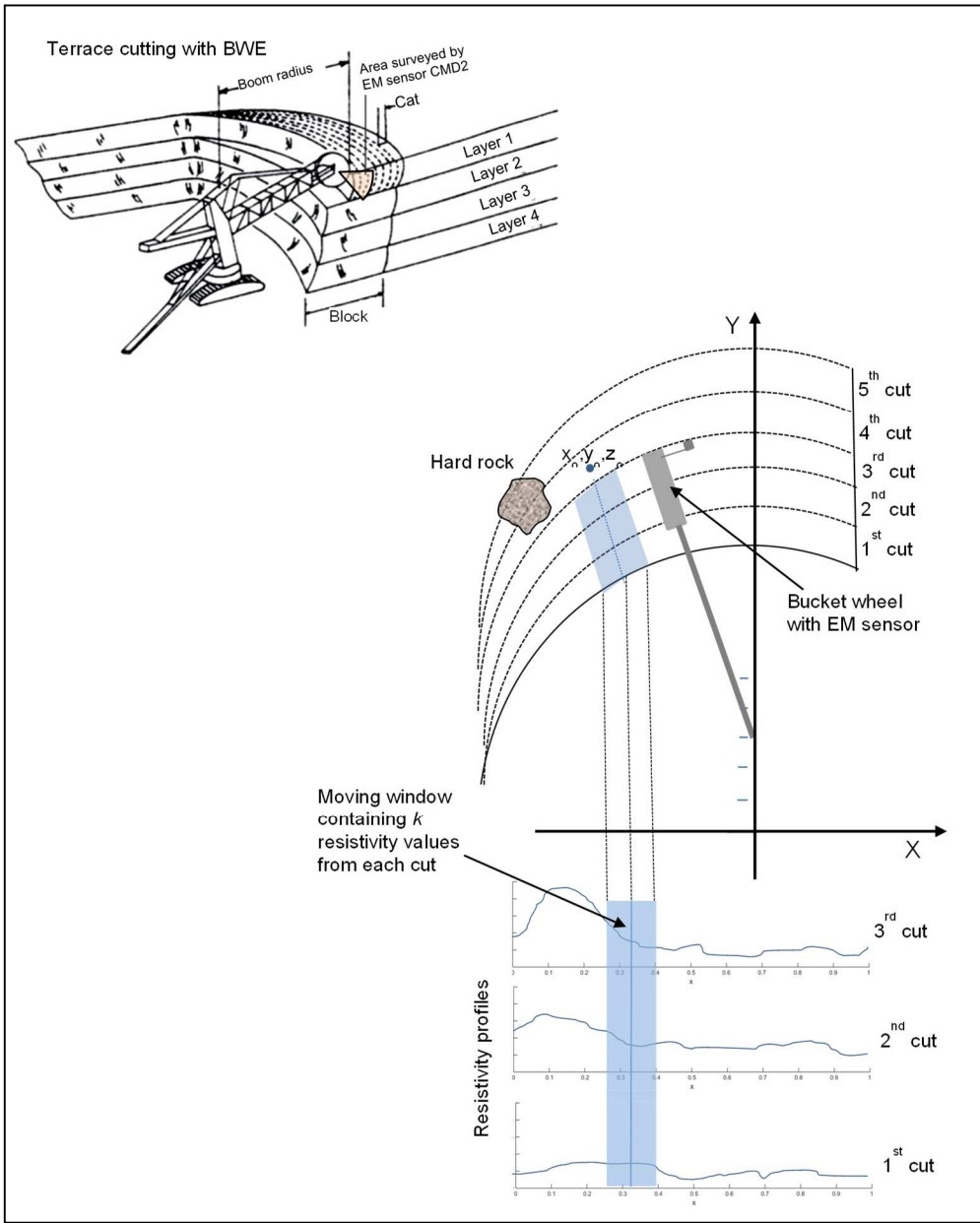


Figure 72 Schematic diagram showing: (Top) Terrace cutting by BWE. (Bottom) Successive resistivity profiles obtained during terrace cutting (3 cuts) and use of moving window to examine local changes in resistivity profiles as BW approaches the hard rock

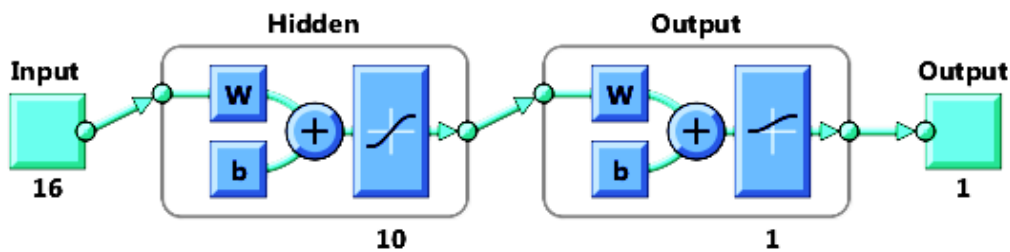


Figure 73 Structure of NNRPR (forward neural network) used for the prediction of the probability of occurrence of a hard rock formation

The confusion matrix obtained after NNRPR training is shown in Figure 74. Class 1 symbolizes the occurrence of hard rock formation while class 0 symbolizes the nonexistence.

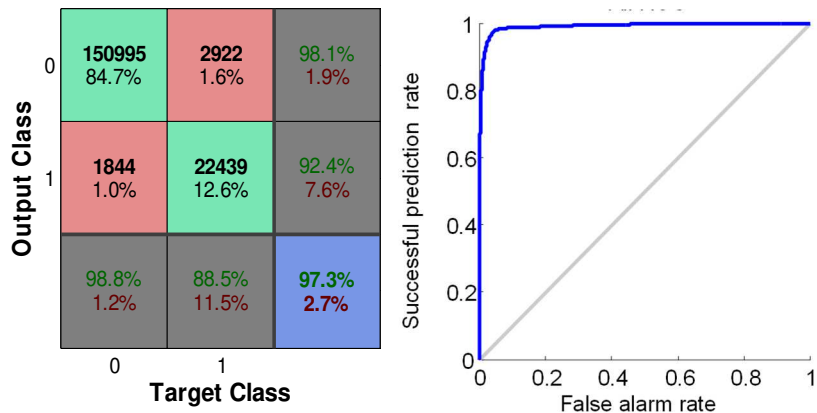


Figure 74 (Left) Confusion matrices for all data showing the number and the percentages of correct and false predictions (Class 0=Non-existence of a hard rock formation, Class 1=Existence of a hard rock formation). (Right) The Receiver-Operator-Curve, or ROC, indicates how the false alarms rate increases as the rate of successful prediction increases.

The percentage of successful predictions is 88.5% while the percentage of false alarms is 1.2%. These percentages are considered acceptable. Figure 74 shows the obtained Receiver-Operator-Curve (ROC) as well, which indicates how the false alarms rate changes as the rate of successful prediction increases. From ROC it is obvious that the achievement of higher successful prediction rate (e.g. 0.98) could result in a considerable higher false alarm rate (0.1).

The trained NNRPR was then used to predict the occurrence of hard rock formations in real data collected with EM sensor (CMD2). These data were collected at the mine face of sector 7 of the South Field Mine of PPC. In the upper middle part of the mine face a hard rock formation was observed. The measurement points, as well as, the constructed resistivity map are shown earlier. The presence of the hard rock formation is clearly shown by the high resistivity values. Seven resistivity profiles with 0.5m spacing were created and then data for five successive cuts (1-5) were derived to be used as input to NNRPR to predict the probability of the occurrence of the hard rock formation. Predicted probabilities for each cut are shown in Figure 75. NNRPR has predicted the probability for a hard rock occurrence at cut 5 at the horizontal position of 7m to the value of 0.92. For the other cuts (1-4) the predicted probability was very low (nearly zero).

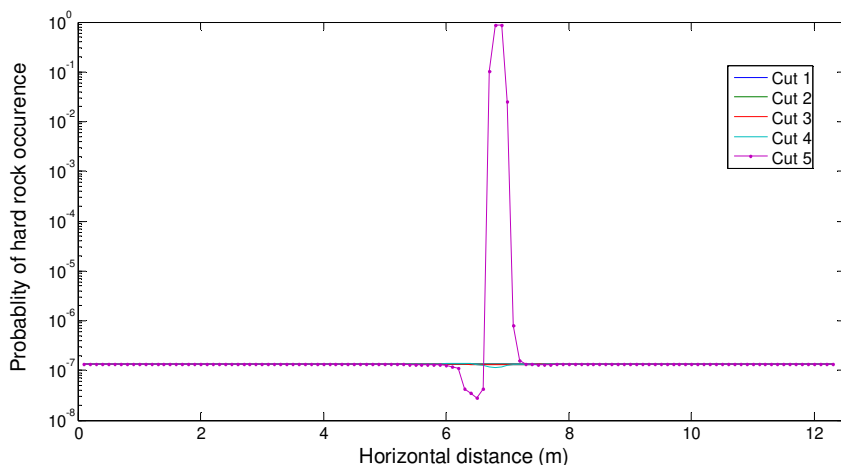


Figure 75 Profiles of the probability for a hard rock occurrence for the examined five successive cuts (1-5)

WP 3.4 Major achievements:

- Overall system design (block diagram) for data collection, processing and evaluation.
- Pre-processing of collected data including removal of abnormal values, coordinates transformation and sorting of collected data into BWE cutting trajectories.
- The assessment of existing methods for EM data evaluation.
- The assessment of the modelling techniques.
- The creation of the synthetic data.
- The development (Matlab codes) and testing of the simple mode evaluation methods (statistical).
- The development (Matlab codes) and testing of the advanced mode evaluation methods (PPI and NNPR development).

2.2.3.5 WP-3.5 Development of the expert system.

For the development of the FIS, the Fuzzy Logic Toolbox of the Mathworks was implemented (Mathworks). The steps for the development of the FIS were:

- definition and fuzzification of the input/output variables;
- creation of the inference rules (application of the fuzzy operator (AND, OR) in the antecedent and implication from the antecedent to the consequent);
- aggregation of the consequents across the rules;
- defuzzification.

During the first stage the initial structure and the parameters of the developed FIS were chosen. The final structure and the FIS and the optimal values of parameters were determined during training. During the training process typical selective mining cases representing different operational conditions were given to FIS as input data and the obtained results were compared to that evaluated by an expert (mining engineers). Furthermore the rules inference mechanism and the response surface plot were examined. Based on the results of this comparison FIS parameters were changed until satisfactory result was achieved.

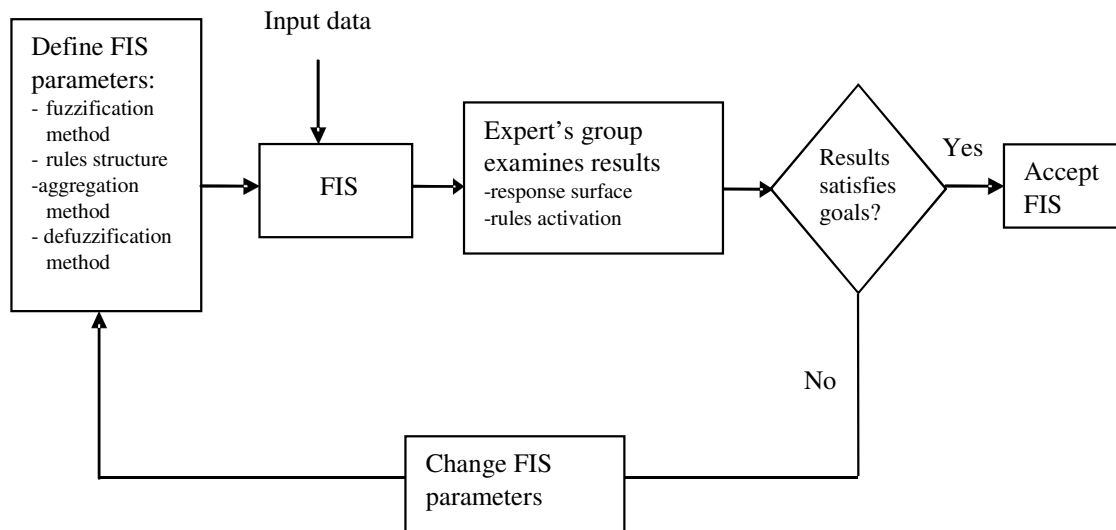
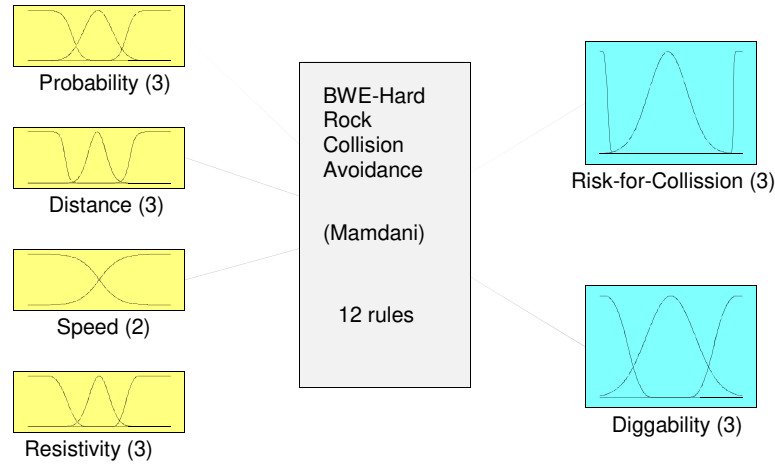


Figure 76 Strategy for developing a FIS for the determination of the collision risk

Based on the description of mining operations and the experts' opinion, the inputs selected for the developed FIS were considered the probability of occurrence of a hard rock formation at a specific position S, the distance of bucket wheel to S, the slewing speed of bucket wheel and the apparent resistivity values of the excavated material.

Two outputs were selected for the FIS, the risk for collision of the bucket wheel with a hard rock formation and the diggability of the excavated formation. The structure of the FIS, consisting of four inputs, two outputs and 12 rules, is shown in Figure 77.



System BWE-Hard Rock Collision Avoidance: 4 inputs, 2 outputs, 12 rules

Figure 77 FIS development in Matlab programming environment (Fuzzy Logic Toolbox)

The fuzzification of the FIS input/output variables converts them to linguistic variables, which are fuzzy sets that are used to add semantic sense to the analysis. The shape of the fuzzy variables is given by the fuzzy membership functions. A degree of membership to a linguistic variable is assigned to each value of the input variable. In this step, the degree μ_i , to which each input variable belongs to the appropriate fuzzy set via membership functions, is determined. The input is always a crisp numerical value and the output is a fuzzy degree μ of membership in the qualifying linguistic set (always in the interval between 0 and 1). The membership functions, used for the fuzzy values of the fuzzy variables, are selected based on expert's experience. The parameters of membership functions were optimized during the training of the FIS. The parameters of the membership functions, which determined during the training process, are shown in Fig. 3.4.

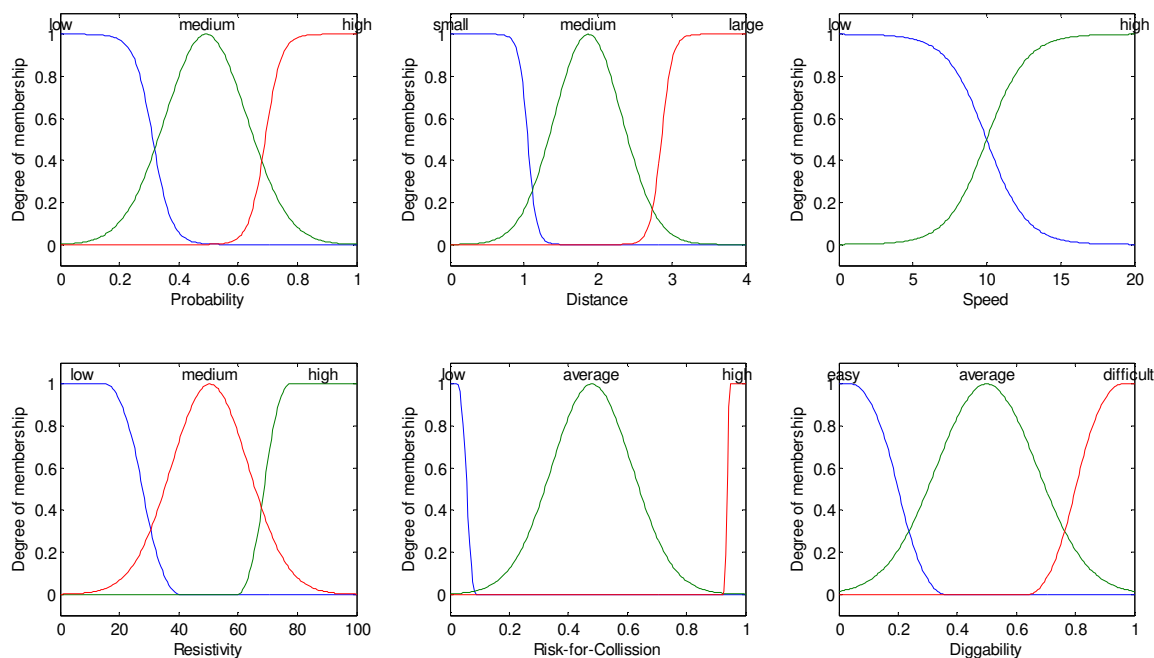


Figure 78 Membership functions of input/output variables.

The rules of the FIS are obtained from information gathered by mining engineers and operators' experience and were optimized during the training of the FIS. Finally, the developed knowledge base of the FIS consists of 12 rules. The fuzzy operator AND was applied to all fuzzy antecedents. The structure of a typical rule, consists of the antecedent, the inference and the weigh. The weigh indicates the importance of a particular rule compared to the others. In the developed FIS, all rules have the same weigh. The results of all rules are combined with the aggregation process into a single fuzzy set for the output variable. From the available aggregation methods (maximum, probabilistic or and summation) the summation method was used.

The input for the defuzzification process is the aggregate output fuzzy set and the output is a crisp number. The most popular defuzzification method is the centroid, which calculates the centre of the area under the curve. Other available methods are: bisector, middle of maximum (the average of

the maximum value of the output set), largest of maximum, and smallest of maximum. In the developed FIS the centroid method was used. The inference mechanism of the developed FIS, which consists of four inputs, 12 rules and two outputs, is shown in Figure 79. Information flows from left to right, to a single output for each rule. Outputs from all rules are aggregated to form outputs fuzzy set. The response surface for Risk of Collision as function of the Probability (of hard rock occurrence) and the Distance (BW to hard rock) is shown in Figure 80.

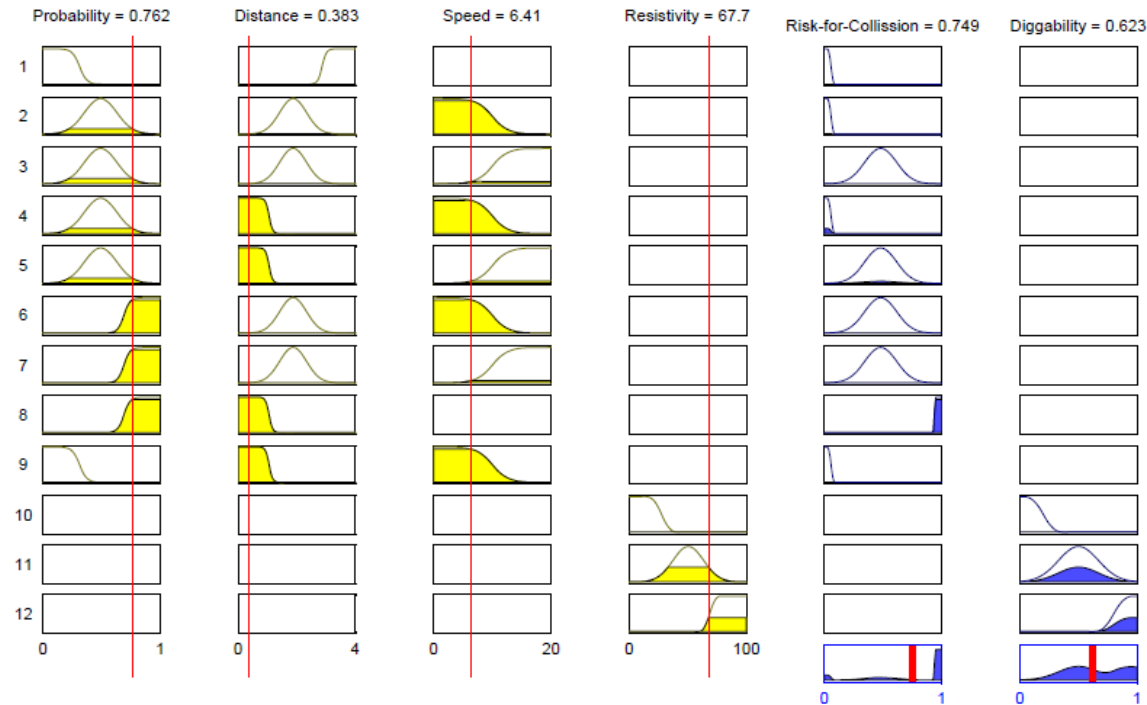


Figure 79. Fuzzy inference mechanism and defuzzification method.

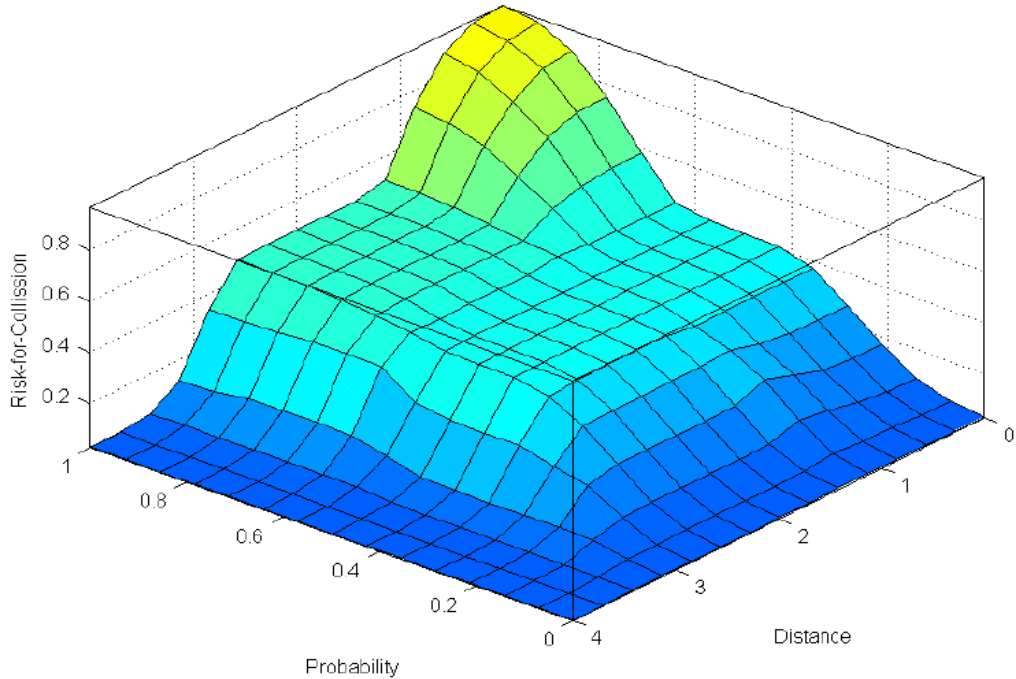


Figure 80. FIS response surface for Risk of Collision as function of the Probability (of hard rock occurrence) and the Distance (BW to hard rock).

Two different versions of the Fuzzy Inference System (FIS) were developed. The first version, presented above, was named AMFIS and it is used during the advanced mode operation of the real-time automated algorithm for data processing and evaluation (Deliverable D3-4). The second version, named SMFIS, is used during the simple mode operation of the real-time automated algorithm for data processing and evaluation. The SMFIS has less inputs (the probability and the distance) and rules compared to AMFIS.

A graphical user-interface (visualization unit) providing all necessary information, in a comprehensive way, to the operator of the BWE was also developed. As shown in Figure 81 the developed visualization unit includes three active panels. The first panel (top left) displays the excavation process while the second panel (bottom left) provides information about the diggability of the excavated material (coloured scale). The third panel (on the right) shows the risk of collision of the BW with a hard rock formation (also in coloured scale) and displays short messages in form of warnings or advices for the operator of the BWE. Depending on the mode of real-time operation (simple or advanced) the visualization unit can also provide information regarding the position BW and the slewing speed of the boom. When risk of collision exceeds a certain level an audio alarm is also activated.

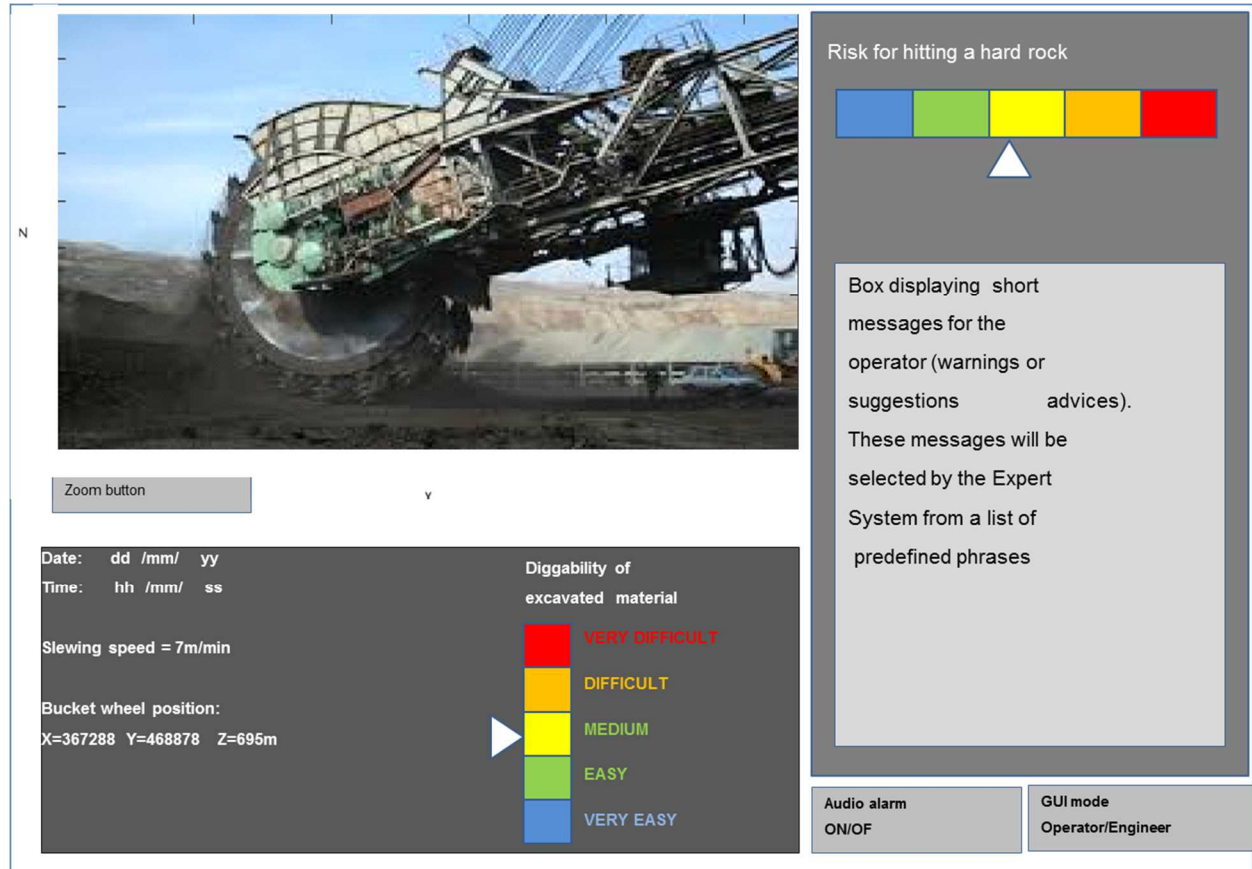


Figure 81 Visualization unit providing all necessary information to the operator of the BWE.

WP 3.5 Major achievements

- Development of Fuzzy Inference Systems for Simple and Advanced mode operation.
- Design of the graphical user-interface and the explanation-guidance facility (visualization unit) of the FIS in order to be comprehensible by the operator of the BWE.

2.2.3.6 WP-3.6 Integration - final testing and evaluation.

Software integration - HAROR standalone application

Software integration aimed to combine the algorithms that have been developed in previous phases and to develop a standalone program (HAROR, HArdROckReconnaissance) for real time mine face inspection during excavation by BWE. This application (HAROR) receives and records real time measurements from EM instrument and from a camera, process-evaluate them and provide information in real time about the diggability of the excavated material, the probability of hard rock occurrence and the risk of collision. It generates also warning alarms for the BWE operator when risk of collision is increased.

HAROR main screen and menus during real-time operation are shown in Figure 82. The main screen is divided into four panels. The first panel (top left) displays the excavation process as it is shown by the connected camera. The second panel (bottom left) provides information about the probability of hard rock occurrence, the effort of BWE (or the diggability of the excavated material) and the risk of collision (hitting a hard rock). These parameters are displayed in a five-level colour scale in order to be easily observable by the operator.

The third panel (on the right) shows buttons which are controlling acquisition, storage and display (plot) of measurements and evaluated parameters during the excavation process. Typical generated plots of the measured resistivity, estimated probability of hard rock occurrence, BWE effort (or diggability) and risk for hard rock hitting are shown in Figure 83. The computational time (comp. time) in seconds is also shown to ensure that the required calculations can be executed in less than 1 second which is the selected sampling time. Higher computational time could result in delays of the real-time procedure. The same panel includes also the button for activation/deactivation of the audio alarm as well as the HAROR info button. The audio alarm is triggered when risk of collision exceeds a certain level. The fourth panel (bottom right) displays several useful information regarding, time location and the current measurements of the connected sensors. Depending on the mode of real-time operation (simple or advanced) this panel can also provide information regarding the BW position and the slewing speed of the boom.

HAROR application was developed in Matlab 9.3 (R2017b) programming environment and its code is given in Appendix A. It contains 16 functions and subroutines and has been developed in order to be used in touch screen due to easiness of learning and using in a demanding environment like mines.



Figure 82 HAROR main screen and menus during real time operation.

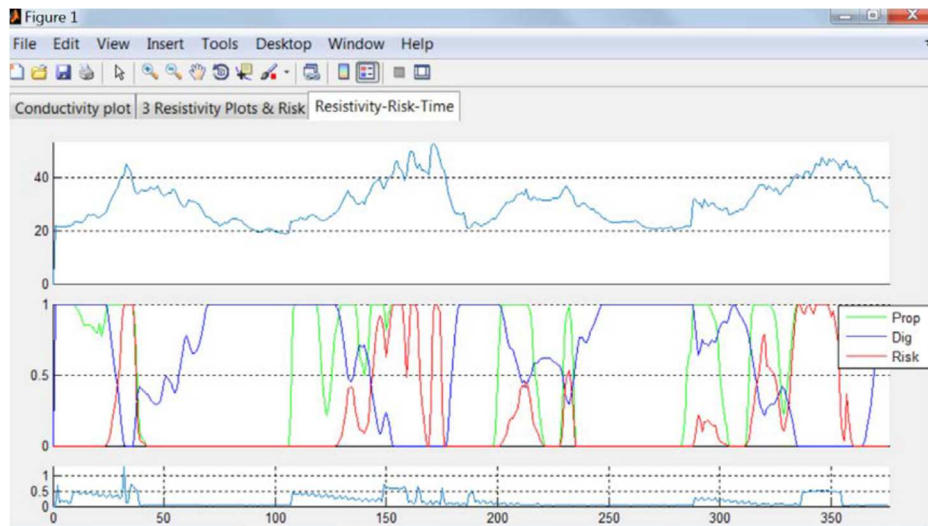


Figure 83 Available plots during HAROR operation.

Hardware integration

The hardware integration included the connection of the geophysical instrument (CMD2), DGPS and optical camera to a rugged laptop computer where the HAROR application was installed. The used computer was a fully rugged laptop (Getac V110). This type of computers was selected because of the harsh and demanding environment in the mine field and inside the BWE operator cabin (Figure 84). Getac V110 has also a fast processor in order to be capable to execute all necessary processes and computations in less than a second.



Figure 84 Getac laptop with the installed HAROR software during its operation (inside BWE operator cabin).

The EM sensor (CMD2) and DGPS were attached to the especially constructed arm next to the bucket wheel (Figure 85). This fixed length arm is built from two different parts, one from steel firmly connected to the BWE and another from a wooden beam, where the EM sensor was attached. Wooden beam ensures that the CMD2 does not interfere with the metallic structure of the BWE. Also a protective PVC enclosure with foamy interior was used to protect CMD2 instrument from a potential fall of material from the mine face during the excavation (Figure 86). The wooden beam carrying CMD2 can be rotated and moved backward and forward manually for adjusting the position of CMD2 sensor.



Figure 85 Mounting of EM instrument and DGPS on the BWE boom.



Figure 86 EM instrument with protective case attached to wooden beam.

FINAL FIELD TEST AND EVALUATION

The final tests included the operation of BWE equipped with the real-time inspection system in especially prepared sites where hard rocks were buried at certain distance in front of the working face. More specifically this last phase included:

- the adjustment of the system to the specific conditions of the South Field Lignite Mine, prior to its installation on the BWE;
- the selection and preparation of the sites for the final field tests in South Field Lignite Mine;
- the mounting of EM sensor, DGPS, optical camera and rugged laptop on the BWE SE1;
- the final test on the selected sites and the evaluation of the results.

Adjustment of the system to specific mine conditions and selection and preparation of the test sites

For the adjustment of the integrated system a number of surveys were conducted in the first bench of South Field Mine. These surveys included the measurements of the resistivity of the geological formations in the vicinity of the final test sites. These measurements were performed on the top of the bench (over bench measurements).

The final tests included the operation of BWE equipped with the real-time inspection system in specially created test sites where hard rocks were buried at certain places in front of the working face.

Results indicated that the system was able to detect the presence of hard rock inclusions in the excavating area and to generate early warnings alarms for the operator of the BWE. It was observed that the reliability of the system was mainly affected by the changing mining conditions and mainly from the distance of the EM sensor from the mine face (effect of varying air gap). However these problems could be avoided in an industrial real-time inspection system mounted on a robotic arm capable to adjust sensor position automatically.

WP 3.6 Major achievements

- The connection of the fuzzy expert system to the automated algorithm for the estimation of the probability of occurrence of a hard rock formation, the diggability and the risk of collision. These estimations were based on the measurements of the apparent specific electrical resistivity of the excavated material obtained by the Electro Magnetic (EM) sensor.
- The modification-enhancement of the existing graphical user-interface (visualization unit) providing all necessary information, including those obtained by the fuzzy expert system in a comprehensive way, to the operator of the BWE.
- The conversion of the above software into a standalone application (HAROR, HArdROckReconnaissance) and its installation on a fully rugged laptop.
- The connection of the geophysical instrument, GPS and optical camera to HAROR application, which was installed on the rugged computer.
- The testing of overall system in the laboratory and in special field sites in TUC installations.
- The preparation of the sites for the final field tests and the adjustment and calibration of the overall system in the mining environment (South Field Lignite Mine).
- The mounting of EM sensor, GPS, optical camera and rugged laptop on the BWE.
- The final tests and the evaluation of the results.

2.2.4 WP-4 Management, coordination, and dissemination

The Kick Off meeting was held between 24th and 25th of September 2015 in Wrocław, Poland. It was organized by Poltegor-Institute. Within this event representatives of all project partners took part.



Figure 87 Kick-off meeting Wrocław, Poland

During KO meeting rules of cooperation, reporting and field tests were established. The places of future meetings were set.

In 2016 progress meetings took place in Prague (March) hosted by VUHU and in Chania (September) hosted by TUC where preliminary results of the project were discussed.

During 2017 two progress meetings took place: in March 2017 in Petrosani in Romania hosted by UP and CE Oltenia and in October in Kouzani in Greece hosted by PPC.



Figure 88 Work progress meeting Petrosani, Romania



Figure 89 Work progress meeting Prague, Czech Republic

During these progress meetings, issues related to the progress of the project as well as future activities were discussed. Each consortium member presented presentations regarding his scope of activity in the project. In 2017, no irregularities were reported and the progress of the project corresponds to the schedule.

In March 2018 the progress meeting in Athens hosted by NTUA took place. During this meeting each task results were presented and the date of international conference closing the BEWEXMIN project was set on June 2018.

2.3 Conclusions

The project BEWEXMIN aimed at the development of solutions to reduce failure rates of bucket wheel excavators operating in difficult mining conditions, where hard rock inclusions and geological formations with high cutting resistance occur. The project included three main research packages. The aim of the first work package was to define requirements to be set during BWE construction in order to obtain dynamic loads of a machine which are as low as possible and proper resistance of load carrying structure. The second work package aimed at the development of a monitoring system of the effort of the load carrying structure of bucket wheel excavator. In the third work package, a real-time mine-face inspection system, based on geophysical methods, for the early detection of hard rock inclusions and geological formations which are difficult to be excavated by bucket-wheel excavators, was proposed.

A part of activities in the first work package were aimed at creating the method of determination of value of force representing impulse loads during calculations of strengths of bucket wheel excavators load bearing structure. All theoretical calculations done within this task were a comparative basis for field tests on real objects. Moreover on the basis of these calculations guidelines regarding technical inspections of individual components of excavators working in hard mineable soils were presented at the final deliverables of the project.

As a result of the theoretical research performed in the project and many years of experience of the authors' team in the field of design and operation of wheel excavators in strip mining, a mathematical model of the process of mining hard mineable soils with heavy-duty working machines was developed. This model was developed on the basis of the analysis of the process of mining tough workable soils with continuous motion and actual values and curves of extreme loads occurring during the operation of bucket wheel excavators. It was created as a result of combination of statistical model of mining forces affecting the excavator's supporting structure with the hypothesis of unitary mining resistance. This combination allows the use of existing long-term experience of mining homogeneous soils with data of the process of mining heterogeneous soils. The basic novelty in relation to the current deterministic model is the replacement of a constant unitary resistance to mining k_A with experimentally determined statistical distribution $k_A(W)$.

The experimental verification of the developed mathematical model proved that the model was formulated correctly. It consisted of the comparison of the curve of the mining force tangential component, obtained as a result of stress measurements at the bucket wheel boom supporting structure with the curve of this component, obtained as a result of measuring the power output of the bucket wheel drive, carried out during mining resistance tests. As a result of the conducted comparisons, it was found that these distributions showed a consistent course of variation, which indicates the correctness of the formulated mathematical model.

Experimental tests were carried out at many excavators during their normal operation in diversified soils, most of them difficult to mine. As a result, a very extensive set of results of instantaneous mining resistance values was obtained. These results were statistically processed and actual distributions (histograms) of the unitary superficial mining resistance values were obtained. Using the developed mathematical model, these histograms can be used in the design and operation of bucket wheel excavators.

The most important practical use of the developed mathematical model is the ability to determine the actual values and nature of the curve of the mining force tangential component at the bucket wheel on the basis of the mining resistance distributions, obtained as a result of statistical research. This allows dimensioning the supporting structure of the newly designed excavator, so that it will not be damaged even in the most difficult geological and mining conditions occurring during the operation of machines in the open pits of a given mine.

Moreover, the selection of the power output of the bucket wheel drive mechanism is made on the basis of the value of the mining force peripheral component, which is decisive for the excavator's capacity. Therefore, it is important that the value of the peripheral component is selected depending on the actual geological and mining conditions present at the locations of the new excavator operation so, that it would be possible to achieve maximum performance under these conditions. It can also be used in current operation, in relation to excavators being upgraded, in terms of adapting the existing mining mechanism to work in soils with increased resistance to mining or its replacement with a new one.

Knowledge of the real distribution of extreme loads affecting the excavator's supporting structure allows predicting the states of its effort in the future and reconstructing its history, which will be the basis for diagnosing the technical condition of machines and avoiding many accidents and disasters.

The applications of the developed mathematical model also include the possibility of a more effective selection of excavators for newly designed as well as existing mine open pits as well as

development of mining processes for these machines, allowing for obtaining optimal efficiency under specific geological and mining conditions.

The mathematical model of extreme loads in the process of mining tough workable soils developed in the project can be used, after minor transformations, in the design and operation of other heavy-duty machines operated in hard mineable strip mines, not only brown coal, but rock raw materials

As part of the project, strength verification of the bucket wheel, which is currently used on excavators, was carried out taking into account the loads from the mining process. The results of calculations of the bucket wheel currently used in the mine on SchRs 4000 excavators indicated local exceedances of stress values in which operational problems are observed. These areas are mainly located in the vicinity of the bucket mounts.

High stress values were also observed in the vicinity of the connection of the rim part of the bucket wheel to the central part in the chute area, for which additional comparative analyses of several modernization solutions were carried out. A design for modernization of the bucket wheel was presented in which the maximum stress values occur outside the zones of welds (as opposed to the original version), where fatigue strength is at least twice as high.

The main aim of the second work package was designing and implementing the BWE monitoring system which was not easy and required solving a number of problems, which included: selection of the optimal statistical method for random loads assessment and development of the relevant algorithm, selection of the appropriate assumption for fatigue accumulation, determining in an experimental way or choosing a series of factors and parameters required for fatigue calculations, developing a method of selecting monitoring sites and measurement points of the load-bearing system, developing a completely new system software (including its multiple additions, corrections and verifications) and proper selection of measuring and processing equipment due to extremely difficult conditions and long-term system operation, as well as a need for data recording, processing and analyzing a very large amount of measurements in a continuous way directly at the tested object with immediate transfer of results to the user.

The designed system of continuous monitoring of the effort of load-bearing structures of opencast mining basic machines has a lot of advantages in relation to the current operation of these machines, the most important of which are:

- the possibility of taking immediate actions preventing failures of load-bearing systems, occurring due to exceeding the thresholds of fatigue strength as well as immediate strength,
- extending the life cycle of the above machines,
- reduction of operating costs of basic machines by reducing the number of failures, and thus reducing the number and duration of stoppages, renovations, etc.,
- achieving an increase of safety of their operation.

Currently, the system is in use at the SchRs 4000.37.5 excavator. Due to the positive results of the research so far, it is planned to implement the system to other mining basic machines in brown coal mines. It is also possible to use the system for all steel constructions subjected to long-term dynamic loads.

The third work package involved the development of the algorithm for automatic data processing obtained from the electromagnetic (EM) sensor (model CMD2) and positioning system (Differential Global Positioning System, DGPS). First, the overall system for data collection, pre-processing and evaluation was designed. Subsequently, existing methods and algorithms were examined for the creation of synthetic data, required during the first phase of the development. Several analytical, statistical and data-driven methods were implemented and tested. Two different evaluation approaches, a relatively simple one called Simple Mode, based on statistical process control and a more sophisticated one, called Advanced Mode, based on Position Prominence Index (PPI) and on Neural-Network based Pattern Recognition (NNPR), were chosen and implemented within Matlab programming environment. Developed models (for both simple and advanced mode) were chosen for testing the algorithms extensively with synthetic data and with real data as well.

Final field tests results indicated that the developed real time mine face inspection system was able to detect the presence of hard rock inclusions in the excavating area and to generate early warnings alarms for the operator of the BWE. The integration of the automated algorithm based on statistical process control, the fuzzy expert system and the visualization unit in a standalone application (HAROR - HArdROckReconnaissance) was proved successful and convenient for real-time monitoring. HAROR is fully parametrized and can be adjusted to operate in different geological and mining conditions.

It was observed that the reliability of the system was mainly affected by the changing harsh mining conditions and the geological settings. Random changes in the distance of the EM sensor from the face and in the height of cut can affect the performance of the system. Moreover the presence, within the reddish clay, of several thin hard and semi hard layers which are diggable by BWE, creates unwanted warnings which should be eliminated by adjusting HAROR parameters.

The knowledge gained from the development of this full-scale system and from the conducted field tests is considered valuable for the next potential step of this research project, which is the development of an industrial grade real time system. An industrial grade system should involve the following:

- A robotic arm (for holding the EM sensor) equipped with a distance measurement sensor and an angle adjustment mechanism.
- Especially manufactured electronics and EM sensor resistant to vibrations, dust, falls and adverse weather conditions.
- Use of EM sensors with capability to change to T-R layout and/or frequency for simultaneous measurements at different depths.
- Transformation of the software code into a lower level programming language (e.g. C++) to reduce the computing time during real time operation. This will allow the use of higher measuring frequency and is anticipated to improve the system accuracy.

2.4 Exploitation and impact of the research results

2.4.1 Actual applications

The monitoring system improved during BEWEXMIN project in WP2 on the basis of theoretical research made in WP1 is currently used in Szczerów Mine on excavator K45. Due to the positive results of the research so far, it is planned to implement the system to other mining basic machines in brown coal mines. It is also possible to use the system for all steel constructions subjected to long-term dynamic loads.

2.4.2 Technical and economic potential for the use of the results

Due to the specific construction and use of mining basic machines, the most sensitive elements deciding on the operational usefulness and operational safety of these machines are their load-bearing structures. These systems are exposed to occurrences of long-term dynamic loads of a random nature and values significantly exceeding the normative ones. In combination with aggressive operational conditions and a very long machine life cycle, it creates favorable conditions for occurrence and development of fatigue cracks, which can lead to serious failures of these systems and even disasters of entire machines. The proof of this is the fact that for 250 major breakdowns of basic machines that have taken place in the 65-year history of Polish opencast brown coal mining, the majority was caused by the fatigue process of load-bearing components. Load-bearing systems of the above machines are protected against exceeding fatigue strength thresholds at a design stage, by dimensioning them in accordance with applicable regulations and standards. However, due to the above-mentioned influence of dynamic loads, their actual values and occurrence frequency cannot be taken into account at the design stage. Therefore, the only effective way to prevent failure occurrences and catastrophes of basic machines is continuous monitoring and ongoing effort evaluation of their load-bearing systems.

The continuous monitoring of load-bearing systems of opencast mining machines has not been performed so far. The tests were carried out in limited time intervals and the results were analyzed after their completion, which due to specificity of fatigue phenomenon prevented further effort forecast of the tested load-bearing structures. Therefore, the Poltegor-Institute has recently undertaken research activities aimed at developing a system of continuous monitoring and ongoing assessment of the effort of load-bearing systems in mining basic machines.

This system is based on continuous measurement of values of dynamic stresses at selected diagnostic points located on the most loaded elements of the tested load-bearing structure. The main task of the system is to assess the fatigue life expressed in hours of effective machine operation, related to the possibility of failure of individual components of the load-bearing structure.

The system is innovative, what is expressed in the fact that the evaluation is carried out continuously and the results are sent immediately to the operator of the machine. Another important novelty is the fact that the above system can be used not only for new machines, but also for machines subjected to long-term use. It is important because the majority of basic mining equipment operating in domestic brown coal mines are machines with a long service life. In addition, this system has an ability to simultaneously evaluate the effort in terms of immediate strength, using the same measuring systems as to assess fatigue strength.

In summary, the system of continuous monitoring of the effort of load-bearing structures of opencast mining basic machines has a lot of advantages in relation to the current operation of these machines, the most important of which are:

- the possibility of taking immediate actions preventing failures of load-bearing systems, occurring due to exceeding the thresholds of fatigue strength as well as immediate strength,
- extending the life cycle of the above machines,
- reduction of operating costs of basic machines by reducing the number of failures, and thus reducing the number and duration of stoppages, renovations, etc.,
- achieving an increase of safety of their operation.

The HAROR system connected with robotic arm built according to assumptions included in WP 3.6 can be a useful tool in mines operating bucket wheel excavators in which non-mineable inclusions or hardly mineable structures occur. It will prevent impact of the bucket wheel with obstacles and thus it will prevent damage to the excavator.

The HAROR system would be also helpful in open cast mines which use two systems of exploitation: continuous and cyclic. Due to the fact that operating costs for continuous system are lower than for cyclic one, the HAROR system will allow for greater use of continuous system and lowering overall costs of exploitation.

2.4.3 Publications / conference presentations resulting from the project

The following list presents publications made within the BEWEXMIN project:

Alenowicz, A. "Requirements set to buckets of BWEs operating in hard mineable soils." Górnictwo Odkrywkowe, 2016.

Alenowicz, J., and A. Bajcar. "Metody ograniczenia awaryjności koparek wielonaczyniowych kołowych eksploatowanych w gruntach trudno urabialnych." IX Międzynarodowy Kongres Górnictwa Węgla Brunatnego. Bełchatów, 2016.

Alenowicz, J., and R. Rosik. "Requirements for load carrying structures of BWE operating in hard mineable soils." Górnictwo Odkrywkowe, 2016.

Bajcar, A. "Ku mniejszej awaryjności". Rynek Inwestycji, nr 15-16/2017-18

Bajcar, A., Onichimiuk, M., Wygoda, M. "Metody ograniczenia awaryjności wielonaczyniowych koparek kołowych w gruntach z wtrąceniami nieurabialnymi". IV Polish Mining Kongress, Kraków 2017.

Bajcar, A., Onichimiuk, M., Wygoda, M. "Methods of decreasing of bucket wheel excavators failures working in soils including unmineable intrusions". Górnictwo Odkrywkowe nr 6, Wrocław 2017.

Bajcar, A., Onichimiuk, M., Wygoda, M., Nowak-Szpak, A., „ Resistances occurring during the exploitation of soils with bucket wheel excavators”, Górnictwo Odkrywkowe nr 4, 2018.

Bajcar, A., Onichimiuk, M., Wygoda, M., Nowak-Szpak, A. „Opory występujące podczas eksploracji gruntów wielonaczyniowymi koparkami kołowymi”, X Międzynarodowy Kongres Górnictwa Węgla Brunatnego. Bełchatów, 2018.

Bajcar, A. "Możliwości wykrywania struktur trudno urabialnych na froncie roboczym wielonaczyniowej koparki kołowej". Konferencja naukowo - techniczna Elgor, Kudowa Zdrój 2017.

Bajcar, A., Rogosz, B. " Praca koparek kołowych w warunkach występowania w urabianym ośrodku utworów o nadmiernych oporach urabiania jak i wtrąceń nieurabialnych" Węgiel Brunatny 2 (103) 2018.

Galetakis, M., T. Michalakopoulos, A. Bajcar, C. Roumpos, M. Lazar, and P. Svoboda. "Project BEWEXMIN: Bucket wheel excavators operating under difficult mining conditions including unmineable inclusions and geological structures with excessive mining resistance." 13th International Symposium Continuous Surface Mining. Belgrade, 2016.

Galetakis, M. et al. "Automatic detection of unmineable inclusions while bucket wheel excavator digging, using electromagnetic (EM) sensor and GPS", Górnictwo Odkrywkowe nr 4, 2018.

Galetakis, M. et al. "Development of a Fuzzy Inference System for avoiding collision of bucket wheel excavator equipped with electromagnetic (EM) sensors with hard rock inclusions", Górnictwo Odkrywkowe nr 4, 2018.

Kiss, R.E., Dinescu, S., Faur, F., Apostu I.E. „ Quick inspection method for working faces in open pits using GIS/GPS tools”, Górnictwo Odkrywkowe nr 4, 2018.

Lazar, M., Risteiu, M., Andras, I., Predoiu, I., "In situ measurements regarding the BWE boom using accelerometers and strain gauges at BWE s operating in CEO open pits", Górnictwo Odkrywkowe nr 4, 2018.

Michalakopoulos, T. et al. „ Requirements of a hard formations early detection system in opencast lignite mines” Górnictwo Odkrywkowe nr 4, 2018.

Moni V., Klouda P., Řehoř M. "Komplexní měření na rýpadle SchRs 1550-4x30/K109", Zpravodaj Hnědé uhlí, 1/2017, ISSN 1213-1660, VÚHU a.s., Most.

Moni V., Klouda P., Řehoř M „ Complex testing of different types of excavators in the Most Basin condition”, Górnictwo Odkrywkowe nr 4, 2018.

Moni v., Šeděnka D.: "Nasazení technické diagnostiky při zprovozňování strojního vybavení hlubinného dolu." Zpravodaj Hnědé uhlí, 1/2017, ISSN 1213-1660, VÚHU a.s., Most.

Nowak-Szpak, A. „Systemy zdalnego kierowania ruchem maszyn górniczych w kopalniach odkrywkowych – propozycja identyfikacyjno-symulacyjnego programu projektowania pracy koparki kołowej”. Górnictwo Odkrywkowe nr 6, Wrocław 2017

Onichimiuk, M., Wygoda, M., Bajcar, A., Pietrusiak, D., Moczko, P. „Determination of the Bucket Wheel Suspension Stiffness”, 9 Computer Aided Engineering 2018, Springer Series: Lecture Notes in Mechanical Engineering, 2019.

Řehoř, M., and V. Moni. "Hodnocení výskytu obtížně těžitelných struktur na lomu Libouš v rámci řešení projektu BEWEXMIN." XXII. ročníku conference - PROBLÉMY PROVOZU, ÚDRŽBY A OPRAV STROJNÍHO ZAŘÍZENÍ, POUŽÍVANÉHO PŘI POVRCHOVÉM DOBÝVÁNÍ. 2016.

Řehoř, M., and V. Moni. "Výskyt, charakteristika a možnosti vyhledávání obtížně těžitelných struktur ve skrývkových zeminách mostecké pánve." Zpravodaj Hnědé uhlí, 2016.

Řehoř, M., and V. Moni "Optimum methodology of hard structures research in the Most Basin condition", Górnictwo Odkrywkowe nr 4, 2018.

Řehoř, M., M. Moni, and P. Svoboda. "Bucket wheel excavators operating under difficult mining conditions including unmineable inclusions and geological structures with excessive mining resistance." Expert report, Most, 2016.

Řehoř M., Moni V., Novák V., Kraus V., Schmidt P.: "RESULTS OF LONG TERM TESTING OF GEOLOGICAL SITUATION AND EXCAVATOR SCHRS 1550-4X30/K109 PARAMETERS DURING THE RELOCATION TO THE POSITION WITH THE WORSE MINING CONDITIONS IN THE LIBOUS MINE (THE MOST BASIN)." SGEM Conference Proceedings "Exploration and mining", VOLUME XVII, p. 765-772, ISBN 978-619-7105-00-1, ISSN 1314-2704, DOI:10.5593/sgem2017/13, SCOPUS, Albena, Bulgaria 2017.

Roumpos, C. et al. "Possibilities for improving work efficiency of continuous surface mining systems operating in rocks with excessive digging resistance", Górnictwo Odkrywkowe nr 4, 2018.

Szewerda, K., "The concept of the numerical computing methods for analysis of operational conditions of bucket wheel excavators"

Triantafyllou, M. et al. „Experimental design for applying geophysical methods in investigating the spatial distribution of hard formations in the excavation face of bucket wheel excavators" Górnictwo Odkrywkowe nr 4, 2018.

Vafidis, A., N. Economou, M. Galetakis, A. Vasiliou, T. Michalakopoulos, and G. Apostolopoulos. "Assessing the potential of ground penetrating radar (GPR) to detect hard geological formations and inclusions during the excavation by bucket-wheel excavators." 13th International Symposium Continuous Surface Mining. Belgrade, 2016.

Vafidis, A., Economou, N., Kritikakis, G., Galetakis, M., Vasiliou, A., Apostolopoulos, G. and Michalakopoulos, T., 2017. Imaging boulders using the GPR method, BCRRA2017, Athens, Greece, 28-30th June.

Vafidis, A., et al. "Assessment of geophysical methods for the detection of hard rock formations in lignite mines employing bucket wheel excavators. The case of South Field lignite mine, Macedonia, Greece.", Górnictwo Odkrywkowe nr 4, 2018.

Vîlceanu, F., Andraş, I., Lazăr, M., "Fatigue Assessment of BWE Boom Members and Joints in Order to Assess their Remaining Lifetime", Górnictwo Odkrywkowe nr 4, 2018.

2.4.4 Other aspects concerning the dissemination of results

On 12-13 June 2018 in Wrocław an international conference closing the BEWEXMIN project took place. It was organised by "Poltegor-Instytut" Institute of Opencast Mining. The conference was held under the honorary patronage of the Polish Minister of Energy, Mr. Krzysztof Tchorzewski. The main purpose of the meeting was to present the completed research work and the main results of the BEWEXMIN project.

The conference was opened by the Director of „Poltegor-Instytut” - Jacek Szczepiński, who presented the current state and prospects of brown coal mining in the world. Over 60 participants representing 7 countries took part in the conference. Such a wide group of participants was an opportunity to exchange experiences and discuss the current state and possibilities of reducing the failure rate of bucket wheel excavators in soils with excessive mining resistance or containing non-mineable inclusions.

The speakers were, among others, representatives of Technical University of Crete, National Technical University of Athens, University of Petrosani, KOMAG Mining Technology Institute, VUHU Výzkumný ústav pro hnědé uhlí from Czech Republic, PGE Górnictwo i Energetyka Konwencjonalna SA, Oltenia Energy Complex from Romania and Public Power Corporation from Greece and Wrocław University of Science and Technology.

During the three thematic sessions, a total of 21 presentations were presented and focused around three thematic topics presented below:

- Optimal adaptation of currently exploited and new bucket-wheel excavators for mining of overburden including interlayers with excessive mining resistance and unmineable inclusions.
- Monitoring system of bucket wheel excavator load carrying structure efforts and method of diagnostic signals analysis for current assessment of threats of load carrying structure damages as well as constant control of residual strength of the structure
- Real-time mine-face inspection system, based on geophysical methods, capable to detect hard rock inclusions and geological formations which are difficult to be excavated by bucket-wheel excavators

A few days earlier, on 22 May during the scientific and technical conference "RISK | 2018" Innovation Technology, the gala of Business and Economy Magazine "Rynek Inwestycji" was held, where "Poltegor-Institute" received the Gold Medal awarded by "Rynek Inwestycji" for developing of advanced methods of risk mitigation related to the operation of bucket wheel excavators in hardly mineable soils. The award acknowledged several years of effort not only of the "Poltegor-Institute", but also of all entities involved in the BEWEXMIN project.

3 LIST OF FIGURES

Figure 1 Theoretical scheme of the impact impulse	15
Figure 2. Triangular model of impulse load	15
Figure 3. Proposed model of impulse force.....	16
Figure 4 Bucket wheel and boom before hitting in the unmineable obstacle	17
Figure 5 Bucket wheel and boom during impact in the unmineable obstacle	17
Figure 6 Deflection of the bucket wheel boom after impact	18
Figure 7 Diagram of boom deflection under the influence of vertical force.....	19
Figure 8 Diagram of deflection of the attached bucket wheel boom with winch force	19
Figure 9 Diagram of distribution of measuring points	20
Figure 10 Attachment of the auxiliary machine to the bucket	20
Figure 11 Diagram of boom deflection under the load (F)	21
Figure 12 Model of the bucket wheel drive	22
Figure 13 Kinematic scheme of the angular gearbox with equivalent scheme	22
Figure 14 Kinematic scheme of main gearbox with equivalent diagram.....	23
Figure 15 Geometrical model of the bucket wheel drive.....	23
Figure 16 Histogram of the distribution of mining resistance values $kA(\Omega)$	27
Figure 17 Geometric model of the bucket wheel excavator's body	28
Figure 18 Physical model of the bucket wheel excavator's body.....	29
Figure 19 Physical model of the bucket wheel excavator's superstructure	29
Figure 20 The method of attaching the bucket wheel hoisting ropes.....	30
Figure 21 Value of the driving torque of the bucket wheel as a function of its rotational	30
Figure 22 The method of loading the bucket wheel	31
Figure 23 Computational model of a multi-bucket excavator	31
Figure 24 Measurement of vibrations by numerical simulations a) place of measurement,	32
Figure 25 Mast 1 deformation forms in relation to selected natural frequencies	33
Figure 26 Forces at the point of fixing the rope, that supports and lifts the bucket wheel boom....	34
Figure 27 Visualization of the collision situation of the bucket wheel hitting an obstacle	34
Figure 28 Preparing of sensors for loading measurement.....	35
Figure 29 Example of vibration curve	36
Figure 30 The geometric model of the bucket wheel	37
Figure 31 Discrete model of the bucket wheel	38
Figure 32 Examples of stress measurement points	41
Figure 33. Selected structural node	43
Figure 34. Deformation measurement point on the boom – left side	44
Figure 35. Deformation measurement point on the boom – right side	44
Figure 36 Examples of modelled welds.....	45
Figure 37 Diagram of notch coefficient values	46
Figure 38 Testing rig.....	46
Figure 39 Rig measurement system prototype	47
Figure 40 Excavator KK 1300.1-CZ/K111	50
Figure 41 Clays in mined block.....	51
Figure 42 Switchboard RM 10	52
Figure 43 Measurement of bucket wheel lateral force	52
Figure 44 Thermovision measurement of teeth and buckets	53
Figure 45 Measuring points at the bucket wheel boom - boom hanging area, lower left girder point P1.03.06	55
Figure 46 Measurement report of static stresses. A lower left girder of the bucket wheel boom	55
Figure 47. Integration of images and measurements of various modalities.	62
Figure 48. Scope of the hard inclusions detection system	63
Figure 49. Simulated 2D models with the resulting radargrams using the GPR 250MHz antenna...64	64
Figure 50. Classification of the examined samples according to their moisture and resistivity values	65
Figure 51. Range of apparent conductivity values deduced from the EM survey on the slope, next to a photo of the mine front. Lower apparent conductivity zones in red are observed next to hard rock layers.	66
Figure 52. Apparent conductivity maps for measurements at the artificial site created at Szczerów Field Mine.....	67
Figure 53 Mounting of EM instrument and differential GPS on the 6m long fixed wooden beam on one of PPC's BWEs in the South Field mine.	69
Figure 54 Conductivity map of the mine face surveyed by the EM instrument mounted on the BW. The layer of hard material, which has a low conductivity value, is clearly detected.	69
Figure 55 Determination of the minimum safe distance between the EM instrument and the BW with respect to electromagnetic interference.....	69
Figure 56 The concept of the new mounting setup	70
Figure 57 Design details of the new mounting arm.	70

Figure 58 3D conductivity map of the mine face surveyed by the EM instrument using the bucket truck. The inclusions of hard material, which has a low conductivity value, are clearly detected ...	71
Figure 59 Block diagram of measurement and data processing system.....	72
Figure 60 Excavation of a block by terrace cutting. The CMD2 instrument follows the slewing movement of the bucket wheel.	73
Figure 61 EM sensor (CMD2) trajectories in X-Y coordinates (UTM) during the excavation of a block by terrace cutting.....	73
Figure 62 EM sensor (CMD2) elevations during the excavation of a block by terrace cutting.....	74
Figure 63 Low depth range 2D cumulative sensitivity for intercoil separation 1.89m and maximum depth of penetration 7m. The instrument is located at horizontal distance $x=0\text{m}$, where maximum sensitivity values occur	75
Figure 64 The apparent resistivity values as estimated by both analytical and numerical approach over a $30\text{m} \times 7\text{m}$ model. Two relatively higher resistivity bodies are buried (their top surface) at depth of 0.5m from the surface within a conductive homogeneous half	75
Figure 65 Application of Simple Mode Hard Rock detection algorithm to synthetic resistivity data. Simulation resamples the last BW cut before hitting the boulder, located at 0.2 m depth (the top of boulder) and 13 m (center) of model. The sampling interval in horizontal direction is 0.1 m and the colour scale corresponds to model resistivity in Ωm	76
Figure 66 Performance evaluation of SMHRD process data windows and threshold limits, using synthetic resistivity data and successive BWE cuts. Cut4 correspond to the last BW cut before hitting on the boulder. Different BW cut depths (0.2, 0.6, 0.8, 1.0, 1.2 m) were examined in 100 different (randomly generated) 2 boulder models. The most successful parameter combination result for the 4 cuts is highlighted with crosses.	77
Figure 67 Apparent resistivity map deduced from experimental data interpolation, acquired by the EM instrument CMD2 along the route marked with white crosses. High resistivity values correspond to an area where hard rock inclusion was observed. Separated data were extracted along 7 resistivity profiles with 0.5m spacing and then data for five successive cuts (1-5) were derived to be used for processing.	77
Figure 68 Part of the mine face surveyed with CMD2. It is located in the overburden bench of sector 7 of South Field mine of PPC. As shown in photo the hard rock inclusion is a lenticular conglomerate formation surrounded by brown-reddish clay layers	78
Figure 69 Example of Simple Mode Boulder Detection application on the 4 th cut of the experimental resistivity data, shown in Figure 67. The area marked with warning alerts (both out of standard deviation -std- and stalta limits) at the positions where steep increase of resistivity values is encountered. The sampling interval along profiles is 0.1m.	78
Figure 70 (Top) Random dataset and their 6 most prominent maxima. Numbers over the red circles indicate their rank. (Bottom) Prominent maxima at the same positions for both passes are detected at 5m. PPI value (black line) is accordingly increased.....	79
Figure 71 Apparent resistivity (left axis) and PPI values (right axis) calculated from 2 successive cut changes (up: cut 2 to 3, down: cut 3 to 4) of the experimental data	80
Figure 72 Schematic diagram showing: (Top) Terrace cutting by BWE. (Bottom) Successive resistivity profiles obtained during terrace cutting (3 cuts) and use of moving window to examine local changes in resistivity profiles as BW approaches the hard rock	82
Figure 73 Structure of NNRPR (forward neural network) used for the prediction of the probability of occurrence of a hard rock formation	82
Figure 74 (Left) Confusion matrices for all data showing the number and the percentages of correct and false predictions (Class 0=Non-existence of a hard rock formation, Class 1=Existence of a hard rock formation). (Right) The Receiver-Operator-Curve, or ROC, indicates how the false alarms rate increases as the rate of successful prediction increases.....	83
Figure 75 Profiles of the probability for a hard rock occurrence for the examined five successive cuts (1-5).....	83
Figure 76 Strategy for developing a FIS for the determination of the collision risk	84
Figure 77 FIS development in Matlab programming environment (Fuzzy Logic Toolbox)	85
Figure 78 Membership functions of input/output variables.	85
Figure 79. Fuzzy inference mechanism and defuzzification method.	86
Figure 80. FIS response surface for Risk of Collision as function of the Probability (of hard rock occurrence) and the Distance (BW to hard rock).	86
Figure 81 Visualization unit providing all necessary information to the operator of the BWE.	87
Figure 82 HAROR main screen and menus during real time operation.	88
Figure 83 Available plots during HAROR operation.	88
Figure 84 Getac laptop with the installed HAROR software during its operation (inside BWE operator cabin).	89
Figure 85 Mounting of EM instrument and DGPS on the BWE boom.....	89
Figure 86 EM instrument with protective case attached to wooden beam.....	89
Figure 87 Kick-off meeting Wrocław, Poland	91
Figure 88 Work progress meeting Petrosani, Romania.....	92
Figure 89 Work progress meeting Prague, Czech Republic	92

4 LIST OF TABLES

Table 1 Experimental values of boom deflections of the K45 bucket wheel excavator	21
Table 2 Theoretical values of the SchRs4000 excavator bucket wheel boom deflections; (Bucket wheel boom vertical deflection under specific force).....	21
Table 3 Reduction of moments of inertia - Drive shaft.....	24
Table 4 Reduction of moments of inertia - angular gearbox	24
Table 5 Reduction of moments of inertia - Main gearbox part 1	24
Table 6 Reduction of moments of inertia - Main gearbox part 2a – the moment transfer.....	24
Table 7 Reduction of moments of inertia - Main gearbox part 2b – inertia.....	25
Table 8 The load of the bucket wheel axis is in direct up.	49
Table 9 Laboratory analyses of the samples (position No 3).....	51
Table 10 The lump size of mined rocks (KK 1300.1 CZ, 29.11.2017).....	53
Table 11. List of lignite mines	59
Table 12. Environmental conditions	59
Table 13. BWE characteristics	59
Table 14. Inverters on BWEs.....	60
Table 15. Excavation characteristics.	60
Table 16. Availability of data relevant to geophysics.	60
Table 17. Formations hard to excavate.	60
Table 18. Installed monitoring infrastructure.	61
Table 19 Part of original data, collected from CMD2 electromagnetic instrument in June 2017 at South Field open pit mine, Ptolemaida, Grece. The last three columns deduced after the coordinates conversion from Lat.-Long. (WGS84') to Cartesian (UTM) geodetic system	72

5 LIST OF ACRONYMS AND ABBREVIATIONS

BWE – Bucket Wheel Excavator
CE OLTEA – SOCITATEA COMPLEXUL ENERGETIC OLTEA SA
DGPS - Differential Global Positioning System
EM - Electromagnetic
FEM – Finite Element Method
GPR – Ground Penetration Radar
HAROR – HardROckReconnaissance – real time mine face inspection system
KOMAG – INSTYTUT TECHNIKI GÓRNICZEJ KOMAG
MBS – Multi Body System
NNPR - Neural-Network based Pattern Recognition
NTUA – NATIONAL TECHNICAL UNIVERSITY OF ATHENS
PGEGLIEK - PGE GÓRNICTWO I ENERGETYKA KONWENCJONALNA SA
POLT – Poltegor Instytut
PPC – PUBLIC POWER CORPORATION AE
PPI - Position Prominence Index
TWB – Two Wheel Bogie
UCRE - THE RESEARCH COMMITTEE OF THE TECHNICAL UNIVERSITY OF CRETE
UPETROS – UNIVERSITATEA DI PETROSANI
VUHU - Výzkumný ústav pro hnědé uhlí a.s.

6 REFERENCES

- Alenowicz, A. (2016). Requirements set to buckets of BWEs operating in hard mineable soils. *Górnictwo Odkrywkowe*(1).
- Alenowicz, J., & Bajcar, A. (2016). Metody ograniczenia awaryjności koparek wielonaczyniowych kołowych eksploatowanych w gruntach trudno urabialnych. *IX Międzynarodowy Kongres Górnictwa Węgla Brunatnego*. Bełchatów.
- Alenowicz, J., & Rosik, R. (2016). Requirements for load carrying structures of BWE operating in hard mineable soils. *Górnictwo Odkrywkowe*(6).
- Al-Shrouf, L. (2014). *Development and implementation of a reliable decision fusion and pattern recognition system for object detection and condition monitoring*. Universitat Duisburg-Essen.
- Alumbaugh, D. L., Newman, G. A., Prevost, L., & Shadid, J. N. (1996). Three-dimensional wideband electromagnetic modeling on massively parallel computers. *Radio Science*(31).
- Arsić, M., Bošnjak, S., Rakin, M., Gnjatović, N., & Savić, Z. (2012). Reliability assessment of welded joints at bucket- wheel excavators based on hypergeometric distribution of defects. *Proceedings of the XX International Conference MHCL'12*. Belgrade.
- Arsić, M., Bošnjak, S., Zrnić, N., Sedmak, A., & Gnjatović, N. (2011). Bucket wheel failure caused by residual stresses in welded joints. *Engineering Failure Analysis*.
- Babiarz, S., & Dudek, D. (2007). *Kronika awarii I katastrof maszyn podstawowych w polskim górnictwie odkrywkowym*. Wrocław: Oficyna Wydawnicza Politechniki Wrocławskiej.
- Bartelmus, W., & Zimroz, R. (2009). A new feature for monitoring the condition of gearboxes in non-stationary operating conditions. *Mechanical Systems and Signal Processing*(23).
- Bartelmus, W., Chaari, F., Zimroz, R., & Haddar, M. (2010). Modelling of gearbox dynamics under time-varying nonstationary load for distributed fault detection and diagnosis. *European Journal of Mechanics* (29).
- Bartelmus, W., Zimroz, R., Sawicki, W., Maniak, M., Woźniak, Z., & Furmaniak, K. (2007). Wybrane zagadnienia diagnostyki wielostopniowej przekładni zębatej ze stopniem planetarnym w układzie napędowym koparki kołowej. *Górnictwo i Geoinżynieria* (31).
- Bošnjak, M. S., Petković, D. Z., Gnjatović, B. N., Jerman, B., & Milenović, L. I. (2012). Finite element and experimental strength analysis of the bucket wheel excavator two-wheel bogie. *Proceedings of the XX International Conference MHCL'12*. Belgrade.
- Bošnjak, S. M., Arsić, M., Zrnić, N. D., Rakin, M. P., & Pantelić, M. P. (2011). Bucket wheel excavator: Integrity assessment of the bucket wheel boom tie-rod welded joint. *Engineering Failure Analysis*(18).
- Bošnjak, S. M., Petković, Z. D., Simonović, A. M., Zrnić, N. D., & Gnjatović, N. B. (2013). 'Designing-in' failures and redesign of bucket wheel excavator undercarriage. *Engineering Failure Analysis*(35).
- Bošnjak, S., & Zrnić, N. (2012). Dynamics, failures, redesigning and environmentally friendly technologies in surface mining systems. *Archives of Civil and Mechanical Engineering* (12).
- Bošnjak, S., Momčilović, D. B., Petković, Z. D., Pantelić, M. P., & N., G. (2013). Failure investigation of the bucket wheel excavator crawler chain link. *Engineering Failure Analysis* (35).
- Bošnjak, S., Pantelić, M., Zrnić, N., Gnjatović, N., & Dordević, M. (2011). Failure analysis and reconstruction design of the slewing platform mantle of the bucket wheel excavator O&K SchRs 630. *Engineering Failure Analysis*(18).
- Bošnjak, S., Petković, Z., Zrnić, N., Pantelić, M., & Obradović, A. (2010). Failure analysis and redesign of the bucket wheel excavator two-wheel bogie. *Engineering Failure Analysis* (17).
- Bošnjak, S., Petković, Z., Zrnić, N., Pantelić, M., & Simić, G., & Simonović, A. (2009). Cracks, repair and reconstruction of bucket wheel excavator slewing platform. *Engineering Failure Analysis* (16).

- Bošnjak, S., Savićević, S. D., Gnjatović, N. B., Milenović, I. L., & Pantelić, M. P. (2015). Disaster of the bucket wheel excavator caused by extreme environmental impact: Consequences, rescue and reconstruction. *Engineering Failure Analysis* (56).
- Bošnjak, S., Zrnić, N., Simonović, A., & Momčilović, D. (2009). Failure analysis of the end eye connection of the bucket wheel excavator portal tie-rod support. *Engineering Failure Analysis*(16).
- Cireş, I., & Nani, V. (2016). Stability control for huge excavator for surface excavation. *Applied Mathematical Modelling*(40).
- Combet, F., & Zimroz, R. (2009). A new method for the estimation of the instantaneous speed relative fluctuation in a vibration signal based on the short time scale transform. *Mechanical Systems and Signal Processing*(23).
- Czmochowski, J., Kowalczyk, M., Pietrusiak, D., Przybyłek, G., & Rusiński, E. (2015). Metodyka oceny stanu technicznego maszyn górniczych w kopalniach odkrywkowych. In *Monografie Politechniki Łódzkiej: Problemy Rozwoju Maszyn Roboczych*. Łódź.
- Dandea, D., & Nan, M. (2013). Design and Simulation of a Control System For the Bucket Wheel Excavator. *Latest Trends in Applied Computational Science*. Malaysia.
- Danicic, D., Sedmak, S., Ignjatovic, D., & Mitrovic, S. (2014). Bucket wheel excavator damage by fatigue fracture – case study. *Procedia Materials Science* 4.
- DIN 22261 Bagger, Absetzer und Zusatzgeräte in Braunkohlentagebauen. (1998). Deutsches Institut für Normung.
- Dreyer, E. (1995). Cost-effective prevention of equipment failure in the mining industry. *Int. J. Pres. Ves. & Piping*. 16.
- Economou, N., & Vafidis, A. (2011). Deterministic deconvolution for GPR data in t-f domain. *Near Surface Geophysics*, 9(5).
- Economou, N., & Vafidis, A. (2012). GPR data time varying deconvolution by kurtosis maximization. *J. of Appl. Geophys.*, 81.
- Francke, J. (2012). A review of selected ground penetrating radar applications to mineral resource evaluations. *Journal of Applied Geophysics*(81).
- Fries, J., Helebrant, F., Jurman, J., Klouda, P., & Moni, V. (2010). Merenje kapaciteta rotornog bagera tipa K 2000. *III. Medunarodni simpozijum energetiko rудarstvo*. Apatin.
- Fries, J., Helebrant, F., Jurman, J., Klouda, P., & Moni, V. (2010). Merenje momenta torzije na vratilu rotornog točka kod velikih mašina. *III. Medunarodni simpozijum energetiko rудarstvo*. Apatin.
- Galetakis, M., Michalakopoulos, T., Bajcar, A., Roumpos, C., Lazar, M., & Svoboda, P. (2016). Project BEWEXMIN: Bucket wheel excavators operating under difficult mining conditions including unmineable inclusions and geological structures with excessive mining resistance. *13th International Symposium Continuous Surface Mining*. Belgrade.
- Galetakis, M., Papadopoulos, S., Vasiliou, A., Roumpos, C., & Michalakopoulos, T. (2014). Development of an expert system for the prediction of the performance of bucket-wheel excavators used for the selective mining of multiple-layered lignite deposits. *12th International Symposium of Continuous Surface Mining*. Aachen.
- Gottvald, J. (2011). Measuring and comparison of natural frequencies of bucket wheel excavator SchRs 1320 and K 2000. Recent Researches in Geography, Geology, Energy, Environment and Biomedicine. *Proceedings of the 4th WSEAS International Conference on Engineering Mechanics, Structures, Engineering Geology*. Corfu Island.
- Gottvald, J. (2012). Analysis of vibrations of bucket wheel excavator SchRs 1320 during mining process. *FME Transactions*(40).
- Großgeräte in Tagebauan Berechnungenrundlaghen. Der Minister für Wirtschaft und Verkehr des Landes Nordrhein-Westfalen I/B2-22-02 (1960).
- Jovančić, P. D., Ignjatović, D., Tanasijević, M., & Maneski, T. (2011). Load-bearing steel structure diagnostics on bucket wheel excavator, for the purpose of failure prevention. *Engineering Failure Analysis*(18).

- Jula, D., Kovacs, I., Dumitrescu, I., Andras, A., & Tomus, O. (2001). Upgrading the Boom Positioning Mechanism of Bucket Wheel Excavators Utilized in Romanian Open Pit Lignite Mines. *microCAD 2011, International Scientific Conference Miskolc*.
- Kavouridis, K., Roumpos, C., Galetakis, M., & Pavloudakis, F. (2008). Methods and Technological Improvements for the Efficient Removal of the Overburden Hard Rock Formations at South Field Lignite Mine. *9th International Symposium 'Continuous Surface Mining'*. Petrosani.
- Klonda, P., Novak, A., Basta, L., Moni, V., & Strakos, K. (2008). Wpływ kształtu i geometrii ostrza organów urabiających w interakcji z urabianą skałą. *Systemy Wspomagania w Zarządzaniu Środowiskiem*. Zabrze.
- Kocańda, S., & Szala, J. (1991). *Podstawy obliczeń zmęczeniowych*. Warszawa: Państwowe Wydawnictwo Naukowe.
- Kovacs, I., Nan, M. S., & Andras, I. (2006). Research regarding the lignite and rock excavation using bucket wheel excavators. *Scientific Bulletin Series C : Fascicle Mechanics, Tribology, Machine Manufacturing Technology*.
- Kovacs, I., Nan, M. S., Andraş, I., Tomuș, O.-B., & Andraş, A. (2010). Comparative study of mechanical rock cutting. *Annals of the University of Petroşani, Mechanical Engineering*(12).
- Kovacs, I., Nan, M., Jula, D., & Tomus, O. (2010). New Buckets Mounted on Rotor Excavators as a Result of Dislocation Tested Process. *International conference on applied computer science*. Malta.
- Kowalczyk, M., Czmochowski, J., & Rusiński, E. (2009). Construction of diagnostic models of the states of developing fault for working parts of the multi-bucket excavator. *Maintenance and Reliability*(2).
- Lele, S. K. (1992). Compact Finite Difference Schemes with spectral-like resolution. *JCP*(103).
- Liehs, K., Zapp, P., & Lierenfeld, T. (2012). Safe and reliable positioning of main mines equipment at RWE Power AG. *World of Mining*(64).
- Musiał, W., & Szepietowski, W. (1988). Durch Anprallen der Schaufeln gegen Findlinge hervorgerufene Belastungen des Auslegergerüstes eines Schaufelradbaggetts. *BRAUNKOHLE*(1/2).
- Nan, M. S., Dandea, D. L., & Simon, B. (2013). The modernization of bucket wheel excavators using intelligent image analysis systems. *Hebezeuge und Fördermittel*(39).
- Nan, M. S., Kovacs, I., & Popescu, F. D. (2008). Balance control by weighting and tensiometric measurements of bucket wheel excavators. *WSEAS TRANSACTIONS on SYSTEMS and CONTROL Issue , 3*(11).
- Nan, M., Kovacs, I., A. I., & Jula, D. (2008). Study of the working regime of the bucket wheel excavators in the conditions of Romanian open pit lignite mines. *8th WSEAS International Conference on SIMULATION, MODELLING and OPTIMIZATION (SMO '08)*. Santander.
- Nieb, T. (2009). Automatic metal end stone detection on bucket wheel excavators used in RWE Power AG's opencast lignite mines. *World of Mining*(61).
- Onichimiuk, M., Wygoda, M., & Wojtowicz, A. (2011). *Uruchomienie systemu monitorowania ustroju nośnego na koparce SchRs 4000*. IGO Poltegor 6286/IGO 2011.
- Pajer, G. (1979). *Tagebaugroßgeräte und Universalbsgger*. Berlin: VBE Verlag Technik.
- Rasper, L. (1975). *The bucket wheel excavator : development - design - application*. Clausthal-Zellerfeld: Trans Tech Publications.
- Řehoř, M., & Moni, V. (2016). Hodnocení výskytu obtížně těžitelných struktur na lomu Libouš v rámci řešení projektu BEWEXMIN. *XXII. ročníku conference - PROBLÉMY PROVOZU, ÚDRŽBY A OPRAV STROJNÍHO ZAŘÍZENÍ, POUŽÍVANÉHO PŘI POVRCHOVÉM DOBÝVÁNÍ*.
- Řehoř, M., & Moni, V. (2016). Výskyt, charakteristika a možnosti vyhledávání obtížně těžitelných struktur ve skrývkových zeminách mostecké pánve. *Zpravodaj Hnědé uhlí*(2).
- Řehoř, M., Moni, M., & Svoboda, P. (2016). *Bucket wheel excavators operating under difficult mining conditions including unmineable inclusions and geological structures with excessive mining resistance*. Expert report, Most.

- Rusiński, E., Czmochowski, J., & Pietrusiak, D. (2012). Selected problems of open cast mining machines design. *Proceedings of the XX International Conference MHCL'12*. Belgrade.
- Rusiński, E., Czmochowski, J., Iluk, A., & Kowalczyk, M. (2010). An analysis of the causes of a BWE counterweight boom support fracture. *Engineering Failure Analysis*(17).
- Rusiński, E., Harnatkiewicz, P., Kowalczyk, M., & Moczko, P. (2010). Examination of the causes of a bucket wheel fracture in a bucket wheel excavator. *Engineering Failure Analysis*(17).
- Sasaki, Y., Kim, J., & Jun, C. (2010). Multidimensional Inversion of Loop-Loop Frequency-Domain EM Data for Resistivity and Magnetic Susceptibility. *Geophysics*, 75.
- Savković, M., Gašić, M., Arsić, M., & Petrović, R. (2011). Analysis of the axle fracture of the bucket wheel excavator. *Engineering Failure Analysis*(18).
- Savković, M., Gašić, M., Petrović, D., Zdravković, N., & Pljakić, R. (2012). Analysis of the drive shaft fracture of the bucket wheel excavator. *Engineering Failure Analysis*(20).
- Strunk, S., & Witzel, J. (2010). Optimizing the production of problematic overburden at the Hambach opencast mine. *World of Mining*(62).
- Szepietowski, W. (2009). Sprzęgła przeciążeniowe w napędzie koła czerpakowego koparek wielonaczyniowych. *Napędy i Sterowanie*(3).
- Szepietowski, W., & Szepietowski, M. (2011). Zabezpieczenia mechaniczne przed nadmiernym obciążeniem dynamicznym koparki kołowej. *Górnictwo Odkrywkowe*(5).
- TGL 13472 Skahltragwerke der Tagebaugroßgeräte Verbinadlich. (1973).
- TGL 13472/2 Skahltragwerke der Tagebaugroßgeräte Verbinadlich. (1977).
- Vafidis, A., Economou, N., Galetakis, M., Vasiliou, A., Michalakopoulos, T., & Apostolopoulos, G. (2016). Assessing the potential of ground penetrating radar (GPR) to detect hard geological formations and inclusions during the excavation by bucket-wheel excavators. *13th International Symposium Continuous Surface Mining*. Belgrade.
- Vołkov, D., & Cerkasov, V. (1969). *Dinamika i procznośc mnigokovszowych ekskavatorów i otwaloobrazovatej*. Moskva: Maszynostrojenie.

Getting in touch with the EU

In person

All over the European Union there are hundreds of Europe Direct information centres. You can find the address of the centre nearest you at:
https://europa.eu/european-union/contact_en

On the phone or by email

Europe Direct is a service that answers your questions about the European Union. You can contact this service:

- by freephone: 00 800 6 7 8 9 10 11 (certain operators may charge for these calls),
- at the following standard number: +32 22999696 or
- by email via: https://europa.eu/european-union/contact_en

Finding information about the EU

Online

Information about the European Union in all the official languages of the EU is available on the Europa website at: https://europa.eu/european-union/index_en

EU publications

You can download or order free and priced EU publications at: <https://publications.europa.eu/en/publications>. Multiple copies of free publications may be obtained by contacting Europe Direct or your local information centre (see https://europa.eu/european-union/contact_en).

EU law and related documents

For access to legal information from the EU, including all EU law since 1952 in all the official language versions, go to EUR-Lex at: <https://eur-lex.europa.eu>

Open data from the EU

The EU Open Data Portal (<https://data.europa.eu/euodp/en/home>) provides access to datasets from the EU. Data can be downloaded and reused for free, for both commercial and non-commercial purposes.

In newly-opened as well as existing lignite mines occur increasingly difficult mining conditions due to the presence of a growing number of unmineable inclusions and inclusions with an excessive mining resistance. During exploitation of such materials there are large dynamic and impulse loads. This results in frequent breakdowns and therefore exclusion of machines from normal operation. The aim of the project was to develop solutions to reduce failure rates of bucket wheel excavators working in such conditions. This could be achieved either by reducing the sensitivity of excavators on pulse load or by efforts to reduce the size of dynamic loads. Research in the BEWEXMIN project included three work packages. The first package included: experimental determination of the dynamic surplus from mass forces and linkage of these surpluses with physico-mechanical characteristics of exploited soils; method for determining alternative computational strength of pulse loads; determination of the requirements for flawless excavator work in specific conditions. In the second work package a way to create a system to monitor stress of excavator's structures leading to continuous assessment of the degree of construction effort, signalling damage possibility, was created. The activities included in the third work package aimed to eliminate or reduce value of pulse loads caused by encountering unmineable obstacle by means of early detection of stones. All three WPs were interrelated and constituted a complete set of activities aiming at the same goal, which was to reduce failure rates of bucket wheel excavators operating in difficult mining conditions.

